2010

Elucidating a role for BBS3 in syndromic and non-syndromic retinal disease

Pamela Reed Pretorius
University of Iowa

ELUCIDATING A ROLE FOR BBS3 IN SYNDROMIC AND NON-SYNDROMIC RETINAL DISEASE

by

Pamela Reed Pretorius

An Abstract

Of a thesis submitted in partial fulfillment
of the requirements for the Doctor of
Philosophy degree in Genetics
in the Graduate College of
The University of Iowa

December 2010

Thesis Co-Supervisors: Professor Val C. Sheffield
Professor Diane C. Slusarski

ABSTRACT

Bardet-Biedl Syndrome (BBS) is a syndromic form of retinitis pigmentosa, characterized by retinal degeneration, obesity, learning disabilities, congenital abnormalities and increased incidences of hypertension and diabetes. Individuals with BBS are blind by the third decade of life. At least fourteen genes are reported to individual cause BBS. This thesis focuses on *BBS3*, with the overall goal of characterizing the function of BBS3 in terms of both syndromic and non-syndromic retinal degeneration.

A member of the Ras family of small GTP-binding proteins, *BBS3* is postulated to play a role in vesicular transport. A second highly conserved transcript of *BBS3*, *BBS3L*, is expressed in the mouse and zebrafish eye. Histological analysis of *Bbs3L* knockout mice at 9 months reveals disorganization of the inner segments, indicative of retinal degeneration. To further evaluate the functional effects of *BBS3* deficiency in the eye, an antisense oligonucleotide (Morpholino) approach was utilized to knockdown *bbs3* gene expression in zebrafish. Consistent with an eye specific role, knockdown of *bbs3L* results in mislocalization of the photopigment green cone opsin and reduced visual function, but not abnormalities of the Kupffer's vesicle or delays in intracellular trafficking of melanosomes, both cardinal features of BBS in the zebrafish. To dissect the individual functions of *BBS3* and *BBS3L*, *BBS3* or *BBS3L* RNA was co-injected with the *bbs3* morpholinos. *BBS3L* RNA, but not *BBS3* RNA, restores green opsin localization and vision. Moreover, only *BBS3* RNA is sufficient to rescue melanosome transport. Together these data demonstrate that *BBS3L* is necessary and sufficient for retinal function and organization.

This work was extended to humans by characterizing the A89V missense mutation in BBS3 identified in retinitis pigmentosa patients. To evaluate the *in vivo* function of the A89V missense mutation in non-syndromic retinal degeneration and BBS,

rescue experiments were performed in the zebrafish. Unlike *BBS3L* RNA, *BBS3L A89V* RNA does not rescue the vision defect seen with loss of *bbs3* in zebrafish; however, *BBS3 A89V* RNA suppresses melanosome transport delays. These data demonstrate that the mutation identified in patients with non-syndromic retinal degeneration is critical and specific for the vision defect.

Abstract Approved: _____
Thesis Co-Supervisor

_____
Title and Department

_____
Date

_____
Thesis Co-Supervisor

_____
Title and Department

_____
Date

ELUCIDATING A ROLE FOR BBS3 IN SYNDROMIC AND NON-SYNDROMIC RETINAL DISEASE

by

Pamela Reed Pretorius

A thesis submitted in partial fulfillment
of the requirements for the Doctor of
Philosophy degree in Genetics
in the Graduate College of
The University of Iowa

December 2010

Thesis Co-Supervisors: Professor Val C. Sheffield
Professor Diane C. Slusarski

Graduate College
The University of Iowa
Iowa City, Iowa

CERTIFICATE OF APPROVAL

_____

PH.D. THESIS

_____

This is to certify that the Ph.D. thesis of

Pamela Reed Pretorius

has been approved by the Examining Committee
for the thesis requirement for the Doctor of Philosophy
degree in Genetics at the December 2010 graduation.

Thesis Committee: _____
Val Sheffield, Thesis Co-Supervisor

_____
Diane Slusarski, Thesis Co-Supervisor

_____
Michael Anderson

_____
Robert Mullins

_____
Curt Sigmund

To my parents: Martin and Paula Gehring
To my husband: Andrew Pretorius
To my daughter: Katja Pretorius

You look at science (or at least talk of it) as some sort of demoralizing invention of man, something apart from real life, and which must be cautiously guarded and kept separate from everyday existence. But science and everyday life cannot and should not be separated. Science, for me, gives a partial explanation for life. In so far as it goes, it is based on fact, experience and experiment..

Rosalind Franklin
Letter to Ellis Franklin

ACKNOWLEDGMENTS

Although an individual does the writing of a thesis, I could never have completed this project without the support, guidance and efforts of numerous people. First, I would like to thank my co-mentors, Dr. Diane Slusarski and Dr. Val Sheffield for instilling in me the qualities of a good scientist. Thank you for your commitment to my training and for encouraging me to stretch my mind. I would also like to thank my committee members Dr. Michael Anderson, Dr. Robert Mullins and Dr. Curt Sigmund for their support and guidance through the years. To the Genetics program, thank you for providing this opportunity.

Additionally I extend my gratitude to the past and current members of the Slusarski and Sheffield labs. You have become a part of my extended family and our conversations have yielded many fruitful returns. A special thank you to Dr. Lisa Baye, Mr. John Beck and Svetha Swaminathan, you have been my partners in crime in the fish lab. Lisa, you have been not only a colleague but also friend, thank you.

Lastly, I would like to thank my family. Mom and dad, you have always encouraged me to reach for my goals and have never wavered in your support, even when I announced the move to Iowa. A special thank you to my husband Andrew, you are my rock. You constantly remind me of the important things in life, from everything to stopping to smell the flowers to spending time with family. Finally, to my daughter Katja, your smiles and giggles have provided me with endless moments of joy as I have assembled my thoughts into this thesis.

ABSTRACT

Hundreds of individually rare, but collectively common Mendelian disorders result in visual impairment. One of these disorders is a heterogeneous syndromic form of retinal degeneration, Bardet-Biedl Syndrome (BBS). This disease is an autosomal recessive disorder characterized by retinal degeneration, obesity, learning disabilities, congenital anomalies, and an increased incidence of hypertension and diabetes. Typically, individuals with BBS experience vision loss during childhood leading to blindness by the third decade of life. At least fourteen genes (*BBS1-BBS14*) are reported to individual cause BBS. This thesis focuses on one of these genes, *BBS3*, with the overall goal of characterizing the function of BBS3 in terms of both syndromic and non-syndromic retinal degeneration using the zebrafish and mouse model systems.

A member of the Ras family of small GTP-binding proteins, *BBS3* is postulated to play a role in vesicular transport. A second highly conserved transcript of *BBS3*, *BBS3L*, has been identified and is expressed predominantly in the mouse and zebrafish eye. The eye-specific expression of *BBS3L* facilitates the dissection of BBS function in the retina independent of alterations to other tissues. To this end, a *Bbs3L* knockout mouse was generated and histological analysis at 9 months reveals disorganization of the inner segments, indicative of early retinal degeneration. To further evaluate the functional effects of *BBS3* deficiency in the eye, an antisense oligonucleotide (Morpholino) approach was utilized to knockdown *bbs3* gene expression in zebrafish. Consistent with an eye specific role, knockdown of *bbs3L* results in mislocalization of the photopigment green cone opsin and reduced visual function, but not abnormalities of the Kupffer's vesicle or delays in intracellular trafficking of melanosomes, both cardinal features of BBS in the zebrafish. To dissect the individual functions of *BBS3* and *BBS3L*, *in vitro* transcribed wild-type human *BBS3* or *BBS3L* RNA was co-injected with the *bbs3* morpholinos. *BBS3L* RNA, but not *BBS3* RNA, restores green opsin localization and

vision. Moreover, only BBS3 RNA is sufficient to rescue melanosome transport, a cardinal feature of BBS in the zebrafish. *Bbs3L* knockout mice as well as a zebrafish *bbs3* knockdown model demonstrate that BBS3L is both necessary and sufficient for retinal function and organization.

This work was extended to humans by characterizing the A89V missense mutation in BBS3 that results in non-syndromic retinal degeneration. To evaluate the *in vivo* function of the A89V missense mutation in non-syndromic retinal degeneration and BBS, rescue experiments were performed in the zebrafish. Unlike wild-type *BBS3L* RNA, *BBS3L A89V* RNA does not rescue the vision defect seen with loss of *bbs3* in zebrafish; however, *BBS3 A89V* RNA is able to suppress the cardinal zebrafish BBS phenotype of melanosome transport, similar to wild-type *BBS3* RNA. These data demonstrate that the *BBS3L A89V* mutation identified in patients with non-syndromic retinal degeneration is critical and specific for the vision defect.

TABLE OF CONTENTS

LIST OF TABLES

LIST OF FIGURES

LIST OF ABBREVIATIONS

ARF	ADP-ribosylation factor
ARL	ADP-ribosylation like factor
BBS	Bardet-Biedl Syndrome
CEP290	Centrosomal protein 290
CNV	Copy number variation
CO-IP	Co-immunoprecipitation
CRX	Cone-rod homeobox
DPC	Days post coitus
DPF	Days post fertilization
EST	Expressed sequence tagged
HPF	Hours post fertilization
IFT	Intraflagellar transport
IS	Inner segment
JBTS	Joubert Syndrome
KV	Kupffer's vesicle
LCA	Leber congenital amaurosis
MARK3	Microtubule affinity-regulating kinase 3
MKKS	McKusick-Kaufman Syndrome gene (also known as *BBS6*)
MKS	Meckel-Gruber Syndrome
MO	Morpholino
NPH	Nephronophthisis
ONL	Outer nuclear layer
OS	Outer segment
PCM-1	Pericentriolar material 1
PNA	Peanut agglutin

PTU	Phenylthiourea
RP	Retinitis pigmentosa
RPE	Retinal pigmented epithelium
RT-PCR	Reverse Transcriptase Polymerase Chain Reaction
SLS	Senior-Loken Syndrome
SNP	Single nucleotide polymorphism
TRIC	Tailless complex polypeptide ring complex
TRIM32	Tripartite motif 32
TRP	Tetratricopeptide repeat
WHO	World health Organization
Wt	Wild-type

CHAPTER I

INTRODUCTION

Visual impairment and blindness have far reaching implications for society. Hundreds of individually rare, but collectively common Mendelian disorders can cause blindness. One of those disorders is a heterogeneous syndromic form of retinal degeneration, Bardet-Biedl Syndrome (BBS, OMIM 209900). Although there is variability in the ocular phenotype between individuals, BBS patients typically present with early and progressive photoreceptor degeneration, leading to both central and peripheral vision loss by the third decade of life (Riise 1987; Leys et al. 1988; Green et al. 1989; Jacobson et al. 1990; Fulton et al. 1993; Carmi et al. 1995a; Beales et al. 1997; Riise et al. 1997; Sheffield 2004; Heon et al. 2005b). Retinitis pigmentosa (RP) is a disorder of retinal degeneration resulting in blindness through the degeneration of rod and cone photoreceptors (Harnett et al. 1988; Green et al. 1989; Bardet 1995; Biedl 1995). To date, there are no effective therapies to delay or arrest retinal degeneration, thus placing a large burden on affected families and on society as a whole. Thus, by understanding the molecular and biological processes controlling retinal degeneration in BBS a better understanding can be had about the complex inheritance of retinal degeneration seen in the general population.

Clinical features of BBS

Bardet-Biedl Syndrome (BBS, OMIM 209900) is a genetically heterogeneous disorder that largely displays an autosomal recessive pattern of inheritance. In the early 1920s, two independent reports by George Bardet and Arthur Biedl gave the first discrete clinical descriptions of this disorder (Bardet 1995; Biedl 1995). This pleiotropic disorder is characterized by retinal degeneration, obesity, polydactyly, renal abnormalities, hypogenitalism and cognitive impairment (Harnett et al. 1988; Green et al. 1989; Bardet 1995; Biedl 1995). In addition, BBS is also associated with an increased susceptibility to

hypertension, diabetes mellitus and heart defects (Harnett et al. 1988; Green et al. 1989; Elbedour et al. 1994). The presence of inter- and intrafamilial phenotypic variation in BBS adds to the complexity of this disorder (Riise et al. 1997; Moore et al. 2005). The greatest phenotypic variability is seen with regards to the degree of obesity, mental retardation and polydactyly. A study conducted on 32 patients from Newfoundland with BBS demonstrated that while all the patients presented with severe retinal degeneration, only two had typical retinitis pigmentosa (Green et al. 1989).

Several minor features not considered to be part of the diagnostic criteria have also been associated with BBS patients. A prospective cohort study conducted in Newfoundland followed 46 BBS patients over 22 years. This study reported a higher incidence of asthma, with hospitalization being required in 68% of the cases (Moore et al. 2005). Several reports of anosmia have also been reported in individuals with BBS (Kulaga et al. 2004; Iannaccone et al. 2005). Although rare, incidences of *situs inversus*, Hirschprung disease, hearing loss, colonic disorders, hypothroidism and chronic serous otitis media have been associated with BBS (Beales et al. 1999; Ansley et al. 2003; Moore et al. 2005; Deffert et al. 2007).

The pleiotropic nature of BBS means that there are both phenotypic as well as genetic overlap with other disorders, often having implications for clinical diagnosis. Impairment of vision and kidney function are phenotypes observed across a range of disorders, due to defects in photoreceptor and renal cilia. The most severe of the overlapping diseases, Meckel-Gruber Syndrome (MKS) is a lethal disorder characterized by encephalocele, polycystic kidneys and polydactyly (Mecke and Passarge 1971). Hypomorphic mutations in *MKS1* have also been associated with BBS (Leitch et al. 2008). McKusick-Kaufmann Syndrome (MKKS) and Joubert Syndrome (JBTS) are both severe pleiotropic disorders that overlap with BBS. An autosomal recessive disorder, MKKS is characterized by postaxial polydactyly, congenital heart defects and hydrometrocolpos (Robinow and Shaw 1979; Stone et al. 2000). Mutations in the *MKKS*

gene were found to cause BBS in some instances (Slavotinek et al. 2000; Stone et al. 2000). JBTS is also an autosomal recessive disorder characterized by retinal dystrophy, renal disease and developmental delay; however, patients present with a molar tooth sign, a malformation of the midbrain-hindbrain, on MRI imaging, setting this disorder apart from BBS (Valente et al. 2008; Brancati et al. 2010). Three other disorders, Senior-Loken Syndrome (SLS), nephronophthisis (NPH) and Leber congenital amaurosis (LCA), present with milder phenotypes and impact fewer organs. The primary features of SLS include retinopathy and nephronophthisis (Loken et al. 1961; Senior et al. 1961). NPH and LCA are the least severe of the disorders overlapping with BBS and result in cystic kidneys and retinopathy, respectively. Interestingly, one gene centrosomal protein 290 (*CEP290),* has been implicated in BBS, JBTS, NPH and LCA further highlighting the extensive overlap between these disorders (den Hollander et al. 2006; Valente et al. 2006; Helou et al. 2007; Leitch et al. 2008).

BBS genetic heterogeneity

BBS displays an autosomal recessive pattern of inheritance, yet is genetically heterogeneous. The genetically heterogeneous nature of BBS was first described in three consanguineous tribes from an isolated Bedouin population in the Negev Region of Israel (Kwitek-Black et al. 1993; Sheffield et al. 1994; Carmi et al. 1995b). The high rate of consanguinity in this population resulted in an increased frequency of the recessive allele. To date, fourteen BBS loci have been identified (Katsanis et al. 2000; Slavotinek et al. 2000; Mykytyn et al. 2001; Nishimura et al. 2001; Mykytyn et al. 2002; Ansley et al. 2003; Badano et al. 2003a; Chiang et al. 2004; Fan et al. 2004; Li et al. 2004; Nishimura et al. 2005; Chiang et al. 2006; Stoetzel et al. 2006b; Stoetzel et al. 2007). Patients with BBS display variable expressivity and it is possible that this variability is a result of genetic modifiers. Perhaps some of these modifiers could be BBS genes themselves or aid in the identification of additional BBS genes.

Despite the identification of fourteen *BBS* genes, approximately 25-30% of the clinically diagnosed BBS families do not have a mutation in any of the fourteen known BBS genes, suggesting that additional disease genes remain to be identified (Stoetzel et al. 2006b; Stoetzel et al. 2007). Both *BBS1* and *BBS10* are reported to be the most commonly mutated loci (Mykytyn et al. 2002; Stoetzel et al. 2006b; Sapp et al. 2010). More recently, mutations in *BBS6, BBS10* and *BBS12* were reported to be disease causing in 36.5% of BBS patients of multiethnic origin (Billingsley et al. 2010). The rare nature of BBS means that many of the genes, such as *BBS3, BBS7* and *BBS8,* account for a small portion of the mutational load (Ansley et al. 2003; Badano et al. 2003a; Chiang et al. 2004; Fan et al. 2004; Stoetzel et al. 2006a; Bin et al. 2009; Pereiro et al. 2010). In some instances, only a single family (*BBS11* and *BBS14*) is associated with the disease (Chiang et al. 2006; Leitch et al. 2008).

Although BBS inheritance is autosomal recessive, a few reports have described pedigrees suggesting oligogenic inheritance. In these cases, two BBS loci are affected, whereby the patient is homozygous or compound heterozygous for mutations at the first BBS locus, and heterozygous at a second BBS locus to manifest the disease. This pattern of inheritance is termed triallelism as three alleles are affected. In the seminal study, a phenotypically normal individual carries two *BBS2* nonsense mutations, while the affected sibling carries the same nonsense mutations in *BBS2* but also has a nonsense mutation in *BBS6* (Katsanis et al. 2001). In a second study, an affected individual was found to carry a homozygous missense mutation in *BBS2* and *BBS4,* while the unaffected siblings and mother carried a homozygous *BBS2* mutation and a heterozygous *BBS4* mutation (Katsanis et al. 2002). In contrast, Mykytyn *et al.* evaluated a cohort of 43 unrelated BBS patients with two mutant *BBS1* alleles for triallelism and did not identify any additional disease causing mutations in *BBS2, BBS4* or *BBS6* (Mykytyn et al. 2003). Thus, in this instance it can be concluded that homozygous *BBS1* mutations are sufficient for disease penetrance. An independent study screened a cohort of 27 BBS patients and

found no evidence of triallelic inheritance; however, a preponderance of heterozygous mutations were observed, consistent with complex inheritance (Hichri et al. 2005). A similar study was undertaken in 19 consanguineous Tunisian families diagnosed with BBS and no evidence of triallelism was detected in the eight BBS genes screened (Smaoui et al. 2006). Screening of an Amish family with MKS identified three affected children with homozygous mutations in BBS6. Interestingly, while the father was a carrier the mother had the same homozygous mutation as the children, however, she did not manifest the disease (Nakane and Biesecker 2005). More recently, *BBS1*, *BBS2*, *BBS4*, *BBS6*, *BBS10* and *BBS12* were screened for mutations in 49 unrelated BBS patients. While this study identified eight patients with variations in three alleles, no solid data was presented in support of triallelism (Hjortshoj et al. 2010). Some families demonstrate inheritance in a triallelic manner; however, the potential pathogenesis of triallelic mutations is still not clear and consequently, requires further evaluation.

Inter- and intrafamilial phenotypic variation is observed in BBS patients, whereby the disorder manifests differently in patients with the same mutation (Riise et al. 1997; Moore et al. 2005). This suggests that there are modifiers of the BBS phenotype. While modifiers could be known BBS genes, they could also be genes that when mutated do not give rise to the BBS phenotype. Three families have been described in which two mutations were found in either *BBS1* or *BBS2* and a third mutation was identified in either *BBS1*, *BBS2* or *BBS6* (Badano et al. 2003a). In this instance, the third mutation results in increased symptom severity and earlier onset and thus epistatically affects the locus with two mutations. A second example of epistatic effect was identified when heterozygous mutations in the non-BBS gene, *MGC1203* (also known as *CCDC28B*), were found to enhance the effect of *BBS1* homozygous mutations (Badano et al. 2006). Together, these studies suggest that mutations at a second locus can modify the BBS phenotype.

Proposed etiology of BBS

Although BBS is rare in the general population, several components of the BBS phenotype, such as retinal degeneration and obesity, are quite common. These phenotypes involve cilia dysfunction in a range of tissues, including, the retina and brain (Mykytyn et al. 2004; Nishimura et al. 2004; Fath et al. 2005; Davis et al. 2007). Moreover, eight highly conserved BBS protein homologues (BBS1, BBS2, BBS3, BBS4, BBS5, BBS7, BBS8 and BBS9) are found in ciliated organisms, but not in non-ciliated organisms (Avidor-Reiss et al. 2004; Chiang et al. 2004; Li et al. 2004; Mykytyn et al. 2004). As a result there has been substantial interest in understanding the pathophysiology underlying BBS. The use of animal models, including mouse, zebrafish, *Caenorhabditis elegans* and *Chlamydomonas,* has provided insight into the functions of BBS genes in both cilia function as well as intraflagellar and/or intracellular transport (Ansley et al. 2003; Blacque et al. 2004; Fan et al. 2004; Kim et al. 2004; Kulaga et al. 2004; Li et al. 2004; Nishimura et al. 2004; Fath et al. 2005; Chiang et al. 2006; Yen et al. 2006). In *Caenorhabditis elegans bbs7* and *bbs8* genetic mutants have ciliary structural defects, including shorter cilia and impaired chemosensation (Blacque et al. 2004). Moreover, *bbs7* and *bbs8* are required for normal localization of the intraflagellar transport (IFT) proteins, IFT88 and IFT80 (Blacque et al. 2004). RNA interference (siRNA) of *BBS5* in *Chlamydomonas* leads to either the partial formation or complete absence of the flagella (Li et al. 2004).

Cilia

An ancient, evolutionarily conserved structure, the cilia projects from the cell surface of most eukaryotic cells. Although ubiquitously present in vertebrate cells, cilia are restricted to sensory neurons in invertebrates (Wheatley et al. 1996). Moreover, cilia are involved in diverse biological roles, including cell motility, movement of fluid, chemosensation, photosensation and mechanosensation (Evans et al. 2006). The

structure of the cilium is composed of a nine microtubule doublet core arranged around a central core (axoneme) (Haimo and Rosenbaum 1981). In the case of motile cilia (9+2), the microtubule doublets are arranged around two central microtubules linked by dynein arms. Non-motile cilia (9+0) lack these central microtubules as well as connecting dynein arms. At the tip of the cilia, the axonemal microtubules and ciliary membrane are linked by a complex of microtubule capping structures (Sloboda 2005). Located at the base of the cilia is the transition zone, which in conjunction with the basal body regulates the transport of molecules into and/or out of the cilium (Bisgrove and Yost 2006).

Intraflagellar and intracellular transport

During cilia formation, new axonemal subunits are added to the distal tip, resulting in elongation of the cilia from the basal body. As protein synthesis does not occur in the cilia, the components of the cilia must be transported along the microtubules by means of intraflagellar transport (IFT) (Kozminski et al. 1993). Microtubules of the axoneme are oriented with their minus-end toward the basal body and their plus-end toward the distal tip of the cilia. The microtubule-based molecular motors move in only one direction and thus require specialized microtubule motors to mediate bidirectional movement along the axonemal microtubule. A plus-end directed motor, kinesin 2 drives anterograde transport toward the distal tip. Once the motor reaches the tip, a transition from anterograde to retrograde trafficking occurs. Cytoplasmic dynein 1B is a minus-end directed motor, facilitating retrograde movement (Cole et al. 1993; Pazour et al. 1998; Signor et al. 1999). These motors associate with IFT particles, which consist of two complexes, A and B (Cole et al. 1998; Piperno et al. 1998). The IFTA complex is essential for retrograde transport, while the IFTB complex functions in anterograde transport.

In comparison to IFT, intracellular transport involves the transport of cargos or organelles along cytoskeletal tracks (kinesins and dyneins along microtubules and

myosins along actin) (Brady et al. 1982; Kozminski et al. 1993; Vale 2003). Similar to IFT, the kinesin motor and cytoplasmic dynein motor are responsible for anterograde and retrograde transport along the microtubule, respectively. Intracellular transport also relies on an additional motor, myosin V to transport along actin (Rogers and Gelfand 1998; Tabb et al. 1998). Cargos of intracellular transport include membrane bound organelles (such as the Golgi) and secretory and endocytic vesicles (Goldstein 2001; Vale 2003). While there are several similarities between IFT and intracellular transport, one major difference does exist. Intracellular transport requires that the cargos be membrane-bound, while in IFT non-membrane bound cargos are transported (Goldstein 2001; Vale 2003).

BBS proteins and their function in cilia

Although mutations in any of the 14 BBS genes cause similar phenotypes, domain prediction analysis of BBS proteins demonstrates that for the most part, BBS proteins do not belong to the same functional protein family (Table 1). Moreover, there is still much to be learned about the molecular basis of this disorder and the precise function of each of the BBS proteins.

The BBSome, a complex of BBS proteins

BBS1, BBS2, BBS5 and BBS7 are novel proteins and show no significant homology to any proteins of known function (Nishimura et al. 2001; Mykytyn et al. 2002; Badano et al. 2003a; Li et al. 2004). BBS7 was identified through shared structural features with BBS1 and BBS2. Both BBS2 and BBS7 contain WD40-like repeat domains and coiled-coil domains, while BBS1 harbors only a coiled-coil domain, which are typically involved in protein interactions (Badano et al. 2003a). BBS4 and BBS8 both contain tetratricopeptide repeat (TPR) domains, which may also mediate different protein-protein interactions (Blatch and Lassle 1999). In cell culture, two pools of BBS4 have been identified. The first pool was identified in the centriolar satellites, where it

interacts with a component of the centriolar satellites, PCM-1 (pericentriolar material 1), as well as $p150^{glued}$, a component of the dynein transport machinery (Kim et al. 2004). The second pool of BBS4 was found inside primary cilia, where it functions in the absence of PCM-1 (Nachury et al. 2007). Taken together, BBS4 functions as a bridge to bring components to the centrosome via interactions with PCM-1, as well as to influence transport inside the cilia. Only one BBS gene, BBS9 (also known as B1, parathyroid hormone-responsive protein) does not appear to contain any known functional domains (Adams et al. 1999).

Recently, seven of the BBS proteins were identified in stoichiometric amounts in a complex termed the BBSome. Using tandem affinity purification of mouse testis, BBS1, BBS2, BBS4, BBS5, BBS7, BBS8 and BBS9 were found to form a 470kDA protein complex that binds to PCM-1 (Nachury et al. 2007). Moreover, the BBSome was found to localize to non-membranous centriolar satellites in the cytoplasm, as well as the cilia membrane (Figure 1) (Nachury et al. 2007). Rabin8, the GTP exchange factor for Rab8 was found to associate with the BBSome at the basal body. Recruitment of the BBSome to the basal body leads to the activation of Rab8 and ultimately cilia biogenesis (Nachury et al. 2007). The presence of these proteins in equal stoichiometric amounts may help to explain the non-allelic heterogeneity observed in BBS patients. As mentioned previously, triallelic inheritance, where patients harbor three mutations in two BBS genes, has been reported in a few BBS cases (Katsanis et al. 2001; Katsanis et al. 2002; Badano et al. 2003b; Beales et al. 2003; Katsanis 2004; Laurier et al. 2006). It has been suggested that the third allele could modify the penetrance or severity of the BBS phenotype. Thus one could hypothesize that having mutations in more than one subunit of the BBSome would have a greater impact on the stoichiometry and biochemical stability of the complex and lead to a more severe phenotype.

BBS3 and its role with the BBSome

BBS3, ADP-ribosylation like factor 6 (ARL6) is a member of the Ras superfamily of small GTP-binding proteins, which is subdivided into ADP-ribosylation factor (ARF) and ARF-like (ARL) subgroups (Pasqualato et al. 2002). Recent work indicates that ARFs and ARLs play a role in the movement of components within the cilia (Takai et al. 2001; Hori et al. 2008; Borovina et al. 2010; Li et al. 2010) . ARF GTPases are well characterized and function in membrane-trafficking pathways as well as regulation of the budding and formation of vesicles through the recruitment of adaptor proteins and/or complexes to the endocytic and exocytic pathways (Memon 2004; Kahn et al. 2006). Although ARL GTPases were identified on the basis of their similarity to ARF proteins, their precise cellular function is largely unknown; however, it has been proposed that ARL proteins play a role in membrane and/or vesicular trafficking as well as organization of the cytoskeleton (Pasqualato et al. 2002; Kahn et al. 2006). Arl2 has been shown to play a role in regulating tubulin folding as well as maintaining microtubule integrity (Bhamidipati et al. 2000; Radcliffe et al. 2000; Antoshechkin and Han 2002). This suggests, that while ARLS may function in trafficking they may also play a role in microtubule dynamics.

One particular ARL protein, ARL6 (also known as BBS3) was initially identified in a J2E erythroleukemia cell line and was proposed to play a role in hemopoietic development (Ingley et al. 1999). The expression pattern of BBS3 was assessed in a bbs3 transgenic *C. elegans* model (*arl-6p::gfp*). GFP signal was observed in the ciliated sensory cells, as well as the ciliated head neurons (Fan et al. 2004). Since ARLs are proposed to have a role in trafficking, time lapse imaging was performed and movement of the GFP tagged bbs3 protein along the ciliary axoneme observed (Fan et al. 2004). Interestingly, movement of BBS3 occurred in both the anterograde and retrograde direction (Fan et al. 2004). This indicates that BBS3 is important for trafficking along the ciliary axoneme. A dynamic pattern of expression was observed for *ARL6* during

early mouse development. *ARL6* mRNA localized around the node, which plays a role in establishing the basic body plan of the embryo, of 7.0-7.5 day post coitum (dpc) mice as well as the neural plate of 8.5 dpc mice (Takada et al. 2005). Thus indicating a role for *ARL6* in early mouse development.

While BBS3 was not identified as a member of the BBSome, its conservation and expression pattern is most similar to that seen with BBSome proteins, highlighting a potential role for BBS3 in ciliogenesis and transport. An additional question that remains is whether loss-of-function of BBS3 affects the BBSomes formation and/or its ability to traffic properly. Co-immunoprecipitation (Co-IP) with BBS2 on testis tissue from wild-type and *Bbs3*$^{-/-}$ mice demonstrates that the BBSome still forms in *Bbs3* null mice (Qihong Zhang observation). Moreover, using sucrose gradient centrifugation, and antibodies against BBS1, 2, 3, 4, 7 and 9 confirms that the size of the BBSome is unaltered with loss of Bbs3, indicating that all components of the BBSome are present (Qihong Zang observation). Knockdown of BBS3 in retinal pigmented epithelium (RPE) cells prevents localization of the BBSome subunits BBS1, BBS8, BBS9 and BBIP10 to the cilium (Jin et al. 2010) (Qihong Zang observation). This indicates that while *BBS3* is not a direct member of the BBSome, it does play a role in targeting this complex to the cilia and may aid in the transport of BBSome cargos. Finally, our lab has identified a second transcript of *BBS3*, *BBS3L*, and has demonstrated that the BBS3L protein product plays an important role in eye structure and function in both the zebrafish and mouse (Chapter 2).

A complex of three chaperonin-like BBS proteins

Three proteins, BBS6, BBS10 and BBS12, are predicted to have chaperonin function and share sequence homology to the chaperonin containing TCP1 family (CCT). All three are members of the type II chaperonin superfamily and contain chaperonin domains (Stone et al. 2000; Stoetzel et al. 2006b; Stoetzel et al. 2007). BBS6, also

known as MKKS, was the first BBS gene identified (Slavotinek et al. 2000; Stone et al. 2000). High homology was observed between BBS6 and the alpha subunit of the *Thermoplasma acidophilum* thermosome, a prokaryotic chaperonin complex (Stone et al. 2000). Interestingly, both proteins have structural similarities to an eukaryotic chaperonin called tailless complex polypeptide ring complex (TriC), a chaperonin involved in the folding of many proteins including tubulin and actin (Frydman et al. 1992). Since the identification of BBS6, two additional proteins, BBS10 and BBS12 have been identified with predicted chaperonin function. BBS10 differs from both BBS6 and BBS12 in that it contains a functional hydrolysis motif, GDGTT[T/S], that is specific to group II chaperonins (Stoetzel et al. 2006b). The presence of this catalytic domain indicates that BBS10 might be an active enzyme (Stoetzel et al. 2006b).

Although not direct components of the BBSome, BBS6, BBS10 and BBS12 form a complex with six CCT proteins (CCT1-5, CCT8) (Seo et al. 2010). The BBS/CCT complex functions by binding to BBS7 (and possible BBS2), a core component of the BBSome, to mediate the association the other BBSome subunits (BBS1, BBS4, BBS5, BBS8 and BBS9) (Seo et al. 2010). Knockdown of CCT proteins using siRNA in HEK293T cells results in reduced association of BBS2 and BBS7 with BBS9, thus the CCT proteins are necessary for BBSome assembly (Seo et al. 2010).

Unincorporated BBS genes

BBS11 or TRIM32 (tripartite motif–containing gene 32) is a member of the TRIM protein family, which is characterized by a RING-finger, a B-Box and a coiled-coil motif. Prior to the association of BBS with a mutation in the B-Box domain, TRIM32 was associated with limb-girdle muscular dystrophy type-2H. A point mutation (D487N) in the highly conserved C-terminal NHL domain is responsible for the muscular dystrophy phenotype (Frosk et al. 2002). It was demonstrated that TRIM32 is an E3 ubiquitin ligase capable of ubiquinating actin (Kudryashova et al. 2005).

Hypomorphic mutations that either cause BBS or have an epistatic effect on the disease have been associated with MKS1 (BBS13) and CEP290 (BBS14) (Leitch et al. 2008). Null mutations in either one of these genes have been previously associated with a more severe cilia disorder, Meckel-Gruber Syndrome (MKS) (Kyttala et al. 2006; Baala et al. 2007; Frank et al. 2008). CEP290 (centrosomal protein 290) is a large gene consisting of multiple domains. The presence of 13 putative coiled-coil domains suggests that this protein mediates interactions between a wide range of gene products explaining its involvement in multiple disorders (Sayer et al. 2006). In contrast, MKS1 encodes a B9 domain whose function is poorly understood (Kyttala et al. 2006)

The association of ten BBS proteins into two different complexes has helped reduce the functional complexity of BBS, but it has raised additional questions as to the role of the remaining non-BBSome proteins. While it is unclear what role BBS11 plays with either of these complexes, it is possible that this E3 ubiquitin ligase interacts transiently with the BBSome to regulate degradation of the complex. BBS3, which shows a conservation pattern similar to that of BBSome proteins, assists in trafficking of the BBSome to the cilia. Additionally, *BBS3* has been implicated in cilia formation and/or function and may play a key role in transport of molecules critical for the proper maintenance of photoreceptors.

Vision, cilia and BBS

BBS is a heterogeneous syndromic form of retinitis pigmentosa (RP), a retinal disease characterized by the degeneration of rod and cone photoreceptors. The retina is located at the back of the eye and consists of seven alternating layers of cells and processes. It is the responsibility of the retina, more specifically the rod and cone photoreceptors, to convert the light signal into a neural signal that can be relayed to the brain via the axons of the ganglion cells. Although there is variability in the ocular phenotype between individuals, BBS patients typically present with early and progressive

photoreceptor degeneration that results in both central and peripheral vision loss by the third decade of life (Riise 1987; Leys et al. 1988; Green et al. 1989; Jacobson et al. 1990; Fulton et al. 1993; Carmi et al. 1995a; Beales et al. 1997; Riise et al. 1997; Heon et al. 2005b). Variability in the ocular components of BBS was found in a study conducted on 34 affected Bedouin individuals harboring mutations in *BBS2*, *BBS3* or *BBS4* (Heon et al. 2005b). In all cases, RP was found to be early-onset and severe, while myopia was found to be associated with BBS3 and BBS4, but not the BBS2 cohort (Heon et al. 2005b). Thus, by understanding the molecular and biological processes controlling retinal degeneration in BBS a better understanding can be had about the complex inheritance of retinal degeneration seen in the general population.

The vertebrate retina contains photoreceptors, highly polarized cells with a modified cilium (connecting cilium) that joins the photosensitive outer segment (OS) to the protein synthesizing inner segment (IS). As the OS is incapable of protein synthesis all proteins required for phototransduction as well as structural components must be synthesized in the IS. The connecting cilium transports cellular components from the IS to the OS that are necessary for the structure and function of the OS (Young 1967; Besharse and Horst 1990). A non-motile cilia, the connecting cilium has a microtubule backbone (axoneme) which is anchored in the IS by the basal body (Rohlich 1975; Besharse and Horst 1990). The photoreceptor OS is often referred to as a modified cilium due to the fact that the axoneme extends almost the entire length of the OS. Transport of cargo is required through the lifetime of the photoreceptor cell as approximately 10% of the OS distal tip is shed daily (Luby-Phelps et al. 2008).

IFT proteins are important in this intraphotoreceptor transport process as they play a key role in both assembly and maintenance of photoreceptor cells (Pazour et al. 2002; Krock and Perkins 2008; Luby-Phelps et al. 2008). Using *Xenopus leavis* photoreceptors, IFT proteins were shown to be abundant in the basal body region and the IS as well as distributed along the OS axoneme (Luby-Phelps et al. 2008). Loss of IFT

genes in vertebrates leads to abnormal OS development, retinal degeneration and mislocalization of photopigments (Pazour et al. 2002; Tsujikawa and Malicki 2004; Sukumaran and Perkins 2009). *Ift88* mutant mice have aberrantly stacked OS disk membranes as well as an accumulation of opsin in the IS (Pazour et al. 2002). The accumulation of photopigment in the IS eventually becomes toxic to the cell and leads to photoreceptor cell death. Zebrafish mutants for i*ft88* and *ift172* fail to form connecting cilium, while *ift57* mutants have shorter OS compared to wild-type (Krock and Perkins 2008; Sukumaran and Perkins 2009). Retina phenotypes observed in *Bbs-null* mice are similar to those seen with loss of IFT genes, suggesting that BBS proteins play a role in transporting proteins through the connecting cilium into the OS of the photoreceptor.

Animal models

Mus musculus

Analysis of BBS knockout mice (*Bbs2*$^{-/-}$, *Bbs4*$^{-/-}$ and *Bbs6*$^{-/-}$) reveals that these mice have major components of the human phenotype including blindness, obesity, renal cysts and neurological deficits (Mykytyn et al. 2004; Nishimura et al. 2004; Fath et al. 2005). Additionally, absence of a BBS protein prevents the formation of flagella during spermatogenesis, however; these knockout mice do develop other motile cilia, as well as, a modified primary cilia in the photoreceptor. Characterization of the retinal phenotype in *Bbs1-knockin, Bbs2*, *Bbs4* and *Bbs6-null* mice has demonstrated that photoreceptors initially form; however, the cells subsequently show a mislocalization of the photopigment rhodopsin and undergo progressive photoreceptor degeneration (Mykytyn et al. 2004; Nishimura et al. 2004; Fath et al. 2005; Abd-El-Barr et al. 2007; Davis et al. 2007). Work with two independently generated *Bbs4-null* mice indicates that Bbs4 plays an important role in establishing both correct structure as well as proper transport of phototransduction proteins (Abd-El-Barr et al. 2007; Swiderski et al. 2007). Interestingly, the photoreceptor degeneration observed in these mice is not a result of

structural defects to the connecting cilium or basal body, but rather the degeneration is a result of disrupted IFT between the IS and OS (Abd-El-Barr et al. 2007). This data would suggest that *Bbs4* is important for the transport of phototransduction proteins, but not for maintaining structural integrity. In an independently generated *Bbs4* knockout mouse increased expression of the stress response genes, *Edn2*, *Lcn2*, *Serpina3n* and *Socs3* was observed in 4 week old mice prior to gross retinal damage (Swiderski et al. 2007). The increased expression of four stress response genes indicates that the retina is undergoing changes prior to the appearance of gross morphological changes. Taken together, these data strongly support a role for BBS proteins in intracellular transport and cilia; thus further substantiating a critical role for BBS genes in the modified photoreceptor cilium for cell maintenance and function.

Danio rerio

Work pioneered by two prior Graduate students in the lab, David Yen and Marwan Tayeh, established the zebrafish as a model for BBS. This system utilizes a morpholino antisense oligonucleotide (MO) approach to transiently knockdown *bbs* gene expression in the zebrafish embryo. Knockdown of *bbs* function in zebrafish generates two prototypical defects: reduction of the size of the Kupffer's vesicle (KV) as well as retrograde transport defects (Chiang et al. 2006; Yen et al. 2006; Tayeh et al. 2008). The KV is a transient ciliated structure readily observed in the tail bud region in early somite stage zebrafish embryos; approximately 12 hours post fertilization (hpf) (Essner et al. 2002). Loss of *bbs* genes results in a reduction of KV size to less than the width of the notochord (Chiang et al. 2006; Yen et al. 2006; Tayeh et al. 2008).

The second prototypical phenotype observed in bbs morphants is delayed trafficking of the melanosome. Zebrafish are able to alter their skin pigmentation by intracellular trafficking of melanosomes within melanophores in response to light and hormonal stimuli (Marks and Seabra 2001; Blott and Griffiths 2002; Skold et al. 2002;

Barral and Seabra 2004). A lysosome-related organelle, the melanosome can be shuttled bidirectionally between the cell periphery and the perinuclear region. Dispersal of the melanosomes to the cell periphery (i.e. anterograde movement) is kinesin directed, while dynein is responsible for the retraction of the melanosomes to the perinuclear region (i.e. retrograde movement) (Marks and Seabra 2001; Blott and Griffiths 2002; Barral and Seabra 2004). Epinephrine treatment triggers a rapid melanosome aggregation in melanocytes, and can be used to evaluate the effect of gene knockdown on cellular trafficking (Wu and Hammer 2000). Typically, stimulating 5-day-old embryos with epinephrine results in melanosome transport within 1.5 minutes while knockdown of *bbs* genes results in statistically significant delay in melanosome transport (Chiang et al. 2006; Yen et al. 2006; Tayeh et al. 2008).

Aims

The purpose of this study was to evaluate the pathophysiology underlying the retinal degeneration observed in Bardet-Biedl Syndrome with respect to *BBS3*. Both the mouse and zebrafish have been established as models for BBS and it is these systems that were used to unravel both the cellular and molecular mechanisms of retinal degeneration in BBS. Knockout mouse lines (*Bbs2*$^{-/-}$, *Bbs3*$^{-/-}$, *Bbs4*$^{-/-}$, *Bbs6*$^{-/-}$), as well as a knockin line (*Bbs1*$^{M390R/M390R}$), have been generated and all recapitulate the human BBS phenotype of retinal degeneration. Interestingly, death of the photoreceptors is preceded by mislocalization of rhodopsin, suggesting that there is a defect in intracellular transport in *Bbs* mutant mice. Thus, these models of BBS offer an opportunity to further study the mechanism underlying photoreceptor cell death. To gain insight into the pathophysiology of BBS, the function of BBS3 in terms of both syndromic and non-syndromic retinal degeneration wias characterized. Specifically this project aimed to: 1. Dissect apart the individual functions of *BBS3*, the canonical *BBS3* transcript, and *BBS3L*, the evolutionarily conserved eye specific transcript, using both the zebrafish and

mouse model systems. This was accomplished by characterizing *BBS3L*, which is unique among BBS gene products as it is expressed predominantly in the eye, suggesting a specialized role in vision. 2. Extend this work to human disease through the characterization of the BBS3 A89V missense mutation that results specifically in non-syndromic retinal degeneration.

Table 1 Predicted protein domains of the fourteen BBS genes

Protein	Chromosomal location	Predicted Protein Domain and/or Family
BBS1	11q13	ß-propeller repeats
BBS2	16q21	ß-propeller repeats
BBS3	3p12-q13	ADP-ribosylation factor like GTPase
BBS4	15q22.3	Tetratricopeptide repeat
BBS5	2q31	Pleckstrin homology domains
BBS6	20p12	Chaperonin
BBS7	4q27	ß-propeller repeats
BBS8	14q32.11	Tetratricopeptide repeat
BBS9	7p14	Parathyroid hormone-responsive B1
BBS10	12q	Chaperonin
BBS11	9q33.1	E3 ubiquitin ligase
BBS12	4q27	Chaperonin
BBS13	17q23	B9 domain
BBS14	12q21.3	Coiled-coil domains

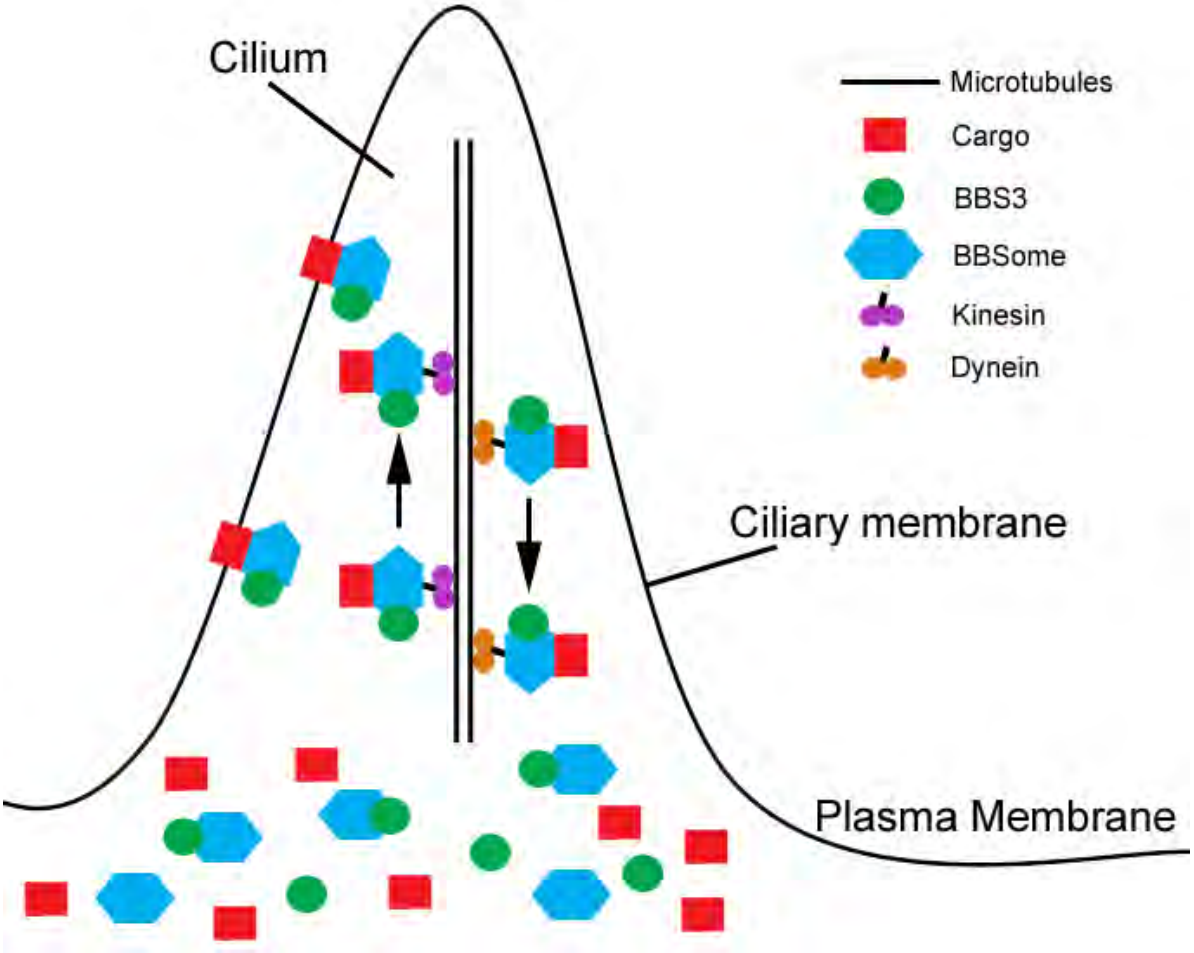

Figure 1 Model for the function of the BBSome. Cilia schematic depicting a model for the function of the BBSome in the targeting of cargo molecules along and/or within the cilia. BBS3 may work to recruit the BBSome and aid in the transport of these cargos.

CHAPTER II

IDENTIFICATION AND FUNCTIONAL ANALYSIS OF THE VISION SPECIFIC BBS3 (ARL6) LONG ISOFORM

Introduction

Bardet-Biedl Syndrome (BBS, OMIM 209900) is a pleiotropic disorder characterized by retinal degeneration, obesity, polydactyly, renal abnormalities, hypogenitalism and cognitive impairment (Harnett et al. 1988; Green et al. 1989; Bardet 1995; Biedl 1995). Additionally, there is an increased incidence of hypertension, diabetes mellitus and heart defects in BBS patients (Harnett et al. 1988; Green et al. 1989; Elbedour et al. 1994). Although there is variability in the ocular phenotype between individuals, BBS patients typically present with early and progressive photoreceptor degeneration, leading to both central and peripheral vision loss by the third decade of life (Riise 1987; Leys et al. 1988; Green et al. 1989; Jacobson et al. 1990; Fulton et al. 1993; Carmi et al. 1995a; Beales et al. 1997; Riise et al. 1997; Heon et al. 2005a).

To date, 14 genes (*BBS1-14*) have been implicated in BBS (Katsanis et al. 2000; Stone et al. 2000; Mykytyn et al. 2001; Nishimura et al. 2001; Mykytyn et al. 2002; Ansley et al. 2003; Badano et al. 2003a; Chiang et al. 2004; Fan et al. 2004; Li et al. 2004; Nishimura et al. 2005; Chiang et al. 2006; Stoetzel et al. 2006b; Stoetzel et al. 2007; Leitch et al. 2008). Analysis of mouse models of BBS (*Bbs1*$^{M390R/M390R}$, *Bbs2*$^{-/-}$, *Bbs4*$^{-/-}$ and *Bbs6*$^{-/-}$) reveals that these mutant mice have major components of the human phenotype including retinal degeneration, obesity, renal cysts and neurological deficits (Mykytyn et al. 2004; Nishimura et al. 2004; Fath et al. 2005; Davis et al. 2007). Multiple lines of evidence suggest that BBS phenotypes involve cilia dysfunction in a range of tissues, including the retina. The vertebrate retina contains photoreceptors, highly polarized cells with a modified cilium, known as a connecting cilium, that joins

the photosensitive outer segment (OS) to the protein synthesizing inner segment (IS). The connecting cilium transports cellular components from the IS to the OS that are necessary for the structure and function of the OS (Young 1967; Besharse and Horst 1990). Intraflagellar transport (IFT) proteins are important in this intraphotoreceptor transport process as they play a key role in both assembly and maintenance of photoreceptor cells (Pazour et al. 2002; Krock and Perkins 2008; Luby-Phelps et al. 2008). Loss of IFT genes in vertebrates leads to abnormal OS development, retinal degeneration and mislocalization of photopigments (Pazour et al. 2002; Tsujikawa and Malicki 2004; Sukumaran and Perkins 2009).

Retina phenotypes observed in *Bbs* mutant mice are similar to those seen with loss of IFT genes, indicating that BBS proteins play a role in transporting proteins through the connecting cilium into the OS of the photoreceptor. For instance, characterization of the retinal phenotype in BBS mouse models has demonstrated that photoreceptor death is preceded by mislocalization of the photopigment rhodopsin (Mykytyn et al. 2004; Nishimura et al. 2004; Fath et al. 2005; Abd-El-Barr et al. 2007; Davis et al. 2007). Recent work with two independently generated *Bbs4-null* mice indicates that Bbs4 plays an important role in establishing both correct structure as well as proper transport of phototransduction proteins (Abd-El-Barr et al. 2007; Swiderski et al. 2007). In the zebrafish model system, individual knockdown of *bbs* genes results in defects in the ciliated Kupffer's vesicle (KV) and delayed retrograde transport within the melanocyte (Chiang et al. 2006; Yen et al. 2006; Tayeh et al. 2008). Moreover, work in *Caenorhabditis elegans* has shown that *bbs1*, *bbs3*, *bbs5*, *bbs7* and *bbs8* localize to the basal body of ciliated cells and are involved in IFT (Ansley et al. 2003; Blacque et al. 2004). Taken together, these data strongly support a role for BBS proteins in intracellular transport and cilia; thus further substantiating a critical role for BBS genes in the specialized connecting cilium of the photoreceptor for cell maintenance and function.

BBS3 is a member of the Ras superfamily of small GTP-binding proteins, which is subdivided into ADP-ribosylation factor (ARF) and ARF-like (ARL) subgroups (Pasqualato et al. 2002). The precise function of ARL proteins is unknown, but it has been proposed that they play a role in membrane and/or vesicular trafficking (Pasqualato et al. 2002). Work in *C. elegans* indicates that *ARL6* is specifically expressed in ciliated cells and undergoes IFT along the ciliary axoneme (Fan et al. 2004). Here we report the identification of a second transcript of *BBS3*, *BBS3L*, and determine that the BBS3L protein product plays an important role in retina structure and function. BBS3L is evolutionally conserved and is unique among BBS gene products as it is expressed predominantly in the eye, suggesting a specialized role in vision. We have established both mouse and zebrafish models to study the function of *BBS3L*, and determined that BBS3L is specifically required for retinal organization and function.

Materials and methods

Ethics statement

The University of Iowa Animal Care and Use Committee approved all animal work in this study.

EST

Expressed sequence tag (EST) data for human and mouse ARL6 was downloaded from NCBI and compared to the known coding region as represented by the NCBI reference sequence (NM_177976.1 and NM_032146.3 for human and NM_019665.3 for mouse).

RT-PCR

RNA was extracted from a pool of 10-20 embryos at the following stages: 8-12 somites, 24, 36, 42, 48, 60, 72, 96 hpf and 5 dpf. Additionally, RNA was extracted from the following adult tissues: fat, brain, heart, whole eye and retina. cDNA was

synthesized using oligo dT primers. The bbs3 primer pair 1, which recognizes both *bbs3* transcripts, was used to evaluate expression. β-actin expression served as a control.

Primers:

bbs3 primer pair 1-F: 5'-AAGGACAAACCATGGCATATC-3'

bbs3 primer pair 1-R: 5'-TTACGTTTTCATCGCTCTGAT-3'

β-actin-F: 5'-TCAGCCATGGATGATGAAAT-3'

β-actin-R: 5'-GGTCAGGATCTTCATGAGGT-3'

Morpholino injections and knockdown efficiency

Antisense oligonucleotides (Morpholino, MO) were designed and purchased from Gene Tools.

bbs3_aug (Tayeh et al. 2008): AGCTTGTCAAAAAGCCCCATTTGCT

bbs3_long: ATTTCAGCTTCAGTACTTACAGTGC

bbs3_6mis (control morpholino): AaCTTGTgAAAtAGCgCCATaTGaT

crx: GGCTGCTTTATGTAGGACATCATTC

Morpholinos (12ng) were air-pressure-injected into one- to four-cell staged embryos. Transcript knockdown efficiency was assessed by RT-PCR as described above using bbs3 long splice-blocking morphants at the following stages: 8-12 somites, 72 hpf and 5 dpf. Primers recognizing both *bbs3* (bbs3 primer pair 1) transcripts were used to assess knockdown efficiency.

Human BBS3 cloning and RNA synthesis

Human BBS3 and BBS3L constructs were generated by TA cloning into the Gateway vector system (Invitrogen), and subsequently subcloned into Gateway expression vectors with a C-terminal mCherry or myc tag (generous gift from the Chien and Lawson Labs).

Primers:

-hBBS3-F: ATGGGATTGCTAGACAGACTTTC

-hBBS3-R: TGTCTTCACAGTCTGGATCTG

-hBBS3L-R: TCTTTTCATGTCTTCACAGTC

For rescue experiments, MO-resistant C-terminally tagged mCherry RNA was synthesized using the mMessage mMachine transcription kit (Ambion). *hBBS3* or *hBBS3L* RNA (8pg) was co-injected with the appropriate morpholino into one- to four-cell staged embryos.

Analysis of Kupffer's vesicle

Embryos with KVs smaller than the width of the notochord (less than approximately 50μm in diameter) were considered reduced, while embryos in which KVs could not be morphologically identified were scored as absent. Live embryos were photographed on a stereoscope with a Zeiss Axiocam camera.

Melanosome transport assay

The melanosome transport assay was performed as previously described (Chiang et al. 2006; Yen et al. 2006; Tayeh et al. 2008). Dark-adapted 6-day-post fertilization embryos were treated with epinephrine (50mg/ml, Sigma, E4375) added to egg water (Westerfield 1993) for a final concentration of 500μg/ml. Melanosome movement was monitored under the microscope and the end-point time recorded. Live embryos were photographed on a stereoscope with a Zeiss Axiocam camera.

Zebrafish Western blot

Embryos were injected with C-terminal myc-tagged human *BBS3* (8pg) or *BBS3L* (8pg) RNA at the 1-2 cell stage. Embryos (n=15) were collected at 8-12 somite, 48 hpf, 4, dpf, 5 dpf and 6 dpf and homogenized in lysis buffer (20mM Tris; 100mM NaCl; 1mM EDTA; 0.5% TritonX-100; 0.5% SDS) with protease inhibitors (0.1 mM PMSF (Roche); 10 μg/mL Leupeptin (Roche)). The supernatant was collected and cell lysates run and transferred using the X Cell SureLock Mini-Cell System under reduced conditions

(Invitrogen). Briefly, the samples were mixed with the NuPAGE LDS Sample Buffer and the NuPAGE Reducing Agent (Invitrogen) and heated at 70°C for 10 minutes. Following separation of the proteins on a pre-cast 4-12% NuPAGE Novex Bis-Tris gel (Invitrogen) the proteins were transferred to nitrocellulose membranes (Li-Cor Biosciences). The membrane was blocked in Odyssey Blocking Buffer (Li-Cor Biosciences) for 1 hour at room temperature and incubated with mouse monoclonl anti-myc (1:2000, 9B11, Cell Signaling) and rabbit polyclonal anti-actin (1:2000, Sigma) primary antibody diluted in Odyssey Blocking Buffer for 1 hour at room temperature. A species-specific fluorescently labeled secondary antibody was diluted in Odyssey Blocking Buffer (1:10,000) and incubated for 45 minutes before scanning and analyses with the Odyssey Infrared Imaging Scanner (Li-Cor Biosciences).

Vision startle response assay

A visually evoked startle response behavioral assay was modified from a previously described assay (Easter and Nicola 1996). Prior to experimentation, 5-day-old zebrafish embryos were light adapted for 1 hour. A visual stimulus was applied by performing rapid changes (approximately 1 second) in white light intensity through abruptly opening and closing the shutter located between the light source and the animal. An abrupt movement of the zebrafish embryo within one second of visual stimuli application was scored as a positive response. After performing five visual stimuli trials spaced at 30 seconds apart, the mechanical stimulus response was evaluated by probing embryos with the tip of a blunt needle. Embryos that failed to respond to the mechanical stimulation, although rare, were not included in the analysis.

Zebrafish retina histology

Embryos were maintained in 0.003% phenylthiourea (PTU) beginning at 70% epiboly to minimize pigmentaion of the retinal pigmented epithelium (RPE). Five day post-fertilized embryos were fixed overnight at 4°C with 4% paraformaldehyde (PFA)

prepared in BT buffer (4% sucrose, 0.1M $CaCl_2$ in 0.1M PO_4, pH 7.3). Embryos were rinsed with phosphate-buffer saline (PBS) and cryoprotected with 15% sucrose and 30% sucrose for 1 hour at 4°C. Optimal cutting temperature compound (OCT, Sakura) was used to infiltrate the embryos overnight at 4°C. Embryos were cryosectioned at -21°C. Sections were collected at 12μm and allowed to dry for 1 hour at 25°C. Gross morphology of the retinas was evaluated with standard hematoxylin/eosin staining.

Immunohistochemistry

Tissues were prepared as described above and 12μm sections collected. The tissues were incubated with blocking solution (5% normal donkey serum, 0.1% tween-20, 1% DMSO in PBS) for 2 hours and then incubated overnight at 4°C with either mouse-anti-green cone opsin (1:500, generous gift from the Hyde lab) or monoclonal mouse rhodopsin (Ret-P1, 1:1000, NeoMarker) diluted in blocking solution. Following washes with PBDT (PBS, 1% DMSO, 0.1% tween-20) sections were incubated for 1.5 hours at 25°C with goat-anti-mouse Alexa 488 (1:400, Molecular Probes) diluted in blocking solution. Nuclei were counterstained with To-Pro3 (1:1000, Molecular Probes) diluted in PBS. Sections were mounted in Vectashield mounting medium (Vector Laboratories) and analyzed using a Leica SP2 laser confocal microscope system with 63x magnification and 3x zoom. Images are representative of maximum projections of five focal planes (z-series).

Green opsin and rhodopsin cell counts

The ratio of mislocalized green opsin cells to total green opsin positive cells was determined from a 12μm thick central retina image taken of a single eye. Mislocalization of green opsin was defined as the presence of green opsin in the outer nuclear layer (ONL) of the retina. The number of independent fish retinas counted per group were as follows: wt *n=9*, bbs3 aug MO *n=10*, bbs3 long MO *n=15*, bbs3 aug MO+ hBBS3L RNA *n=5*, bbs3 long MO+hBBS3 RNA *n=5*. Scorers were masked to the genotype of

the embryos. Rhodopsin cell counts were performed in a similar manner. The number of independent fish retinas counted per group were as follows: wt *n=6*, bbs3 aug MO *n=8*, bbs3 long MO *n=7*.

Statistical analysis

To evaluate the statistical significance for KV formation as well as opsin localization, the Fisher's exact test with the two-tailed p-value was reported. A One-Way Analysis of Variance (one-way ANOVA) paired with the Tukey Honestly Significant Difference (HSD) test was performed to assess statistical significance for the melanosome transport assay.

Mouse Western blot

Brain, whole eye and retina tissue was collected from adult wild-type mice. Tissues were lysed and homogenized in triple detergent lysis buffer (50mM Tris-Cl, pH 8.0; 150mM NaCl; 0.02% NaN_3; 0.1% SDS; 1% NP-40; 0.5% Na Deoxycholate; H_2O) with protease inhibitor cocktail (10µl/ml, Sigma) and the samples clarified by centrifugation. A Bradford assay was performed prior to running samples using the X Cell SureLock Mini-Cell System (Invitrogen). Samples were mixed with the NuPAGE LDS Sample Buffer containing NuPAGE Reducing Agent (Invitrogen) and the mixture heated at 70°C for 10 minutes. Protein extracts were loaded onto a 4-12% NuPAGE Novex Bis-Tris PAGE gel (Invitrogen) and resolved prior to PVDF membrane (Amersham Biosciences) transfer. The membrane was blocked in blocking buffer (5% nonfat milk, 1% bovine serum albumin (BSA)) for 1 hour at room temperature and then incubated with rabbit anti-mouse Bbs3 primary antibody (1:8000) diluted in 5% nonfat milk for 1 hour at room temperature. A species-specific HRP-conjugated secondary antibody (1:10000, Santa Cruz) was diluted in 5% nonfat milk and incubated for 1 hour at room temperature before detection with ECL reagent (GE Healthcare/Amersham Biosciences).

Generation of Bbs3L mutant mice

A targeting plasmid was constructed by amplifying the 5' and 3' regions of *Bbs3L* using genomic DNA isolated from the 129/SvJ mouse strain. The consensus splice sites were ablated to alter the slice donor and splice acceptor sites flanking exon 8, the exon responsible for the long transcript.

Primers:

splice donor: 5'-CTGCTGTCACAAAAAACAGTACACTAAGTATCTG-3'

splice acceptor: 5'- CAGATACTTAGTGTACTGTTTTTTGTGACAGCAG-3'

Following mutagenesis, these regions were cloned into the targeting vector pOSDUPDEL (a gift from O. Smithies, University of North Carolina, Chapel Hill, NC, USA). The targeting construct was linearized with *Not*I and electroporated into R1 embryonic stem (ES) cells (129 X 1/SvJ3 129S1/Sv). Double selection of ES cells was carried out for the presence of the neomycin gene (Neo) and the absence of the thymidine kinase gene (TK). To identify *Bbs3L*-targeted ES cells, G418-resistnt clones were screened for by PCR. One ES cell line was used to produce chimeras that were bred with C57BL/6J mice to generate Bbs3L heterozygous ($Bbs3L^{+/-}$) mice on a mixed background. These mixed background offspring were evaluated for germline transmission by PCR, and the resulting Bbs3L heterozygotes ($Bbs3L^{+/-}$) crossed to pure 129/SvEv mice for seven generations to enrich for the pure 129/SvEv background. Heterozygous mice were intercrossed and the progeny genotyped by PCR using primers to identify the presence of the targeted allele. Presence of the wild-type and mutant allele was determined by using a three primer pool: forward primer specific to the wild-type allele, forward primer specific to the mutant allele and a reverse primer that recognizes both alleles.

Primers:

Bbs3 wild-type allele-F: 5'-TTGGAGATTTGTCTCCCTCTG-3'

Bbs3 mutant allele-F: 5'-GCTACCCGTGATATTGCTGAA-3'

Bbs3 both alleles-R: 5'-AAAAGGGCATAAAAGCACCTC-3'

Mouse weight studies

$Bbs3^{+/+}$, $Bbs3L^{+/-}$ and $Bbs3L^{-/-}$ animals were weighed weekly for ten months. Sample sizes range from 1-17 mice, with the older ages having fewer mice.

Histological analysis of *Bbs3L*$^{-/-}$ mice

Enucleated eyes were fixed in 4% PFA in PBS (pH 7.4). Following 2-4 hours of fixation at 4°C, the anterior chamber and lens of the eye was removed and the eyecup was further fixed overnight at 4°C in 4% PFA. The eyecups were rinsed with PBS and cryoprotected through a series of 5%:20% sucrose incubations (2:1, 1:1, 1:2) at room temperature before an overnight incubation at 4°C in 20% sucrose. Eyecups were infiltrated with 2 parts 20% sucrose in 1 part OCT (Sakura) for thirty minutes at room temperature. Cryosectioning occurred at -21°C and sections were collected at 7μm. Gross morphology of the retinas was evaluated with hematoxylin/eosin staining after the sections were allowed to dry for at least 1 hour at 25°C.

Immunohistochemistry of *Bbs3L*$^{-/-}$ mice

Immunohistochemistry was performed on cryosections of *Bbs3L*$^{+/+}$ and *Bbs3L*$^{-/-}$ mouse retinas. The sections were blocked with bovine serum albumin (BSA, 1 mg/ml) in PBS for 15 min and then incubated for 1 hour at room temperature with either rabbit anti-mouse Bbs3 (1:100), mouse anti-cellular retinaldehyde-binding protein (1:1,000, CRALBP), biotinylated peanut agglutinin (1:100, PNA, Vector Laboratories) or monoclonal mouse rhodopsin (1:1000, RET-P1, NeoMarker) in PBS. Following washes with PBS, sections were incubated for 30 minutes at room temperature with a species specific secondary antibody: goat-anti-rabbit Alexa 488 (1:200, Molecular Probes), Texas Red Avidin D (1:200, Vector Laboratories) or goat-anti-mouse Alexa 546 (1:200, Molecular Probes). Nuclei were counter stained with either 4', 6-diamidino-2-phentlindole (DAPI, Molecular Probes) or To-Pro-3 (1:1000, Molecular Probes). Sections were mounted in Aqua Mount (Lerner Laboratories) and analyzed using either

an Olympus BX-41 microscope with a SPOT RT digital camera (Diagnostic Instruments) or a Bio-Rad 1024 confocal microscope system. Images from the confocal are representative of multiple focal planes (z-series).

Results

Identification of a second BBS3 transcript in human, mouse and zebrafish

Expressed sequence tag (EST) data for human *BBS3* (*ARL6*) was compared to the known coding region of the gene. Although most of the ESTs were virtually identical to the *BBS3* reference sequence, a few were found to contain 13 extra base pairs. Interestingly, all ESTs that contained this alternative sequence originated from retina or whole eye libraries, suggesting that this second longer transcript, *BBS3L*, has an expression pattern that is limited to the eye.

BBS3L results from differential splicing that leads to the inclusion of a 13 base pair exon and a shift in the open reading frame generating different C-terminal regions (Figure 2A). The striking conservation of the C-terminal region of the long isoform in human, mouse and zebrafish strongly suggests that bbs3L has functional relevance (Figure 2B). To determine if the *bbs3* and *bbs3L* transcripts have similar tissue-specific expression in other species, RT-PCR of zebrafish and mouse tissues was performed. Zebrafish *bbs3* is expressed in all adult tissues examined (fat, brain, heart, whole eye and retina), while *bbs3L* expression is limited to the eye (Figure 3A). Similar tissue expression patterns for *Bbs3* and *Bbs3L* were observed in the mouse with the addition of low levels of *Bbs3L* mRNA in the brain (Figure 4). A developmental profile in zebrafish embryos reveals that while *bbs3* is expressed throughout early development, *bbs3L* is not expressed until 48 hours post fertilization (hpf) (Figure 3B). This is a time when retinal neuroepithelial cells are exiting the cell cycle and differentiating into photoreceptor cells, the light sensing cells of the retina (Hu and Easter 1999).

Knockdown of *bbs3* results in characteristic BBS phenotypes

To determine the functional role of bbs3L in development and to distinguish the individual roles of the two bbs3 protein products, we utilized antisense oligonucleotide mediated gene knockdown (morpholinos, MO) in zebrafish. Two independent MOs were utilized: one targeting the splice junction specific to the long transcript (bbs3 long MO) and the other a previously described MO targeting both transcripts (bbs3 aug MO) through blocking of the translational start site (Tayeh et al. 2008) (Figure 5A). RT-PCR was used to determine the knockdown efficiency of the bbs3 long MO on staged embryos and demonstrated knockdown of the long transcript through at least 5 days post fertilization (dpf) (Figure 5B). Additionally, the *bbs3* transcript is unperturbed in *bbs3L* knockdown embryos.

Knockdown of *bbs* function in zebrafish generates two prototypical defects: reduction of the size of the Kupffer's vesicle (KV) as well as retrograde transport defects (Chiang et al. 2006; Yen et al. 2006; Tayeh et al. 2008). As previously demonstrated, alterations in the formation of the ciliated KV was the earliest observable phenotype resulting from knockdown of both bbs3 transcripts by the bbs3 aug MO (Tayeh et al. 2008). At the 8-10 somite stage (12-14 hpf) in wild-type and control injected embryos the KV has formed in the posterior tailbud. The KV diameter is approximately 50μm and is larger than the width of the notochord (Figure 6A and B). Injection of the bbs3 aug MO resulted in a reduction of KV size to a width less than that of the notochord (Figure 6C). Knockdown of both bbs3 transcripts by the aug MO results in a statistically significant increase in embryos with KV defects (Fisher's exact test, $p<0.001$) (Figure 6D and Table 2). Of note, injection of the bbs3 long MO does not lead to KV defects (Figure 6D and Table 2).

The second prototypical phenotype observed in *bbs* MO-injected embryos (morphants) is delayed trafficking of melanosomes. Zebrafish are able to adapt to their

surroundings through intracellular trafficking of melanosomes within melanophores in response to light and hormonal stimuli (Marks and Seabra 2001; Blott and Griffiths 2002; Skold et al. 2002; Barral and Seabra 2004). To test the rate of this movement, 5-day old zebrafish were dark adapted, to maximally disperse the melanosomes (Figure 6E and F) and then treated with epinephrine to chemically stimulate the retrograde transport of melanosomes (Nascimento et al. 2003; Yen et al. 2006; Tayeh et al. 2008) (Figure 6G). Wild-type and control injected embryos show rapid movement of melanosomes to a perinuclear location averaging 1.4 minutes, whereas bbs3 aug MO injected embryos demonstrated a statistically significant delay, averaging 2.1 minutes (ANOVA with Tukey, $p<0.01$) (Figure 6H and Table 2). In contrast, the rate of melanosome movement in bbs3 long knockdown embryos is statistically the same as control embryos, averaging 1.5 minutes (Figure 6H and Table 2).

To test for MO-specificity as well as differential function of the two *bbs3* transcripts, human RNAs of both *BBS3* and *BBS3L* were used. Embryos co-injected with a combination of MO and RNA were evaluated for suppression of MO induced KV and melanosome transport defects. Co-injection of *BBS3* RNA with the aug MO did not rescue the KV defect but was sufficient to suppress the melanosome transport delay; however, co-injection of the aug MO with *BBS3L* RNA was not able to suppress either MO-induced defect (Table 2). Overexpression of *BBS3*, but not *BBS3L*, RNA alone results in an alteration to the KV. To evaluate protein expression, myc-tagged *BBS3* and *BBS3L* RNA was injected into the 1-cell embryos and Western blot analysis performed using an antibody against myc to detect the tagged proteins. Protein expression was confirmed out to 5 dpf (Figure 7). Taken together, our data demonstrates that *bbs3L* plays a role independent from KV formation and melanosome transport and that human *BBS3* can partially compensate for the loss of zebrafish *bbs3*.

bbs3 long knockdown causes a vision defect in zebrafish

Since BBS patients develop retinitis pigmentosa and the *BBS3L* transcript is differentially expressed in the eye, we sought to functionally test the role of bbs3 in vision. The zebrafish retina develops rapidly; at 60 hpf the retina is fully laminated and by 3 dpf zebrafish embryos are visually responsive (Branchek 1984; Easter and Nicola 1996; Schmitt and Dowling 1999). Zebrafish elicit a characteristic escape response when exposed to rapid changes in light intensity and this startle response can be used as an assay for vision function (Easter and Nicola 1996). In this assay, the behavior of a 5-day old embryo was monitored in response to short blocks of a bright, stable light source (Easter and Nicola 1996) (t=0, Figure 8A). The typical response, a distinct C-bend and a change in swimming direction, is scored over a series of 5 trials, timed 30 seconds apart (t=139ms, Figure 8A). Uninjected embryos respond on average 3.09 times (Figure 8B and Table 3). Cone-rod homeobox (*crx*) gene knockdown was used as a control for vision impairment as loss of this gene is known to affect photoreceptor formation in zebrafish (Liu et al. 2001; Shen and Raymond 2004). *crx* knockdown embryos respond an average of 1.28 times (ANOVA with Tukey, $p<0.01$) (Figure 8B). Knockdown using either the bbs3 aug or bbs3 long MO resulted in a statistically significant (ANOVA with Tukey, $p<0.01$) reduction in the number of responses (1.81 and 1.77 times respectively) compared to controls, indicating vision impairment (Figure 8B and Table 3). These data support a key role for *bbs3L* in vision function.

To functionally test the specific role of both *bbs3* and *bbs3L* in vision, rescue experiments were performed. To investigate whether bbs3 could compensate for loss of *bbs3L*, human *BBS3* RNA was co-injected with either the bbs3 aug or the bbs3 long MO. Although *BBS3* RNA was sufficient to suppress the melanosome transport delays associated with bbs3 aug morphant embryos (Table 2), *BBS3* RNA was insufficient to rescue the vision impairment induced by loss of *bbs3* and/or only *bbs3L* (Figure 8B and Table 3). Conversely, co-injection of *BBS3L* RNA with either bbs3 morpholino was

sufficient to rescue the vision defect (ANOVA with Tukey, $p<0.01$) (Figure 8B and Table 3). Interestingly, overexpression of *BBS3*, but not *BBS3L*, results in visual impairment. Based on these rescue experiments, bbs3L is necessary and sufficient for vision function.

hBBS3L is sufficient to rescue green opsin mislocalization in bbs3 morphant zebrafish

Previous work has demonstrated that *Bbs1 M390R* knockin, *Bbs2*, *Bbs4* and *Bbs6* mutant mice initially form photoreceptors; however, the photoreceptors subsequently show a mislocalization of rhodopsin, a photopigment protein, to the cell bodies of the outer nuclear layer (ONL) and undergo progressive photoreceptor degeneration (Mykytyn et al. 2004; Nishimura et al. 2004; Fath et al. 2005; Abd-El-Barr et al. 2007; Davis et al. 2007). By gross histology, wild-type, bbs3 aug and bbs3 long morphant zebrafish embryo retinas displayed a fully laminated retina at 5 dpf (Figure 9A, 9B and 9C). Ganglion cell outgrowth and optic nerve formation was evaluated using the ath5:GFP [Tg(atoh7:GFP)] transgenic line, a marker of ganglion cell and axon outgrowth (Masai et al. 2003). We found that gross retinal ganglion axon trajectories were not perturbed in *bbs3* aug or long morphants (Pamela Pretorius observation).

While the overall architecture of the retina appeared morphologically normal at 5 dpf, we investigated photopigment localization in *bbs3* morphants. Photopigments are known to localize to the outer segment of the zebrafish photoreceptor (Vihtelic et al. 1999). As the vision startle response assay evaluates cone function in the 5 dpf zebrafish embryo, cone photopigment localization was assessed using an antibody specific to green cone opsin. In the wild-type retina, green opsin is found in the outer-segment of the green cone photoreceptor (Figure 10A). In *bbs3* aug and *bbs3* long morphants green opsin expression was not restricted to the outer segments of the photoreceptors; rather, green opsin was also detected in the cell bodies of the outer nuclear layer throughout the entire retina (Figure 10B and E).

To determine whether there is a functional difference between *BBS3* and *BBS3L* in its ability to rescue the green opsin localization in the photoreceptors of MO-injected embryos rescue experiments were performed. The first question addressed was if *BBS3L* RNA was sufficient to rescue green opsin localization in morphant embryos. Expression of wild-type human *BBS3L* RNA led to improved green opsin localization in both *bbs3* aug and *bbs3L* morphant embryos (Figure 10D and G). The percentage of cells mislocalizing green opsin was quantified and indeed *BBS3L* RNA was able to statistically rescue the green opsin defect in *bbs3* aug morphants (Fisher's exact test, $p<0.01$) (Figure 11 and Table 3). We next investigated whether *BBS3* could compensate for loss of *bbs3L* in the zebrafish retina. Co-injection of wild-type human *BBS3* RNA failed to rescue green opsin localization in *bbs3* aug and *bbs3L* morphant embryos (Figure 10C and F and Figure 11 and Table 3). These data are consistent with the vision startle response rescue data and supports the hypothesis that *BBS3L* has an eye specific role. Moreover, these data support a specific role for *bbs3L* in the retina and for localization of proteins within the photoreceptor cell.

Loss of *bbs3* results in rhodopsin mislocalization in the zebrafish retina

While rod cells are not functional at 5 dpf, when the vision startle response assay is performed, the cells do express the photopigment rhodopsin (Bilotta et al. 2001). Similar to green cone opsin, rhodopsin localizes to the photoreceptor outer segments in wild-type zebrafish embryos (Vihtelic et al. 1999) (Figure 12A). Interestingly, knockdown of *bbs3*, but not *bbs3L*, results in mislocalization of rhodopsin to the cell bodies of the outer nuclear layer (Figure 12B and 12C). Moreover, the percentage of cells mislocalizing rhodopsin was quantified and a statistically significant difference observed between wild-type and *bbs3* aug morphant embryos (Fisher's exact test, $p<0.01$) (Figure 13). Taken together, this experiment suggests a possible cell type

specific function for the *bbs3* transcripts; however, additional experiments are necessary to confirm this.

Bbs3 is expressed in ganglion and photoreceptor cells in mouse and human retinas

A polyclonal antibody against a central region of the mouse Bbs3 peptide, which is conserved across human and mouse, was generated to recognize both isoforms of Bbs3. Cellular localization of Bbs3 was assessed in donor human and mouse retinal tissue. Immunohistochemistry was performed on transverse cryosections from adult human and adult mouse eyes using the Bbs3 antibody. Staining revealed expression of Bbs3 (green) in the ganglion cell layer and the nerve fiber layer as well as the photoreceptor cells of both mouse (Figure 14A and 15A) and human retinal tissue (Figure 14D and 15D). Cellular retinaldehyde-binding protein (CRALBP, red) was used as a marker for Muller cells in both mouse (Figure 14B) and human retinal sections (Figure 14E). The merge represents the co-localization of Bbs3 (green) and CRALBP (red) in the Muller cells of the ganglion cell layer of the mouse (Figure 14C) and human (Figure 14F) retina. Additionally, a cone outer segment marker, peanut agglutinin (PNA, red), was used to demonstrate photoreceptor labeling in both mouse (Figure 15B) and human retinal sections (Figure 15E). The merge represents the co-localization of Bbs3 (green) and PNA (red) in the photoreceptor cells of both mouse (Figure 15C) and human (Figure 15F). The specificity of the BBS3 antibody for immunohistochemistry was confirmed through both Western blot analysis and peptide blocking of the antibody on wild-type mouse retina (Figure 16A and B).

Bbs3L$^{-/-}$ mice display structural abnormalities

To characterize the effects of *Bbs3L* loss on mammalian photoreceptors, a targeted knockin of the long form of Bbs3 was carried out by altering the splice donor and acceptor sites flanking exon 8, leading to the exclusion of exon 8 upon homologous

recombination (Figure 17). This approach leads to the preservation of *Bbs3* expression in the *Bbs3L-null* mice. RT-PCR confirmed the generation and transmission of the *Bbs3L* allele in +/- and -/- mice (Figure 18). Unlike previously generated BBS knockout mice, which are obese by 7 months of age, male and female Bbs3L$^{-/-}$ mice do not become obese (Figure 19A and 19B) (Mykytyn et al. 2004; Nishimura et al. 2004; Fath et al. 2005; Davis et al. 2007). This supports the idea that *Bbs3L* function is restricted to the retina and is consistent with the zebrafish knockdown studies.

Gross histological examination of 8-month-old wild-type and homozygous Bbs3L$^{-/-}$ mutant mice revealed that while all cell layers were present (Figure 20A and D), the inner segments of the photoreceptors were disrupted in a majority of the mutant mice as compared to wild-type (Figure 20B and E). In wild-type mice, the inner segment layer is arranged in a parallel array; while in the Bbs3L-null mice the parallel arrangement of the IS was eccentric with individual inner segments randomly oriented. Additionally, immunohistochemistry with the Bbs3 antibody (green), which recognizes the endogenous Bbs3 protein that is still present, and rhodopsin (red) in Bbs3L$^{-/-}$ mice further confirms inner segment disorganization in Bbs3L$^{-/-}$ mutant mice compared to wild-type (Figure 20C and F).

Discussion

The present study identifies and characterizes the eye-enriched transcript *BBS3L* using both the zebrafish and mouse model systems. While typical BBS genes are ubiquitously expressed and lead to multiple phenotypes in human, mice and zebrafish, *BBS3L* expression is restricted to the eye and serves as a useful tool for understanding the specific pathophysiology of BBS proteins in blinding diseases. By knockdown in zebrafish, we find that *bbs3L* is required for visual function and localization of the photopigment green cone opsin; however, *bbs3L* is dispensable for the cardinal features of BBS in zebrafish, including KV formation and intracellular transport of melanosomes.

Moreover, *BBS3L* RNA, but not *BBS3* RNA, is sufficient to rescue both the vision defect as well as green opsin localization. These data provide strong evidence that *bbs3L* is specifically required for retinal organization and function.

Immunohistochemistry using an antibody that recognizes both Bbs3 and Bbs3L indicates strong expression of the protein in the ganglion cell layer, nerve fiber layer and photoreceptor cells in both human and mouse retinas. By using this antibody on *Bbs3L-null* mouse retinas, we can deduce that *Bbs3* is expressed in both the photoreceptors and ganglion cells. This is consistent with expression data indicating that *Bbs3L* is enriched in the retina.

We have previously demonstrated that knockdown of *bbs* genes in the zebrafish leads to KV defects and melanosome transport delays (Chiang et al. 2006; Yen et al. 2006; Tayeh et al. 2008). As previously reported, knockdown of *bbs3* using the aug morpholino yields both KV and melanosome transport defects; however, knockdown of only *bbs3L* does not affect the KV or transport of melanosomes. The lack of these cardinal features is not surprising given that *bbs3L* is not expressed at the KV stage and that in adult zebrafish the long transcript is only expressed in the eye. Since *bbs3* and *bbs3L* are identical except for the splicing of the last exon, we cannot technically knockdown *bbs3* alone without affecting *bbs3L*. Based on rescue data, *bbs3* knockdown alone appears to be responsible for both the KV and melanosome transport defects seen with the aug morpholino. Importantly, bbs3 and bbs3L do not seem to be functionally interchangeable. Expression of *BBS3L* RNA, at a time and place when the endogenous transcript is not present, does not rescue the cardinal features of BBS in the zebrafish that result from knockdown of both transcripts. Moreover, overexpression of *BBS3* in the whole embryo cannot restore vision loss resulting from the knockdown of only *bbs3L*. It should be noted that melanosome transport is evaluated after the vision startle assay; therefore, overexpressed BBS3 is functional at the time of the vision assay. Although bbs3 may have some effect on vision that is below the detection level of our assay, we

have demonstrated that bbs3L function is both necessary for vision and sufficient to rescue vision loss in the zebrafish.

Similar to the zebrafish results, a *Bbs3L-null* mouse lacks the observed phenotypes of previously published *Bbs-null* mice, such as obesity (Mykytyn et al. 2004; Nishimura et al. 2004; Fath et al. 2005; Davis et al. 2007). The effect of *Bbs3* in the mouse retina may be more significant as *Bbs3L-null* mice present with only a variable mild disruption of the normal architecture. This indicates that in the mouse retina, *Bbs3* is able to partially compensate for loss of *Bbs3L*. Moreover, the difference in phenotype between zebrafish and mouse could potentially be due to the ratio of cones and rods found in each model system. One hypothesis is that *bbs3L* plays a major functional role in cones, but only a minor role in rods. This hypothesis is supported by the presence of rhodopsin mislocalization in *bbs3*, but not *bbs3L*, morphants. Additionally, at the stages examined in the zebrafish, cones are the only functional photoreceptors in the retina, whereas mice have a rod-dominated retina (Young 1985; Bilotta et al. 2001). These attributes are important to consider when looking at the role of BBS in human disease progression, as humans rely on their fovea, a specialized cone-dominant structure in the center of the macula, for visual acuity. Continued characterization of the *Bbs3L-null* mouse may shed more light on this difference between the mouse and zebrafish system, as well as elucidate a more definitive role for *BBS3L* in the retina.

Taken together, these data demonstrate that the *BBS3L* transcript is specifically required for retinal organization and function. While we have identified a second transcript of *BBS3*, a gene known to cause BBS, we would not expect patients with mutations affecting only BBS3L to present with BBS. Based on our findings in both a zebrafish and mouse model of *BBS3L*, patients with mutations in BBS3L alone would present with a non-syndromic retinal disease, characterized by photoreceptor dysfunction and death. Indeed, recent homozygosity mapping of a consanguineous Saudi family has identified a missense mutation in BBS3 that leads to non-syndromic RP (Abu Safieh et

al. 2009). Functional characterization of this mutation in the zebrafish may provide additional clues to the role of BBS3 in the eye. Thus this eye specific transcript, *BBS3L*, will serve as a useful tool for understanding the pathophysiology of other blinding diseases. In addition, our data indicate that expression of *BBS3L*, rather than *BBS3*, would be needed for gene therapy aimed at treatment of blindness in BBS3 patients.

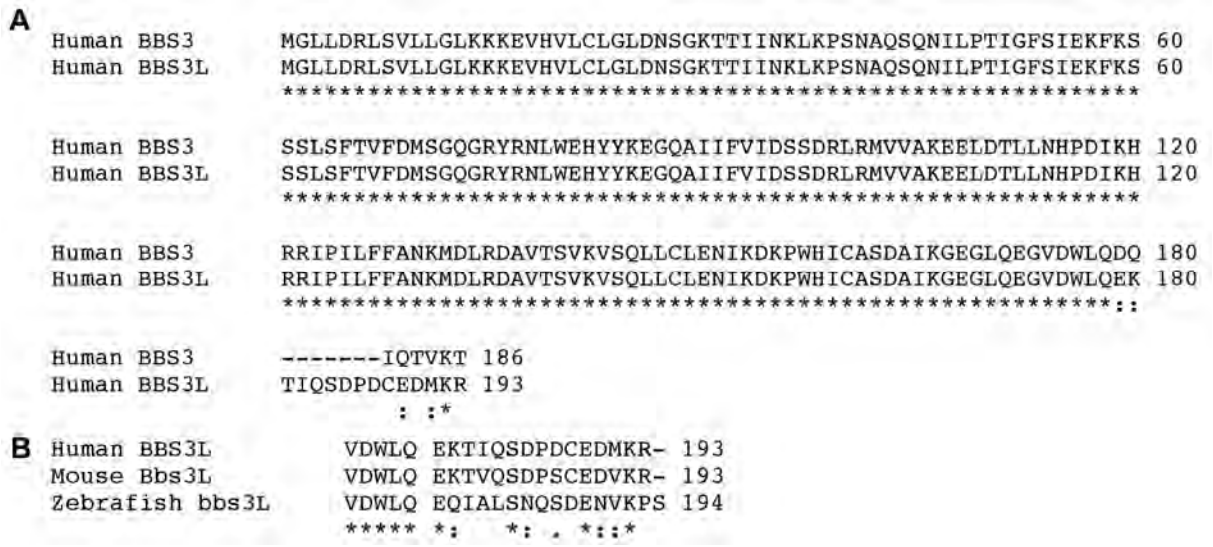

Figure 2 Identification of a second *BBS3* transcript. (A) Alignment of human BBS3 and BBS3L proteins. (B) C-terminal end alignment of human, mouse and zebrafish BBS3L protein. Asterisks (*) indicate identical amino acids shared in all alignments, while colons (:) and periods (.) represent conserved amino acids.

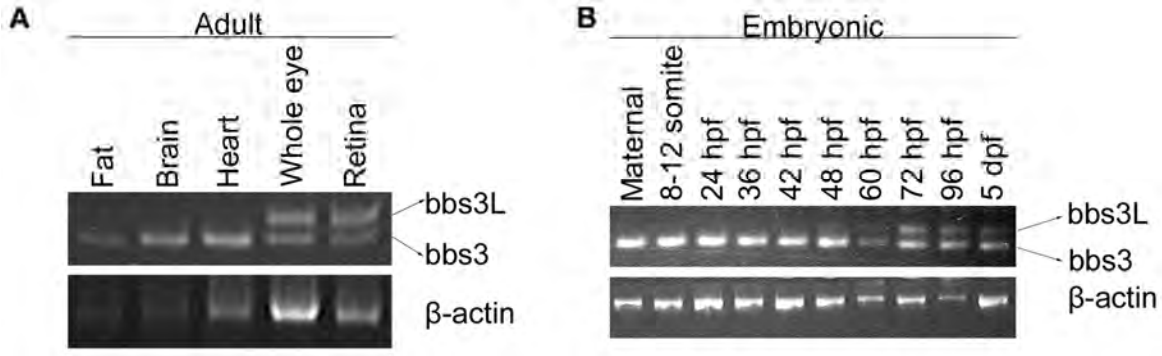

Figure 3 Expression of zebrafish *bbs3* and *bbs3L*. (A) RT-PCR tissue expression profile of zebrafish *bbs3* and *bbs3L* transcripts in wild-type adult zebrafish tissues: fat, brain, heart, whole eye and retina. β-actin was used as a positive control. *bbs3* is expressed in all adult tissues examined, while *bbs3L* expression is limited to the eye. (B) RT-PCR developmental expression profile of *bbs3* and *bbs3L* at the following stages: maternal, 8-12 somites, 24, 36, 42, 48, 60, 72, 96 hpf and 5 dpf. *bbs3* is expressed throughout development, while the long form is present by 48 hpf, correlating with photoreceptor development.

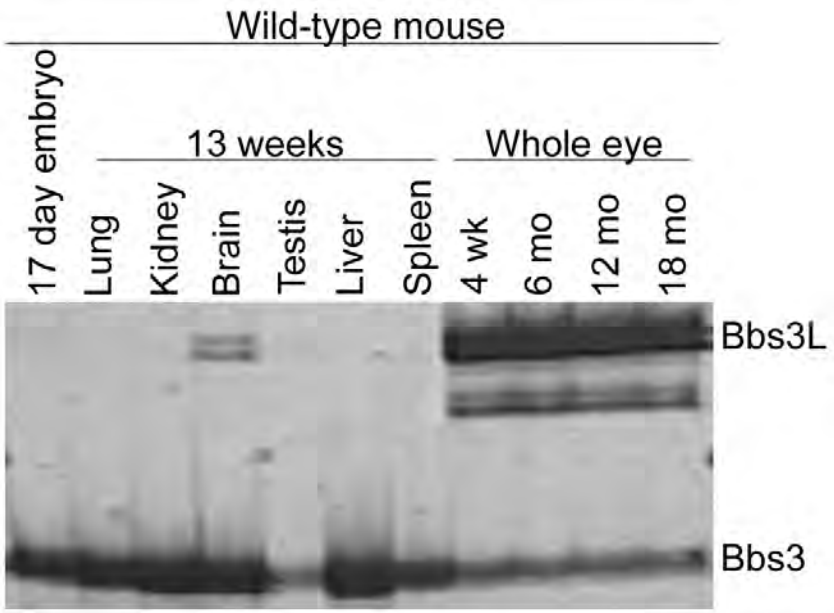

Figure 4 Expression of Bbs3 and Bbs3L in wild-type mouse tissues. RT-PCR run on a silver stained denaturing gel used to initially identify the long transcript of *Bbs3* in mouse tissues. The middle bands are a result of polymerase stuttering.

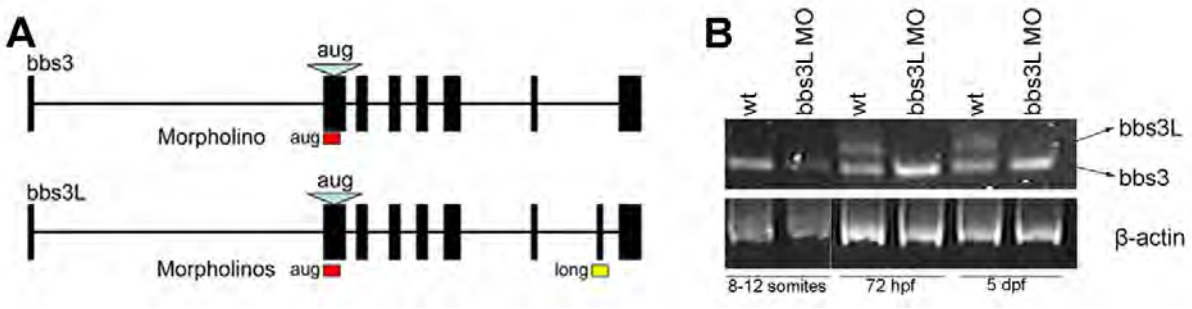

Figure 5 *bbs3* gene structure and *bbs3L* knockdown efficiency. (A) Schematic depicting the *bbs3* gene structure and antisense oligonucleotide strategy used to target either both transcripts (bbs3 aug MO) or to target only *bbs3L* (bbs3 long MO) in zebrafish embryos. The *bbs3* aug MO targets the start site of the gene and thus hits both transcripts, while the *bbs3L* MO is a splice-blocking morpholino that only targets the long form. (B) RT-PCR from staged *bbs3L* morphant embryos at 8-12 somites, 72 hpf and 5 dpf. The *bbs3L* transcript is absent through 5 dpf injected embryos indicating successful knockdown. Note that the *bbs3* transcript is unperturbed in *bbs3L* morphants.

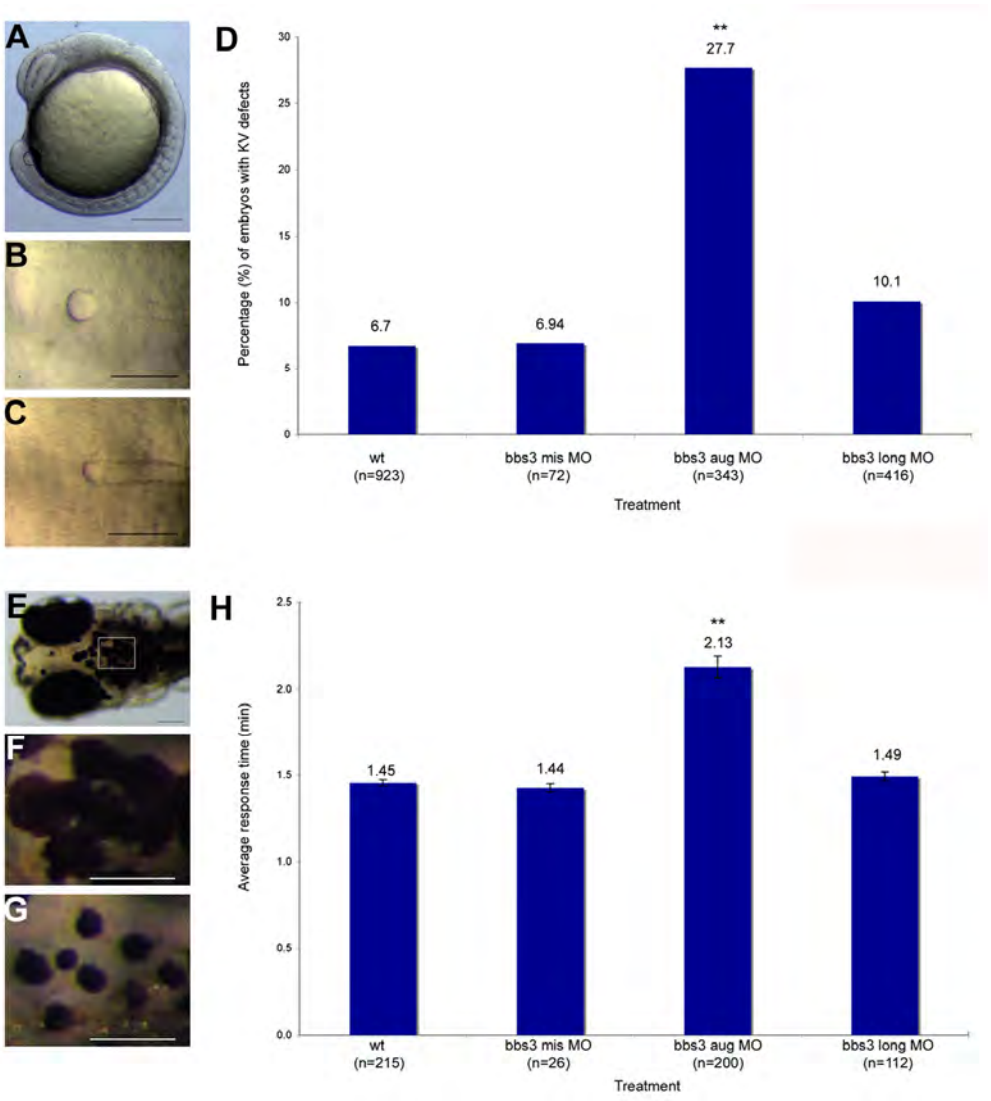

Figure 6 Cardinal features of BBS knockdown in zebrafish. (A-C) Images of live zebrafish embryos at 8-10 somite stage. Scale bar 200μm. (A) Side view of an embryo highlighting the location of the Kupffer's Vesicle (circle), the ciliated structure located in the tailbud. (B) Dorsal view of a normal sized KV from a wild-type embryo. (C) *bbs3* aug MO-injected embryos with a reduced KV. (D) The percentage of embryos with KV defects (reduced or absent) in uninjected, control MO, bbs3 aug MO and bbs3 long MO injected embryos. The sample size (n) is noted on the x-axis. **Fisher's Exact test, $p<0.001$. (E-G) Epinephrine-induced melanosome transport of wild-type 6-day old larvae. Scale bar 100μm. (E) Melanosome transport is observed in cells on the head of the embryos. Boxed region is magnified for F and G. (F) Wild-type larvae prior to epinephrine treatment and (G) the endpoint at 1.45 minutes after epinephrine treatment. (H) Epinephrine-induced retrograde transport times. The sample size (n) is noted on the x-axis. **ANOVA with Tukey, $p<0.01$.

Table 2 Summary of percentage abnormal Kupffer's Vesicle and melanosome transport times

	Abnormal KV (percentage)	n	Melanosome transport (min)	n
wild-type	6.7	923	1.45	215
bbs3 aug MO	27.7**	343	2.13++	200
bbs3 aug MO + hBBS3 RNA	21.2**	85	$1.85++	58
bbs3 aug MO + hBBS3L RNA	24.1**	108	2.01++	46
bbs3 long MO	10.1	416	1.49	112
bbs3 long MO + hBBS3 RNA	19.7**	127	1.53	35
bbs3 long MO + hBBS3L RNA	5.5	109	1.51	46
hBBS3 RNA	27.7**	83	1.49	48
hBBS3L RNA	8.0	25	1.48	19

**Fisher's exact test, $p<0.01$ as compared to wild-type

++ANOVA with Tukey test, $p<0.01$ as compared to wild-type

$ANOVA with Tukey test, $p<0.05$ as compared to morpholino

n, sample size

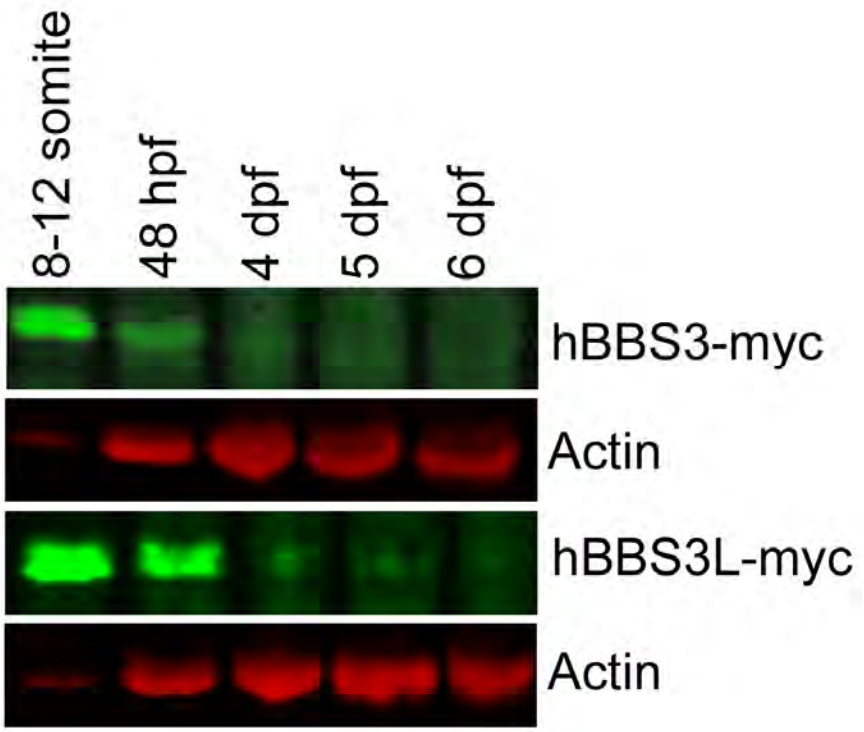

Figure 7 BBS3 and BBS3L protein expression. Western blot analysis of staged zebrafish embryos injected with either human *BBS3* or *BBS3L* myc-tagged RNA. Both proteins are present through 5 days post fertilization. Actin served as a control.

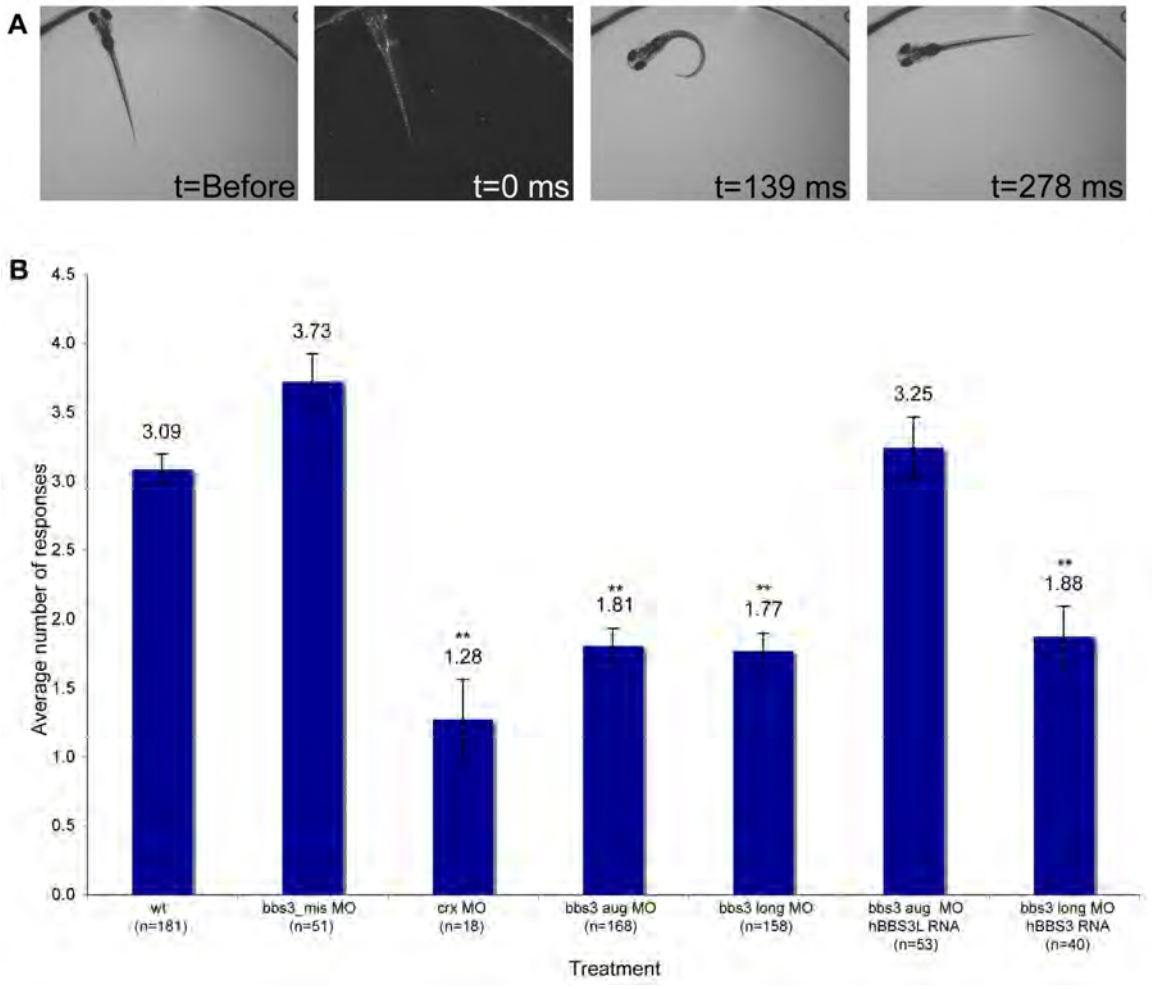

Figure 8 Vision startle response in zebrafish. (A) Vision function was assayed in 5-day old embryos by testing embryos sensitivity to short blocks in light at 30 second intervals for 5 trials (adapted from Easter and Nicola 1996). Selected images from a time-lapse collection before and immediately after a one second block in light. The typical response, a distinct C-bend, is scored as a positive response as shown in time point 139ms. ms, milliseconds. (B) Quantification of the vision startle response for each treatment. Cone-rod homeobox (*crx*) gene knockdown was used as a control for vision impairment. *bbs3* morphants lacking either both transcripts or only the long transcript showed a statistically significant reduction in the number of responses, indicating visual impairment. Rescue experiments using human *BBS3L* or *BBS3* RNA co-injected with the bbs3 morpholinos demonstrated that *hBBS3L* RNA is sufficient to rescue the vision defect associated with knockdown, while h*BBS3* is not sufficient to rescue the vision defect. The sample size (n) is noted on the x-axis. **ANOVA with Tukey, $p<0.01$.

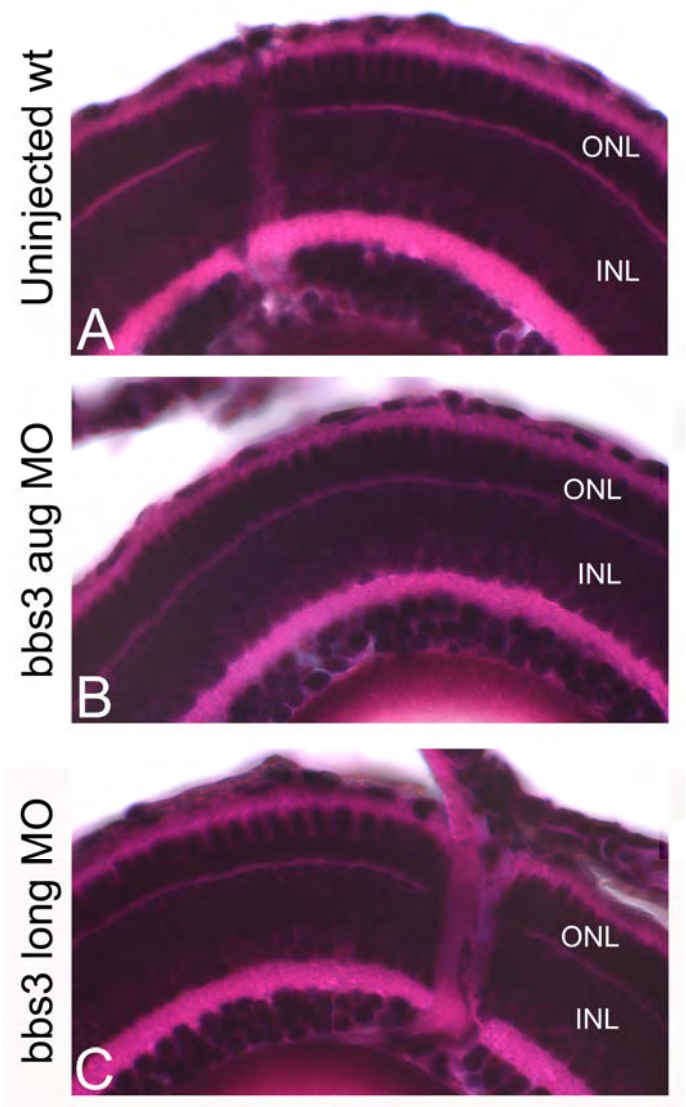

Figure 9 Retina histology in *bbs3 aug* and *bbsL* MO-injected embryos. Brightfield images of hematoxylin/eosin histological staining of transverse sections through 5 dpf zebrafish embryos (A) wild-type (B) bbs3 aug MO (C) bbs3 long MO. Embryos were chemically treated to inhibit the pigment of the retinal pigment epithelium (RPE) to enable visualization of the outer segments. At 5 dpf zebrafish embryos retinas were fully laminated. ONL, outer nuclear layer; INL, inner nuclear layer.

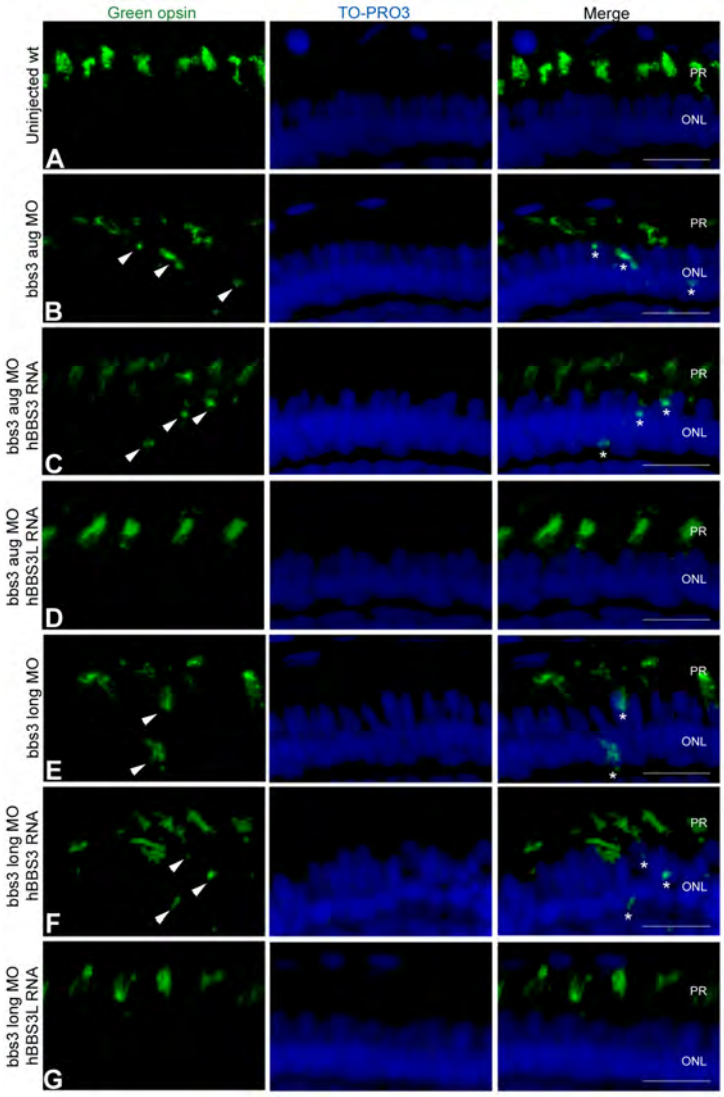

Figure 10 Green opsin mislocalization and rescue in 5-day old *bbs3* morphant zebrafish. Immunofluorescence of green cone opsin (green) on transverse cryosections of 5-day old embryos (A) uninjected wild-type, (B) *bbs3* aug MO, (C) *bbs3* aug MO and *hBBS3* RNA, (D) *bbs3* aug MO and *hBBS3L* RNA, (E) *bbs3* long MO, (F) *bbs3* long MO and *hBBS3* RNA and (G) *bbs3* long MO and *hBBS3L* RNA. To-Pro3 was used to counterstain the nuclei (blue). In *bbs3* aug (B) and *bbs3* long morphants (E), green opsin was not restricted to the outer segment of the photoreceptors and was detected in the cell bodies of the outer nuclear layer (arrowheads and asterisks). Expression of *hBBS3L* RNA improved green opsin localization in both *bbs3* aug (D) and *bbs3L* (G) morphants. Of note, *hBBS3* RNA failed to rescue green opsin localization in *bbs3* aug (C) and *bbs3* long (F) morphant embryos (arrowheads and asterisks). PR, photoreceptor; ONL, outer nuclear layer. Scale Bar 10μm.

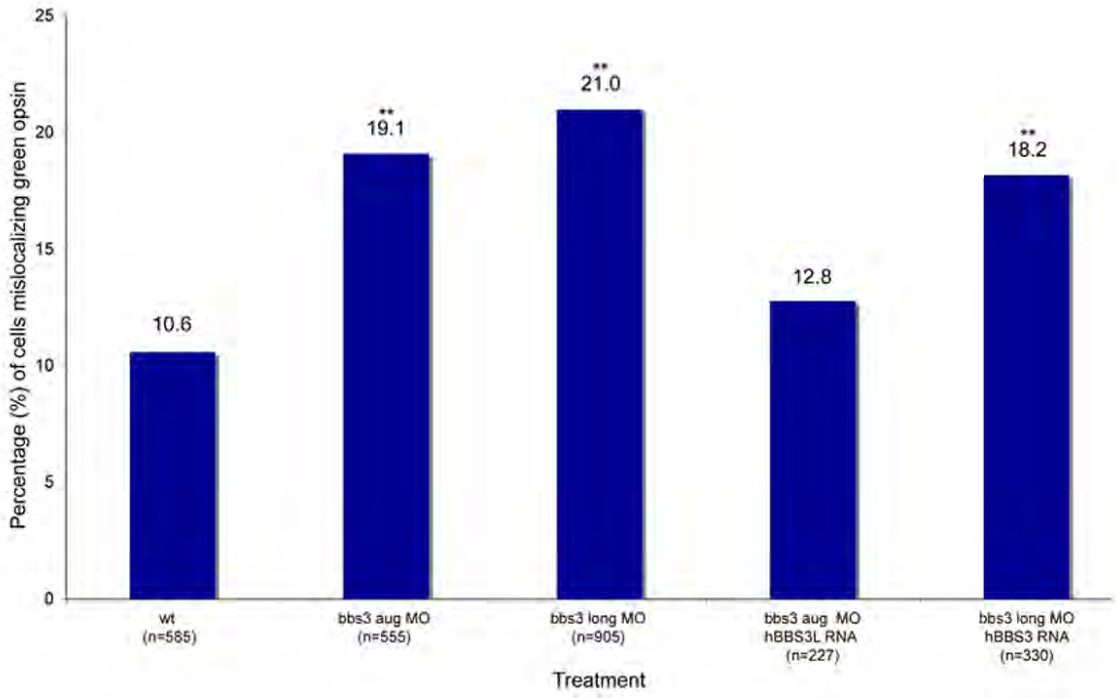

Figure 11 The percentage of cells mislocalizing green cone opsin. The sample size (n) is noted on the x-axis and represents the total number of green opsin positive cells counted. **Fisher's exact test, $p<0.01$.

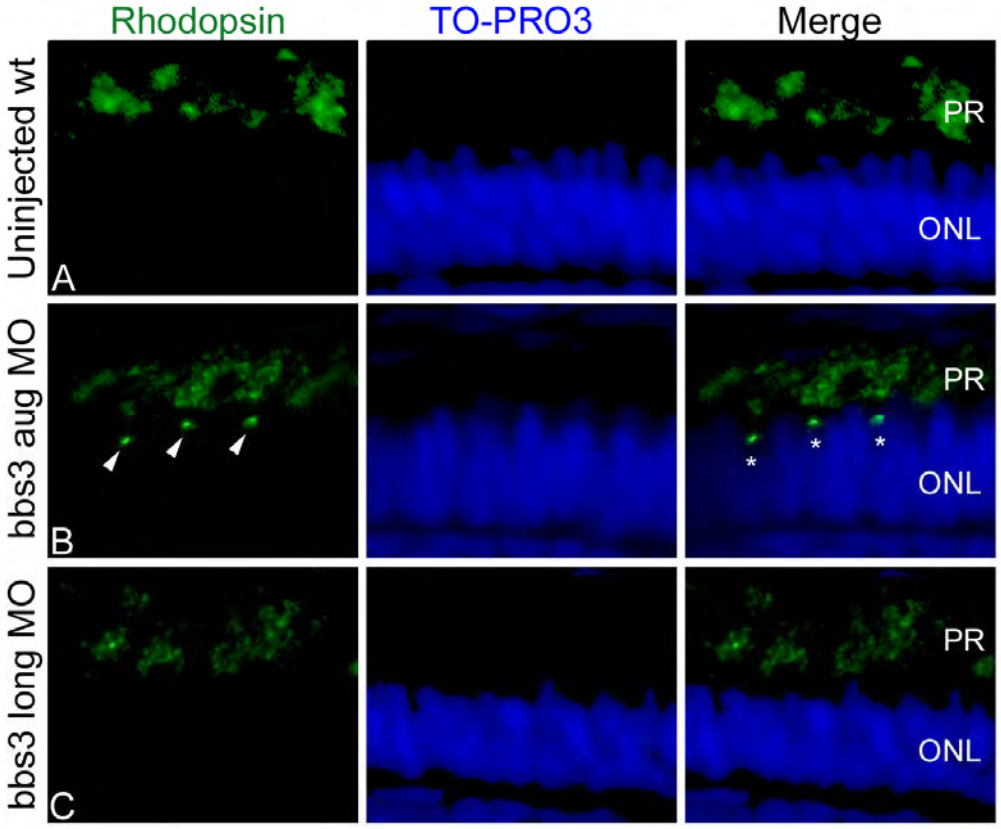

Figure 12 Rhodopsin mislocalization in 5-day old *bbs3* morphant zebrafish. Immunofluorescence of rhodopsin opsin (green) on transverse cryosections of 5-day old embryos (A) uninjected wild-type, (B) *bbs3* aug MO, (C) *bbs3* long MO injected embryos. To-Pro3 was used to counterstain the nuclei (blue). In *bbs3* aug injected embryos (B), rhodopsin was not restricted to the outer segment of the photoreceptors and was detected in the cell bodies of the outer nuclear layer (arrowheads and asterisks). PR, photoreceptor; ONL, outer nuclear layer.

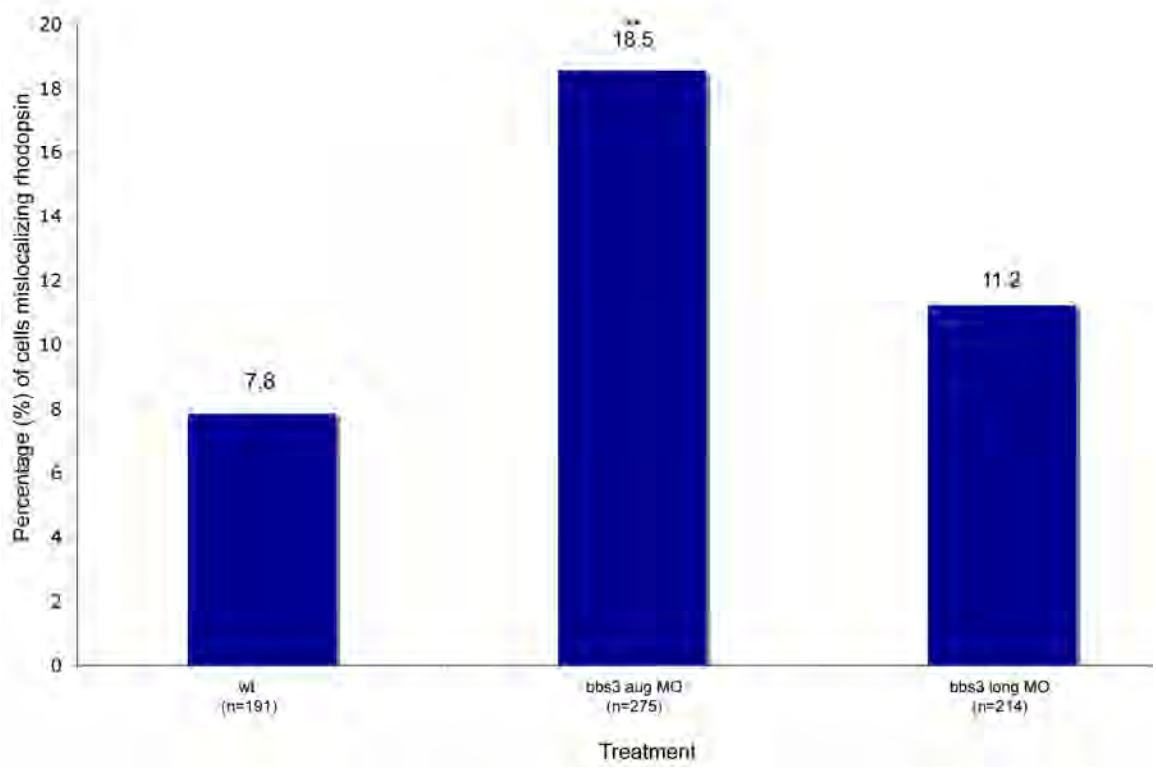

Figure 13 The percentage of cells mislocalizing rhodopsin. The sample size (n) is noted on the x-axis and represents the total number of green opsin positive cells counted. **Fisher's exact test, $p<0.01$.

Table 3 Summary of vision startle assay and percentage of green cone opsin mislocalization

	Vision (# of responses)	n	Mislocalized green opsin(%)	n
wild-type	3.09	181	10.6	585
bbs3 aug MO	1.81^{++}	168	19.1**	555
bbs3 aug MO + hBBS3 RNA	2.13^{++}	54	20.4**	496
bbs3 aug MO + hBBS3L RNA	3.25	53	12.8	227
bbs3 long MO	1.77^{++}	158	21.0**	905
bbs3 long MO + hBBS3 RNA	1.88^{++}	40	18.8**	330
bbs3 long MO + hBBS3L RNA	2.70	53	10.9	357
hBBS3 RNA	1.50^{++}	44	NA	NA
hBBS3L RNA	2.53	17	NA	NA

$^{++}$ANOVA with Tukey test, $p<0.01$ as compared to wild-type

**Fisher's exact test, $p<0.01$ as compared to wild-type

n, sample size

NA, not evaluated

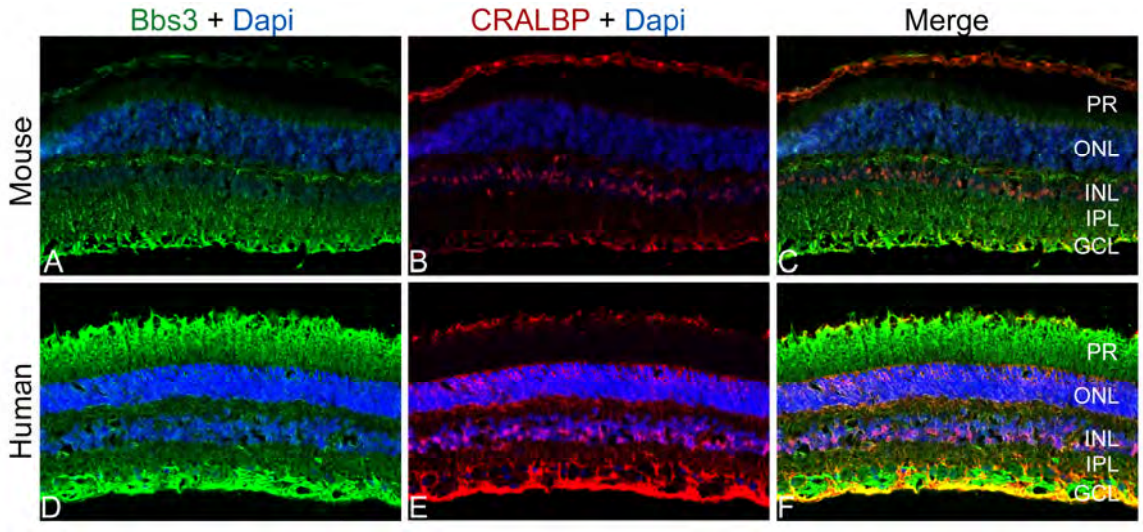

Figure 14 Localization of BBS3 to the ganglion cell layer in human and wild-type mouse retinas. Immunohistochemistry triple labeling of cryosections taken from 8-month old wild-type mouse retinas (A-C) and human donor eyes (D-F). Localization of BBS3 (green) using an antibody generated against a central region of the mouse Bbs3 peptide, which recognizes both Bbs3 and Bbs3L (A and D). Cellular retinaldehyde-binding protein (CRALBP, red) was used as a marker for Muller cells (B and E). Nuclei were counterstained with DAPI (blue). Bbs3 was found robustly in the ganglion cell layer of human and mouse retinas. PR, photoreceptor; ONL, outer nuclear layer; INL, inner nuclear layer; IPL, inner plexiform layer; GCL, ganglion cell layer.

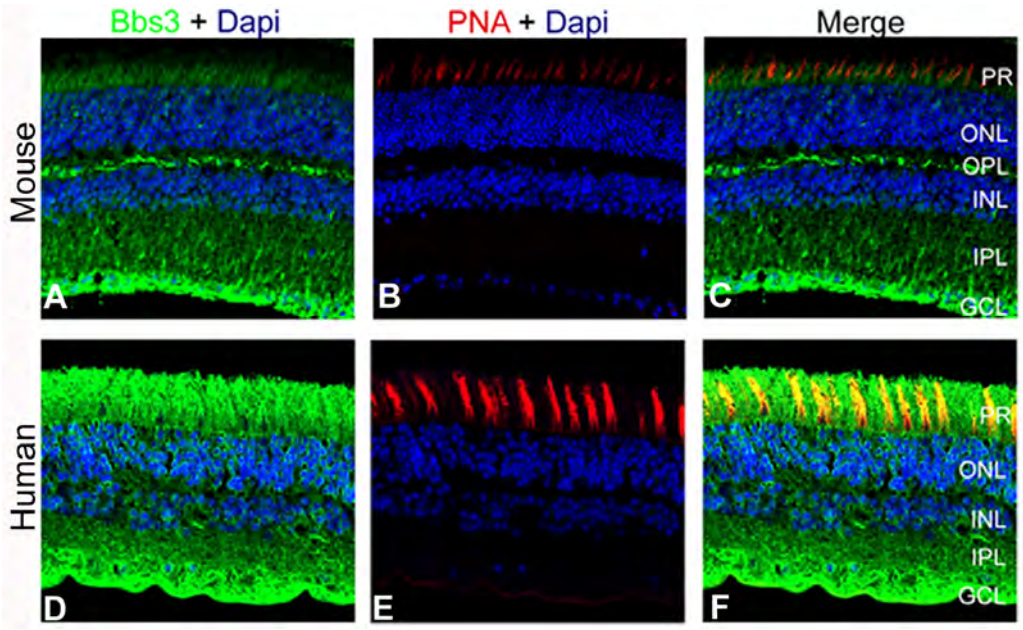

Figure 15 Localization of BBS3 to the photoreceptor cell layer in human and wild-type mouse retinas. Immunohistochemistry triple labeling of cryosections taken from 8-month old wild-type mouse retinas (A-C) and human donor eyes (D-F). Localization of BBS3 (green) using an antibody generated against a central region of the mouse Bbs3 peptide, which recognizes both Bbs3 and Bbs3L (A and D). Peanut agglutinin (PNA, red) was used as a marker for cone outer segments (B and E). Nuclei were counterstained with DAPI (blue). Bbs3 was found robustly in the ganglion cell layer as well as the photoreceptor cell layer of human and mouse retinas. PR, photoreceptor; ONL, outer nuclear layer; OPL, outer plexiform layer; INL, inner nuclear layer; IPL, inner plexiform layer; GCL, ganglion cell layer.

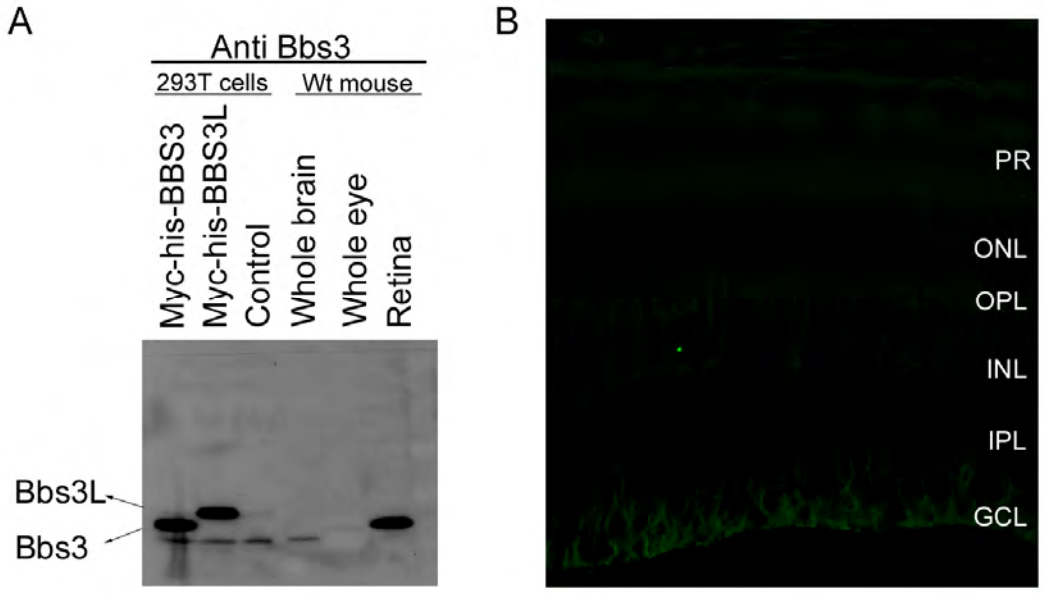

Figure 16 Specificity of the Bbs3 antibody (A) Western blot analysis of brain, whole eye (minus lens) and retina from adult wild-type mouse. Cell lysates from 293T cells transfected with either myc-his-BBS3 or myc-his-BBS3L served as controls. (B) Bbs3 antibody blocking with peptide. Peptide blocking was used to further confirm the specificity of the Bbs3 antibody on wild-type mouse tissue. PR, photoreceptor; ONL, outer nuclear layer; OPL, outer plexiform layer; INL, inner nuclear layer; IPL, inner plexiform layer; GCL, ganglion cell layer.

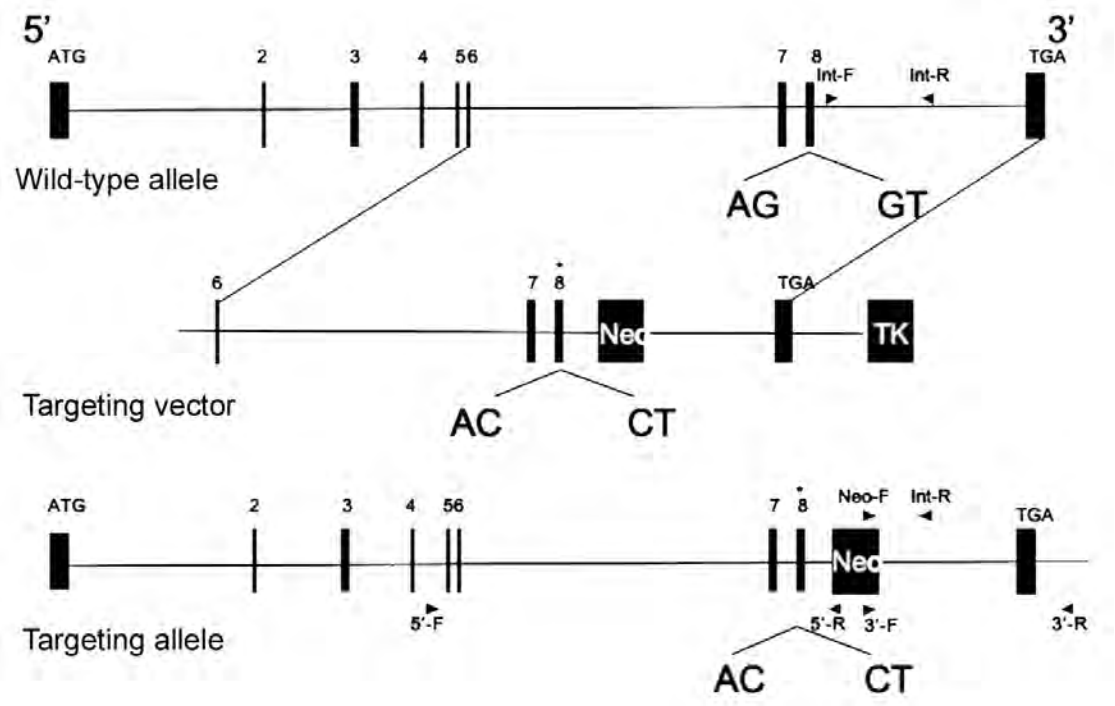

Figure 17 Generation of the *Bbs3L* mutant mice. A schematic for the targeted alteration of the splice donor and acceptor sites of exon 8 (asterisk) found in the Bbs3L transcript. Homologous recombination leads to the inclusion of these altered sites and the loss of Bbs3L specific exon.

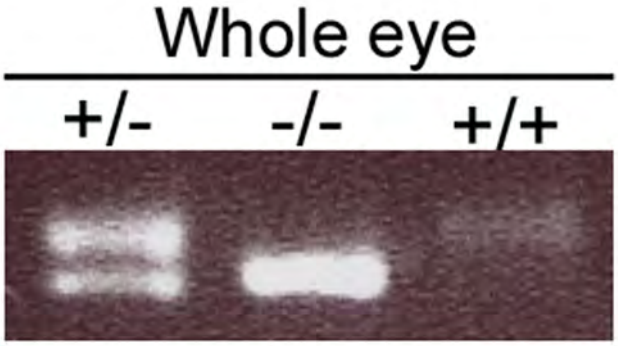

Figure 18 Expression of *Bbs3* and *Bbs3L* in *Bbs3L*-targetted mice. RT-PCR analysis of *Bbs3* and *Bbs3L* expression in the whole eye from heterozygous (+/-), homozygous (-/-) and wild-type (+/+) mice.

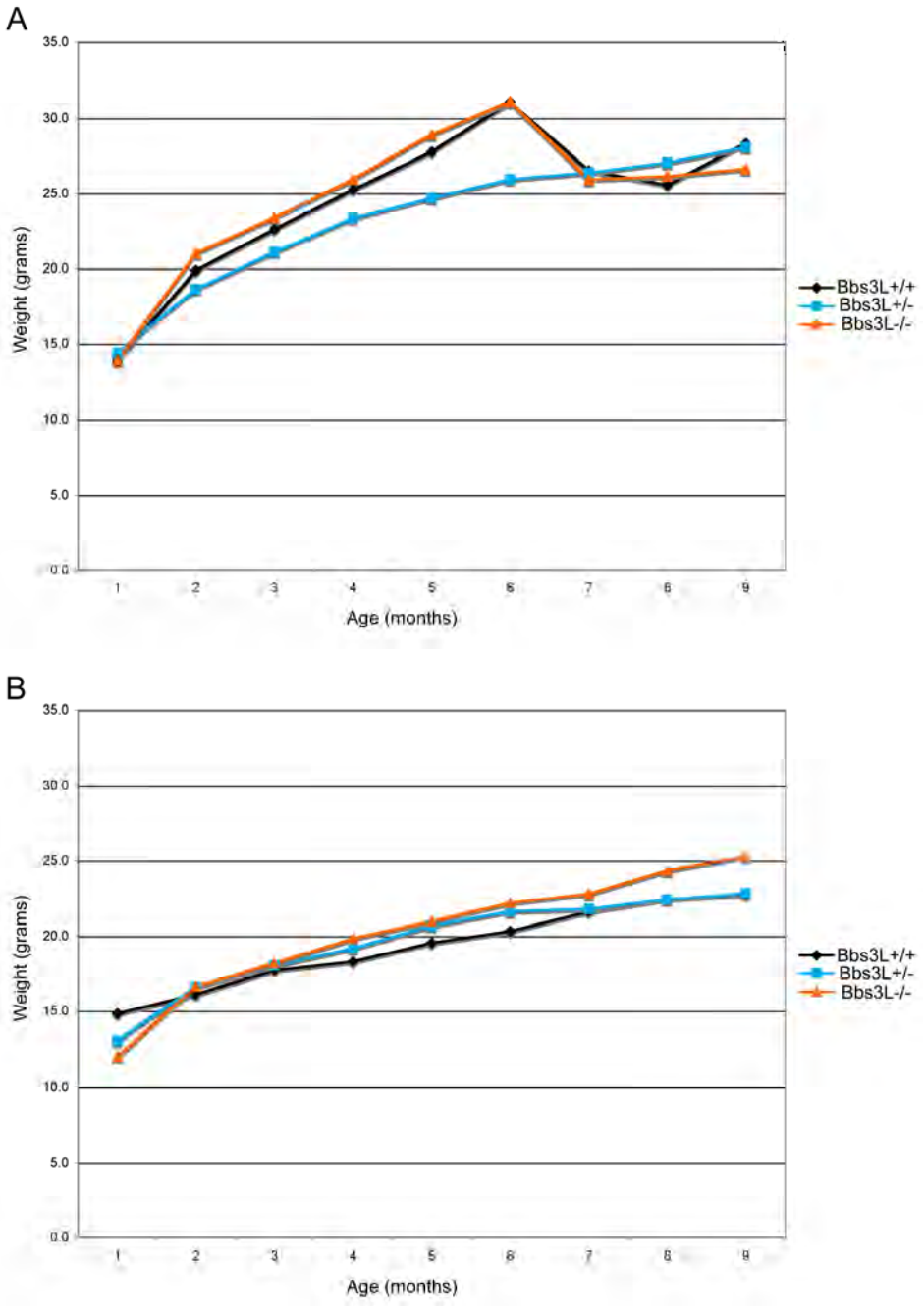

Figure 19 Weight gain by Bbs3L$^{+/+}$, Bbs3L$^{+/-}$ and Bbs3L$^{-/-}$ mice. (A) Bbs3L male mice weight verses age comparison. (B) Weight gain verses age in female Bbs3L mice.

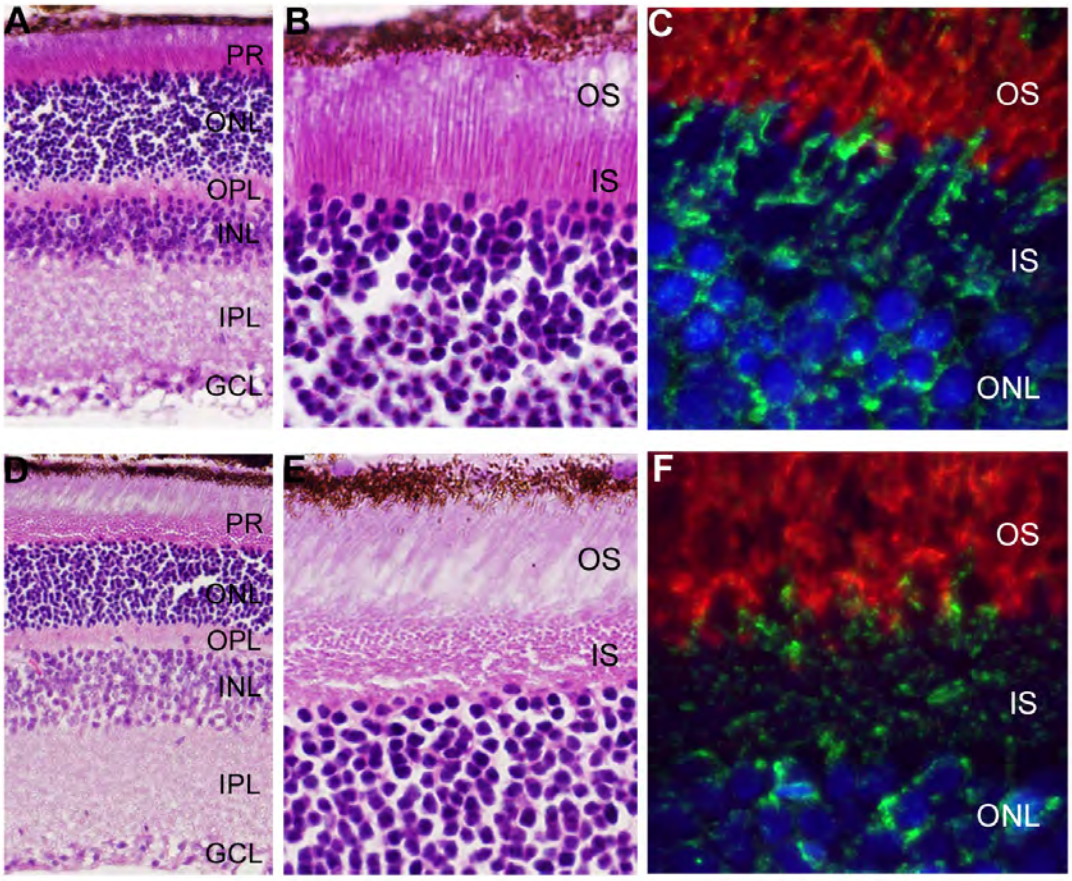

Figure 20 Initial characterization of the *Bbs3L* mutant mouse. Hematoxylin/eosin staining of cryosections from 8-month old *Bbs3L*$^{+/+}$ (A and B) and *Bbs3L*$^{-/-}$ (D and E) mouse retinas. Disruption of the normal photoreceptor architecture was observed in *Bbs3L*$^{-/-}$ mice. Immunohistochemistry analysis of cryosections from (C) wild-type and (F) targeted mutant retinas using the Bbs3 antibody (green) and rhodopsin (red), a marker for rod photoreceptor outer segments. To-Pro3 was used as a counterstain for nuclei. PR, photoreceptor; OS, outer segment; IS, inner segment; ONL, outer nuclear layer; OPL, outer plexiform layer; INL, inner nuclear layer; IPL, inner plexiform layer; GCL, ganglion cell layer.

CHAPTER III

FUNCTIONAL ANALYSIS OF BBS3 A89V THAT RESULTS IN NON-SYNDROMIC RETINAL DEGENERATION

Introduction

An autosomal recessive disorder, Bardet-Biedl Syndrome (BBS, OMIM 209900) is characterized by retinitis pigmentosa, obesity, polydactyly, renal abnormalities, hypogenitalism and cognitive impairment (Harnett et al. 1988; Green et al. 1989; Bardet 1995; Biedl 1995). Moreover, BBS patients are at an increased risk of developing hypertension, diabetes and heart defects (Harnett et al. 1988; Green et al. 1989; Elbedour et al. 1994). Treatment for several of the BBS phenotypes is currently available, for example polydactyly can be surgically corrected while obesity can be controlled with diet and exercise. No effective therapies are currently available to treat the early and progressive photoreceptor degeneration observed in patients (Riise 1987; Leys et al. 1988; Green et al. 1989; Jacobson et al. 1990; Fulton et al. 1993; Carmi et al. 1995a; Beales et al. 1997; Riise et al. 1997; Heon et al. 2005b). To date, 12 BBS (*BBS1-12*) genes are reported to individually cause BBS (Katsanis et al. 2000; Slavotinek et al. 2000; Mykytyn et al. 2001; Nishimura et al. 2001; Mykytyn et al. 2002; Ansley et al. 2003; Badano et al. 2003a; Chiang et al. 2004; Fan et al. 2004; Li et al. 2004; Nishimura et al. 2005; Chiang et al. 2006; Stoetzel et al. 2006b; Stoetzel et al. 2007). Additionally, hypomorphic mutations in *MKS1* and *CEP290* have been associated with BBS, representing *BBS13* and *BBS14* respectively (Leitch et al. 2008). The BBS genes belong to multiple protein families and function cannot be defined based on homology; however, recent advances in molecular pathophysiology and animal models have helped to elucidate why 14 different genes can lead to the same phenotype. Work in mouse, zebrafish, *Caunorhabditis elegans* and *Chlamydomonas* has provided multiple lines of evidence supporting a role for BBS proteins in cilia function and intraflagellar and/or

intracellular transport (Ansley et al. 2003; Blacque et al. 2004; Fan et al. 2004; Kulaga et al. 2004; Li et al. 2004; Mykytyn et al. 2004; Nishimura et al. 2004; Fath et al. 2005; Chiang et al. 2006; Yen et al. 2006; Davis et al. 2007; Tayeh et al. 2008). Although progress has been made in understanding the pathophysiology of BBS, there are major gaps in our understanding of the precise cellular function of the BBS proteins.

BBS3 (ARL6, ADP-ribosylation factor-like), a member of the Ras family of small GTP-binding proteins, was initially identified as a BBS gene through computational genomics and high-density Single Nucleotide Polymorphism (SNP) genotyping (Chiang et al. 2004; Fan et al. 2004). Several mutations (G2X, T31M, T31R, P108L, R122X, G169A and L170W) leading to BBS have been reported throughout BBS3 (Chiang et al. 2004; Fan et al. 2004; Pereiro et al. 2010). Knockdown of *bbs3* using an antisense oliognucleotide (Morpholino) results in two cardinal features of BBS in the zebrafish: reduced size of the ciliated Kupffer's Vesicle (KV) and delays in intracellular melanosome transport (Tayeh et al. 2008; Pretorius et al. 2010). These prototypical phenotypes are preset with knockdown of all BBS genes in the zebrafish (Chiang et al. 2006; Yen et al. 2006; Tayeh et al. 2008; Pretorius et al. 2010). Recently, we identified a second longer eye specific transcript of *BBS3*, *BBS3L*, which is required for retinal organization and function in both the mouse and zebrafish (Pretorius et al. 2010). Knockdown of either both *bbs3* transcripts or *bbs3L* alone leads to vision impairment in zebrafish. To determine the functional requirement of each transcript, RNA encoding either human *BBS3* or *BBS3L* was co-injected with the *bbs3* aug morpholino, which targets both transcripts. We determined that human *BBS3* RNA is sufficient to suppress the melanosome transport delays, but not the vision defect. In contrast, *BBS3L* RNA was sufficient to rescue the vision defect; however, it was unable to suppress the cardinal phenotypes of BBS seen in the zebrafish, supporting a retina specific role for BBS3L (Pretorius et al. 2010).

BBS is rare in the general population; however, the study of this disease can offer insight into normal retinal development as well as provide an understanding of the pathophysiology involved in non-syndromic forms of BBS. Homozygosity mapping of a consanguineous Saudi Arabian family has identified a missense mutation (A89V) in *BBS3* that leads to non-syndromic retinitis pigmentosa (Abu Safieh et al. 2009; Aldahmesh et al. 2009). The identification of specific mutations in the same gene that results in either syndromic or non-syndromic retinitis pigmentosa will provide insight into tissue specific functional regions of BBS3 in the retina. Moreover, understanding the functional domains of proteins involved in vision aids in our understanding of not only the disease state, but also normal vision development.

Here we report the functional characterization of the *BBS3* missense mutation (A89V), which occurs in a highly conserved region of BBS3. The function of the BBS3 A89V mutation was evaluated by utilizing gene knockdown of *bbs3* coupled with RNA rescue in the zebrafish. We examined the intracellular transport of melanosomes, a cardinal feature of BBS gene knockdown in the zebrafish, and visual function using a vision startle assay. The A89V mutation can suppress the melanosome transport defects, but not the vision impairment observed with loss of *bbs3*. Thus, the missense mutation identified in patients with non-syndromic retinal degeneration has uncovered an amino acid in BBS3 that is necessary for vision. The A89V mutation is able to function in melanosome transport, demonstrating that the mutant form of the protein retains the ability to function in tissues typically affected by BBS. Additionally, preliminary studies examining the overexpression of mutant forms of BBS3 were performed to elucidate the molecular and cellular functions of several key BBS3 amino acids. The mutations investigated include a G2A mutation, which should abolish the predicted myristoylation of BBS3, T31R which locks BBS3 in a GDP-bound state (inactive) and Q73L, a constitutively active (GTP-bound) form of the protein. Overexpression of BBS3 G2A and Q73L resulted in vision impairment. This was the only overexpression phenotype

observed with any of the mutations. Finally, the functional difference between the two BBS3 isoforms was evaluated in progenitor cells of the undifferentiated retina. These studies revealed that BBS3 and BBS3L have a similar cytoplasmic distribution throughout the cell.

Materials and methods

Ethics Statement

The University Animal Care and Use Committee at the University of Iowa approved all animal work in this study.

Animal care

Adult zebrafish were maintained under standard conditions and embryos collected from natural spawnings (Westerfield 1993). Embryos were staged using previously described criteria (Kimmel et al. 1995).

Conservation

Using the Ensemble genome (release 59), orthologs to *BBS3* were identified by performing BLAST algorithms with the human *BBS3* sequence (ENST00000335979). Sequences were aligned using ClustalW (Larkin et al. 2007).

Morpholino injections

Antisense morpholinos (MO) were air pressure injected into one- to four-cell staged embryos at a concentration of 12 ng for *bbs3* and 1 ng for *crx*.

Morpholino sequences:

bbs3_aug (Tayeh et al. 2008; Pretorius et al. 2010): AGCTTGTCAAAAAGCCCCATTTGCT

crx (Shen and Raymond 2004): ATGTAGGACATCATTCTTGGGACGG

DNA constructs and RNA synthesis

The G2A, T31R, Q73L and A89V mutation were generated by introducing the appropriate nucleotide change into C-terminally myc tagged hBBS3 or hBBS3L constructs using the Quick Change II site-directed mutagenesis kit (Stratagene).

Primers:

BBS3 G2A-F: 5'-GAATGCCACCATGGCATTGCTAGACA-3'

BBS3 G2A-R: 5'-GTCTGTCTAGCAATGCCATGGTGGCA-3'

BBS3 T31R-F: 5'-GATAATAGTGGCAAAAGGACGATCATTAACAAAC-3'

BBS3 T31R-R: 5'-GTTTGTTAATGATCGTCCTTTTGCCACTATTATC-3'

BBS3 Q73L-F: 5'-GTTTGACATGTCAGGTCTAGGAAGATACAGAAATC-3;

BBS3 Q73L-R: 5'-GATTTCTGTATCTTCCTAGACCTGACATGTCAAAC-3'

BBS3 A89V-F: 5'-GGAACACTATTATAAAGAAGGCCAAG-3'

BBS3 A89V-R: 5'-CACTACTATCAATGACAAAAATAATAA-3'

RNA was synthesized using the mMessage mMachine transcription kit (Ambion) and injected into 1-2 cell embryos at a concentration of 8 pg.

Melanosome transport assay

The melanosome transport assay was performed as previously described (Chiang 2006; Yen 2006; Tayeh 2008). Briefly, epinephrine (500 μL/mL, Sigma E437) treatment was applied to dark-adapted 6-day-old embryos. The movement of the melanosomes from the periphery to the perinuclear region was timed and recorded. A stereoscope equipped with a Zeiss Axiocam camera was used to image live embryos.

Vision startle response

Zebrafish embryos change swimming directions in response to rapid changes in light intensity. Prior to performing the vision startle assay, 5 day post-fertilized (dpf) embryos were light adapted for 1 hour. Embryos were exposed to five trials of rapid changes in light intensity spaced at 30 second intervals and the response, a distinct C-

bend, scored (Nishimura et al. 2010; Pretorius et al. 2010). Cone-rod homeobox (*crx*) gene knockdown was used as a control for vision impairment. To ensure motility, embryos were probed with a blunt needle on their flank, invoking the same response observed in the vision assay.

Statistical analysis

Statistics for both the melanosome transport and vision startle assay were calculated using the One-Way Analysis of Variance (one-way ANOVA) paired with the Tukey Honestly Significant Difference (HSD) test.

Western blot

Embryos were injected with C-terminal myc-tagged human *BBS3L* (8pg) and *BBS3L A89V* (8pg) RNA at the 1-2 cell stage. Embryos (n=15) were collected at the following time points: 72 hpf, 4 dpf and 5 dpf. Collected embryos were homogenized in lysis buffer (20mM Tris; 100mM NaCl; 1mM EDTA; 0.5% Triton X-100; 0.5% SDS) with protease inhibitor (0.1 mM PMSF (Roche); 10 μg/mL Leupeptin (Roche)) and the supernatant collected. Whole cell lysates were run and transferred using the X Cell SureLock Mini-Cell System under reduced conditions (Invitrogen). Samples were mixed with NuPAGE LDS Sample Buffer and NuPAGE Reducing Agent (Invitrogen), heated at 70°C for 10 minutes and run on a pre-cast 4-12% NuPAGE Novex Bis-Tris gel (Invitrogen). Protein was transferred to a PVDF membrane (Amersham) for film development and to nitrocellulose membranes (Li-Cor Biosciences) for fluourescence detection. For film development the membrane was blocked in 5% milk (Carnation) for 1 hour and then probed with either mouse monoclonal anti-Myc (1:2000, 9B11, Cell Signaling) or rabbit polyclonal anti-actin (1:2000, Sigma) antibody overnight at 4°. Horseradish peroxidase-conjugated species-specific secondary antibodies (1:10,000, Jackson ImmunoResearch) were used for detection of primary antibodies. For fluorescence detection the membrane was blocked in Odyssey Blocking Buffer (Li-Cor

Biosciences) for 1 hour at room temperature. Following blocking, the membrane was incubated with mouse anti-myc (1:2000, Cell Signaling) and rabbit anti-actin (1:2000, Sigma) primary antibody diluted in Odyssey Blocking Buffer for 1 hour at room temperature. A species-specific fluorescently labeled secondary antibody was diluted in Odyssey Blocking Buffer (1:10,000, Li-Cor Biosciences) and incubated for 45 minutes before scanning and analyses with the Odyssey Infrared Imaging Scanner (Li-Cor Biosciences).

Heat shock

DNA was injected into embryos at the one-two cell stage to generate transient transgenics that mosaically expressed the gene product. Embryos were maintained in 0.003% phenylthiourea (PTU) beginning at 70% epiboloy to minimize pigmentaion of the retinal pigmented epithelium (RPE). At 20 hpf, embryos were collected and heat shocked for 30 minutes at 37˚C. Following heat shock embryos were transferred to fresh egg water and maintained under standard conditions until imaging was performed. Embryos were screened for protein expression using a standard fluorescent microscope to detect the eGFP tag of the gene product. Expression of the downstream gene product was typically observed 30 minutes to an hour after heat shock application.

Confocal imaging of BBS3 localization

At 24 hpf, live embryos were anesthetized with Tricane (RPI) and embedded in 1% low melt agarose (IBI Scientific) on a coverslip. Embryos were oriented such that the eye was facing up. BBS3-GFP positive cells were imaged with a Leica SP2 laser confocal microscope system and images colleted at 63x magnification and 3x zoom at 1μm steps. Transmitted light images were also collected and overlayed with the fluorescence images. Images are representative of maximum projections of multiple focal planes (*z*-series).

Results

BBS3 conservation and BBS3L mutant expression

Previous homozygosity mapping with a consanguineous family from Saudi Arabia identified a novel missense mutation (A89V) in *BBS3* that results in non-syndromic retinitis pigmentosa (Abu Safieh et al. 2009; Aldahmesh et al. 2009). Comparison across vertebrate species with available full-length BBS3 sequences demonstrates that the A89V mutation occurs in an evolutionarily conserved region of the protein, suggesting that the alanine at position 89 (A89V) may have an essential function within the protein (Figure 21). The location of the mutation upstream of the C-terminus would impact both BBS3 and BBS3L, as this region is identical between the two isoforms (Figure 22). Additionally, the missense mutation is located downstream of the phosphate binding loop (P-loop), which is important for binding triphosphates of the GTP nucleotide (Wiens et al. 2010). To test whether BBS3L A89V is stably expressed in the developing zebrafish we performed Western blot analysis on embryos injected with either myc-tagged BBS3L or BBS3L A89V. Using an antibody against myc to detected the tagged protein, we found that similar to BBS3L, the missense mutation was present through 5 days post fertilization (dpf) (Figure 23). Thus, the BBS3 A89V missense mutation is in an evolutionally conserved region of the protein and would be present in both BBS3 and BBS3L. Moreover, the mutation does not impact BBS3L stability.

BBS3 A89V functions in melanosome transport

Knockdown of *bbs3* using a morpholino (MO) that targets both transcripts (bbs3 aug MO) results in intracellular melanosome transport delay, a phenotype related to syndromic disease and shared among all BBS genes (Chiang et al. 2006; Yen et al. 2006; Tayeh et al. 2008; Pretorius et al. 2010). In response to light or hormonal stimuli, zebrafish alter their skin pigmentation through intracellular melanosome transport within the melanophore (Marks and Seabra 2001; Blott and Griffiths 2002; Skold et al. 2002;

Barral and Seabra 2004). To test the rate of cellular trafficking, 6-day old zebrafish embryos were dark adapted and treated with epinephrine to induce retrograde melanosome transport (Figure 24A). Retrograde transport results in the movement of the dispersed melanosomes to a perinuclear location (Figure 24B). Rescue experiments were performed by co-injecting RNA encoding hBBS3 or hBBS3 A89V with the bbs3 aug MO. Wild-type embryos demonstrate rapid melanosome movement, averaging 1.45 minutes, whereas knockdown of bbs3 leads to a statistically significant delay in transport (ANOVA with Tukey, $p<0.01$) (Figure 24C and Table 4). We have previously demonstrated that human BBS3, but not human BBS3L, can suppress the melanosome transport delays, thus we focused on *BBS3* to investigate the role of the *A89V* mutation in syndromic disease (Pretorius et al. 2010). Similar to *BBS3* RNA, co-injection of *BBS3 A89V* RNA with the *bbs3* aug MO can restore transport times to wild-type levels (Figure 24C and Table 4). These results demonstrate that the BBS3 A89V missense mutation can function to suppress the cardinal BBS phenotype of intracellular melanosome transport. This is consistent with the observation that the human patients harboring the BBS3 A89V mutation do not present with BBS related phenotypes, such as obesity, polydactyly, renal anomalies or cognitive impairment.

BBS3L A89V does not function in vision

Both the mouse and zebrafish model systems have demonstrated that BBS3L is necessary for proper retinal function. Additionally, rescue experiments in the zebrafish have shown that human BBS3L is sufficient to suppress the *bbs3* aug MO-induced vision defect (Pretorius et al. 2010). Since patients with the BBS3 A89V mutation present with only retinitis pigmentosa, we sought to functionally test the role of this mutation in vision by co-injecting *BBS3L* and *BBS3L A89V* RNA in *bbs3* knockdown embryos. Visual function was evaluated by using a natural escape response that is elicited when zebrafish embryos are exposed to rapid changes in light intensity (Easter and Nicola 1996;

Pretorius et al. 2010). In the vision startle assay, an embryos response to five short blocks in bright light are monitored and recorded. Visually responsive embryos change swimming directions in response to short blocks of bright light (Figure 25A). Wild-type embryos respond on average 3.77 times (Figure 25B and Table 5). Cone-rod homeobox (*crx*) gene knockdown was used as a control for vision impairment as *crx* is necessary for photoreceptor formation in the zebrafish (Liu et al. 2001; Shen and Raymond 2004). *crx* knockdown embryos respond an average of 2.39 times, indicative of vision impairment (Figure 25B and Table 5) (ANOVA with Tukey, $p<0.01$). *bbs3* aug MO injected embryos show a statistically significant (ANOVA with Tukey, p,0.01) reduction in the number of responses as compared to wild-type (Figure 25B and Table 5) (Pretorius et al. 2010). Co-injection of *BBS3L* RNA with the *bbs3* aug MO restored visual responsiveness back to wild-type levels, indicating that *BBS3L* RNA was sufficient to rescue vision (Figure 25B and Table 5). Conversely, *BBS3L A89V* RNA was not able to restore visual function back to wild-type levels as embryos responded on average 1.60 times (Figure 25B and Table 5). Western blot analysis confirms expression of hBBS3L A89V through 5 dpf, when the vision assay is performed (Figure 23). The inability of *BBS3L A89V* to restore vision provides strong functional support that this missense mutation leads to non-syndromic retinitis pigmentosa.

Structural-functional characterization of BBS3

Although it has been proposed that BBS3 plays a role in BBSome localization to the cilia, little is known about the precise function of BBS3 in its regulation of diverse cellular processes (Jin et al. 2010). A member of the Ras superfamily of small GTPases, BBS3 cycles between a GDP-bound inactive state and a GTP-bound active state. To address questions concerning the function of key regions of BBS3, three point mutations were characterized. The first mutation, a glycine to alaninine change at position two (G2A) is predicted to ablate myristoylation and possible disrupt BBS3 localization to the

membrane (Figure 26). Two mutations, a T31R mutation, which locks the protein in an inactive GDP-bound state, and a Q73L mutation, which locks the protein in a GTP-bound or active state, were used to characterize the proteins GTPase activity (Figure 26) (Wiens et al. 2010). Additionally, the BBS3 T31R mutation has also been associated with BBS patients (Fan et al. 2004). To test whether the point mutations were stably expressed Western blot analysis was performed on embryos injected with myc-tagged BBS3 or BBS3 containing either the G2A, T31R or Q73L mutation. While BBS3 was robustly expressed through 5 dpf (Figure 27A), expression of the point mutations was only observed through 24 hpf (Figure 27B), suggesting that these mutations impact protein stability.

To evaluate these point mutations for overexpression defects the individual RNAs were injected and the cardinal features of BBS, KV defects and intracellular transport delays, as well as vision evaluated. Overexpression of the mutant forms of BBS3 resulted in no KV or melanosome transport defects. Interestingly the only phenotype observed was visual impairment with overexpression of either *BBS3 G2A* or *BBS3 Q73L* (Table 6). This is an interesting observation, as overexpression of wild-type *BBS3* results in KV defects as well as visual impairment (Table 2 and 3), suggesting that these mutations might have some impact on BBS3 function.

Localization of heat shock BBS3 and BBS3L in the retina

Previous studies have demonstrated that BBS3 and BBS3L are not functionally redundant. This lack of redundancy could be a result of either differential localization within the cell or due to different binding partners (Pretorius et al. 2010). To further elucidate the functional differences between the two *BBS3* transcripts, the localization of BBS3 and BBS3L was investigated in the zebrafish retina. Additionally, introduction of mutations, such as those described above, may also impact protein localization. Therefore, a pilot study examining wild-type BBS3 and BBS3L expression in the

zebrafish retina was performed. To temporally regulate BBS3 and BBS3L expression the two transcripts were independently cloned downstream of the heat-shock-inducible promoter (Figure 28). Temporal regulation of genes allows for easy assessment of protein localization at later points in development, and also allows for closer recapitulation of BBS3L expression, as this transcript is not endogenously expressed until 42 hpf (Pretorius et al. 2010). To evaluate BBS3 and BBS3L expression DNA was injected into the 1-4 cell staged. Injection of DNA into zebrafish embryos results in a mosaic pattern of expression and allows for the assessment of single cells. Once the embryos have developed to the appropriate time, in this case, 24 hpf, the promoter is activated upon the application of heat, thus turning on the downstream gene of interest (Kwan et al. 2007). Using these heat shock constructs, questions can be asked concerning the role of *BBS3* in different cell types (i.e. undifferentiated versus differentiated) over the course of zebrafish retinal development. Localization of hBBS3 and hBBS3L was evaluated in the undifferentiated retina (progenitor cells) following heat shock. Confocal analysis of 24 hpf zebrafish retina reveals that hBBS3 and hBBS3L have similar cytoplasmic distribution in the undifferentiated retina (Figure 29).

Discussion

The present study utilizes the zebrafish to examine the function of BBS3 A89V in intracellular transport, a phenotype associated with the knockdown of BBS genes, and vision. This mutation was identified in a consanguineous Saudi Arabian family that presented with only retinitis pigmentosa (Abu Safieh et al. 2009; Aldahmesh et al. 2009). The polymorphism phenotyping program, PolyPhen, predicts that the BBS3 A89V missense mutation is a benign non-synonomous SNP; however, the alanine at position 89 is highly conserved in vertebrates, suggesting that this amino acid has an essential function. Using RNA rescue experiments we demonstrate that unlike *BBS3L* RNA, the *BBS3L A89V* RNA does not rescue the vision defect observed with loss of *bbs3*.

Although the A89V mutation is not functional in vision, *BBS3 A89V* RNA is able to suppress the cardinal zebrafish BBS phenotype of melanosome transport. Taken together, these data demonstrate that the BBS3 A89V mutation identified in patients with non-syndromic retinal degeneration is critical and specific for the vision defect.

This study highlights the importance of functionally evaluating mutations that fall within different splice variants of a single gene for disease or tissue specific relevance. It is estimated that alternative splicing affects 94% of multi-exon human genes (Pan et al. 2008; Wang et al. 2008). Multiple splice isoforms with potentially diverse functions can be generated from a single gene, thus contributing to phenotypic complexity in disease. Recently, a retina specific splice variant was identified for another BBS gene, *BBS8* (Riazuddin et al. 2010). A splice-site mutation was identified in *BBS8* that resulted in the skipping of a retina specific exon (Riazuddin et al. 2010). This mutation results in affected individuals presenting with non-syndromic retinitis pigmentosa, similar to what was observed with patients harboring the BBS3 A89V missense mutation (Riazuddin et al. 2010). While the *BBS3 A89V* mutation does not fall within in a splice-site, it is located such that it impacts both the canonical BBS isoform as well as the eye specific BBS3L isoform. Thus, mutations targeting a gene with multiple isoforms can have different affects on disease presentation.

Our finding that the BBS3 A89V missense mutation is specific for vision demonstrates that this region is important for proper function of the protein in the eye. While no known domains are predicated to map to this region of BBS3, it is possible that the A89V mutation abrogates the interaction of BBS3 with a retina specific modifier and/or retina specific binding partner. Mutations in another BBS gene, centrosomal protein 290 (CEP290), also result in phenotypic variation. This gene has been implicated in numerous diseases, in particular BBS and isolated blindness (Coppieters et al. 2010). While this gene has been implicated in several syndromic diseases, a mouse model for Cep290, the rd16 mouse in which a few exons of the gene are missing, only manifests

early onset retinal degeneration (Chang et al. 2006). Moreover, additional splice isoforms are predicted for Cep290 and Western blot analysis supports the notion that there are retina specific isoforms (Chang et al. 2006). These observations for BBS8, Cep290 and now BBS3 indicate that mutations need to be evaluated in the context of both isoform and tissue specificity. Moreover, this study highlights the importance of functionally testing human disease mutations to further elucidate their underlying pathophysiology in disease.

This study also provides an initial characterization of three mutations (G2A, T31R and Q73L) that should abrogate the normal function of BBS3 through pilot overexpression studies in the zebrafish. Three phenotypes were evaluated, alterations to the KV, defects in intracellular trafficking and impairment of vision. Interestingly, prevention of BBS3 myristoylation (G2A) and locking BBS3 in the active state (Q73L) leads to visual impairment. While I am hesitant to make inferences from only overexpression studies, it does suggest that these point mutations do not inactivate the protein. Additional studies should be performed to investigate the ability of these mutations to rescue either the cardinal features of BBS or visual impairment. Finally, these studies demonstrate that BBS3 and BBS3L have similar cytoplasmic distribution in the undifferentiated (progenitor cells) zebrafish retina at 24 hpf. It will be interesting to evaluate BBS3 and BBS3L expression at later time points, such as 5 dpf when the zebrafish retina has differentiated and functional cone cells are present. Moreover, localization of BBS3 point mutations (G2A, T31R, Q73L and A89V) in both the undifferentiated (progenitor cells) and differentiated (photoreceptor cells) in the zebrafish retina will provide additional information concerning the mechanism of BBS3 and BBS3L function in the eye.

```
H. sapien       MGLLDRLSVLLGLKKKEVHVLCLGLDNSGKTTIINKLKPSNAQSQNILPTIGFSIEKFKS 60
P. troglodytes  MGLLDRLSVLLGLKKKEVHVLCLGLDNSGKTTIINKLKPSNAQSQNILPTIGFSIEKFKS 60
C. familiaris   MGLLDRLSGLLGLKKKEVHVLCLGLDNSGKTTIINKLKPSNAQSQDIVPTIGFSIEKFKS 60
R. nervegicus   MGLLDRLSGLLGLKKKEVHVLCLGLDNSGKTTIINKLKPSNAQVQDIVPTIGFSIEKFKS 60
M. musculus     MGLLDRLSGLLGLKKKEVHVLCLGLDNSGKTTIINKLKPSNAQSQDIVPTIGFSIEKFKS 60
B. taurus       MGLLDRLSGLLGLKKKEVHVLCLGLDNSGKTTIINKLKPSNAQSQDIVPTIGFSIQKFKS 60
D. rerio        MGLFDKLAGWLGLKKKEVNVLCLGLDNSGKTTIINQLKPSNAQAQDIVPTIGFSIEKFKT 60
T. rubripes     MGLFDKLAGWLGLKK-EVNVLCLGLDNSGKTTIINRLKPSNAQAQDIVPTIGFSIEKFKT 59
                ***:*:*:  ***** **:****************:******* *:*:*******:***:

H. sapien       SSLSFTVFDMSGQGRYRNLWEHYYKEGQAIIFVIDSSDRLRMVVAKEELDTLLNHPDIKH 120
P. troglodytes  SSLSFTVFDMSGQGRYRNLWEHYYKEGQAIIFVIDSSDRLRMVVAKEELDTLLNHPDIKH 120
C. familiaris   SSLSFTVFDMSGQGRYRNLWEHYYKEGQAIIFVIDSSDRLRMVVAKEELDTLLNHPDIKH 120
R. nervegicus   SSLSFTVFDMSGQGRYRNLWEHYYKDGQAIIFVVDSSDKLRMVVAKEELDTLLNHPDIKH 120
M. musculus     SSLSFTVFDMSGQGRYRNLWEHYYKDGQAIIFVIDSSDKLRMVVAKEELDTLLNHPDIKH 120
B. taurus       SSLSFTVFDMSGQGRYRNLWEHYYKEGQAIIFVIDSSDKLRMVVAKEELRTLLNHPDIKH 120
D. rerio        SSLSFTVFDMSGQGRYRNLWEHYYKEGQAIIFVIDSGDKLRMVVAKEELDTLLNHPDIKH 120
T. rubripes     SSLSFTVFDMSGQGRYRNLWEHYYKEGQAIIFVIDSADKLRMVVAKEELDTLLNHPDIKH 119
                ************************:*******:**.*:********** **********

H. sapien       RRIPILFFANKMDLRDAVTSVKVSQLLCLENIKDKPWHICASDAIKGEGLQEGVDWLQDQ 180
P. troglodytes  RRIPILFFANKMDLRDAVTSVKVSQLLCLENIKDKPWHICASDAIKGEGLQEGVDWLQDQ 180
C. familiaris   RRIPILFFANKMDLRDAVTSVKVSQLLCLENIKDKPWHICASDAIKGEGLQEGVDWLQDQ 180
R. nervegicus   RRIPILFFANKMDLRDAVTSVKVSQLLCLENIKDKPWHICASDALKGEGLQEGVDWLQDQ 180
M. musculus     RRIPILFFANKMDLRDSVTSVKVSQLLCLESIKDKPWHICASDAIKGEGLQEGVDWLQDQ 180
B. taurus       RRIPILFFANKMDLRDALTSVKVSQLLCLEDIKDKPWHICASDAIKGEGLQEGVDWLQDQ 180
D. rerio        RRIPLLFFANKMDLRDALSAVKVSQLLCLENIKDKPWHICASDAVKGEGLLEGVDWLQDQ 180
T. rubripes     RRIPILFFANKMDVRDALSSVKVSQLLCLENIKDKPWHICATDALKGEGLQEGVDWLQDQ 179
                ****:********:**::::**********.**********:**:***** *********

H. sapien       IQTVKT 186
P. troglodytes  IQTVKT 186
C. familiaris   IQAVKT 186
R. nervegicus   IQAVKT 186
M. musculus     IQAVKT 186
B. taurus       IQSVKT 186
D. rerio        IRAMKT 186
T. rubripes     IKTIKT 185
                *:::**
```

Figure 21 Multi-species alignment of BBS3 demonstrating the conservation among vertebrates. Shaded box highlights the sight of the A89V mutation. Asterisks (*) indicate identical amino acids, while colons (:) and periods (.) represent conserved amino acids.

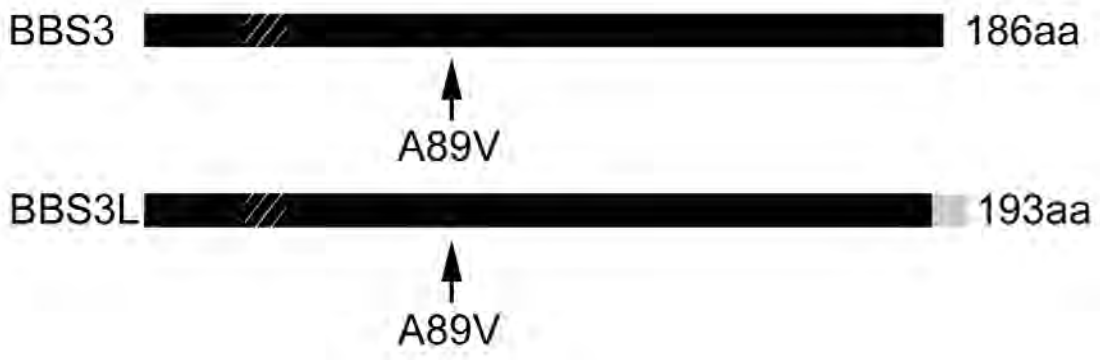

Figure 22 Schematic depicting the location of the A89V mutation in human BBS3 and BBS3L isoforms. The hatched box depicts the location of the P-loop motif and the grey box on the C-terminus of BBS3L denotes the region of difference between the two isoforms.

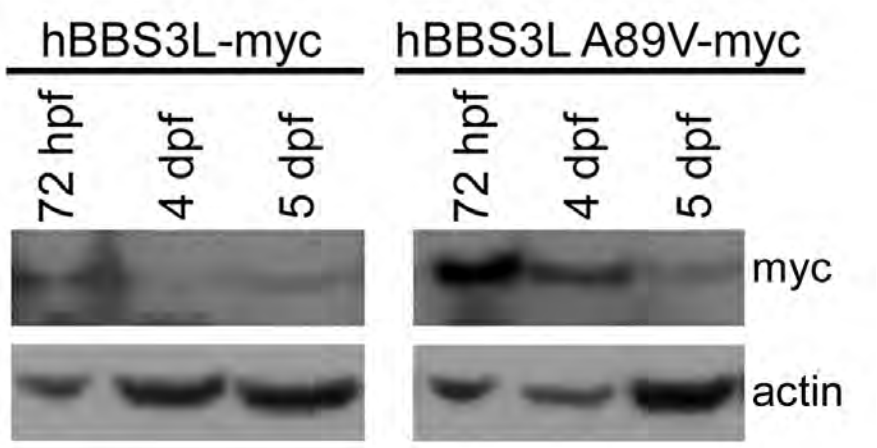

Figure 23 BBS3L and BBS3L A89V protein expression. Western blot analysis of staged zebrafish embryos injected with either hBBS3L or hBBS3L A89V myc-tagged RNA. Both proteins are present through 5 days post fertilization. Actin served as a control.

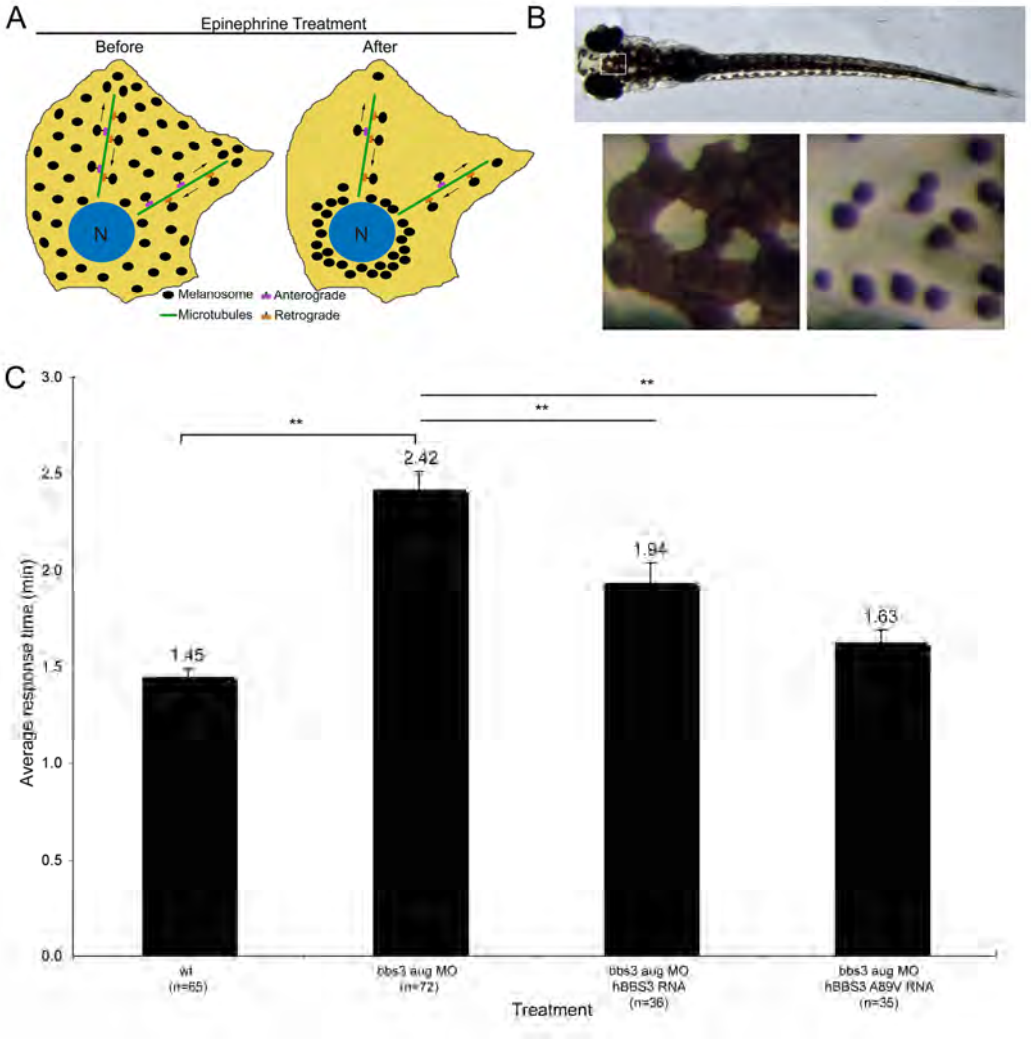

Figure 24 BBS3 A89V functions in melanosome transport. (A) Schematic illustrating the retrograde movement of melanosomes within the melanocyte from the periphery before epinephrine treatment to the perinuclear region after epinephrine treatment. (B) Dorsal view of a dark-adapted wild-type 6-day-old zebrafish embryo. Boxed head region is magnified below the full embryo. The left hand image shows melanocytes prior to epinephrine treatment, while the right hand panel depicts the same melanocytes at the end-point of retrograde transport. (C) The graph summarizes the average epinephrine-induced response times in minutes for each experimental group. Both *hBBS3* and *hBBS3 A89V* RNA are able to suppress the transport time seen with knockdown of *bbs3*. Sample size (n) is denoted on the x-axis. ** $p<0.01$, ANOVA with Tukey.

Table 4 Summary of abnormal Kupffer's vesicle and melanosome transport times for BBS3 A89V

	Abnormal KV (percentage)	n	Melanosome transport (min)	n
wild-type	3.9	232	1.45	65
bbs3 aug MO	19.7**	208	2.42++	72
bbs3 aug MO + hBBS3 RNA	13.2**	38	$$1.94++	36
bbs3 aug MO + hBBS3 A89V RNA	26.9**	115	$$1.63	35
bbs3 aug MO + hBBS3L A89V RNA	18.4**	87	2.22++	33
bbs3 long MO	4.6	195	1.48	63
bbs3 long MO + hBBS3 RNA	10.3	39	NA	NA
bbs3 long MO + hBBS3 A89V RNA	5.9	102	1.53	32
bbs3 long MO + hBBS3L A89V RNA	3.2	95	1.47	29
hBBS3 A89V RNA	15.7**	83	1.48	37
hBBS3L A89V RNA	8.6	70	1.45	26

**Fisher's exact test, $p<0.01$ as compared to wild-type

++ANOVA with Tukey test, $p<0.01$ as compared to wild-type

$$ANOVA with Tukey test, $p<0.01$ as compared to morpholino

n, sample size

NA, not evaluated

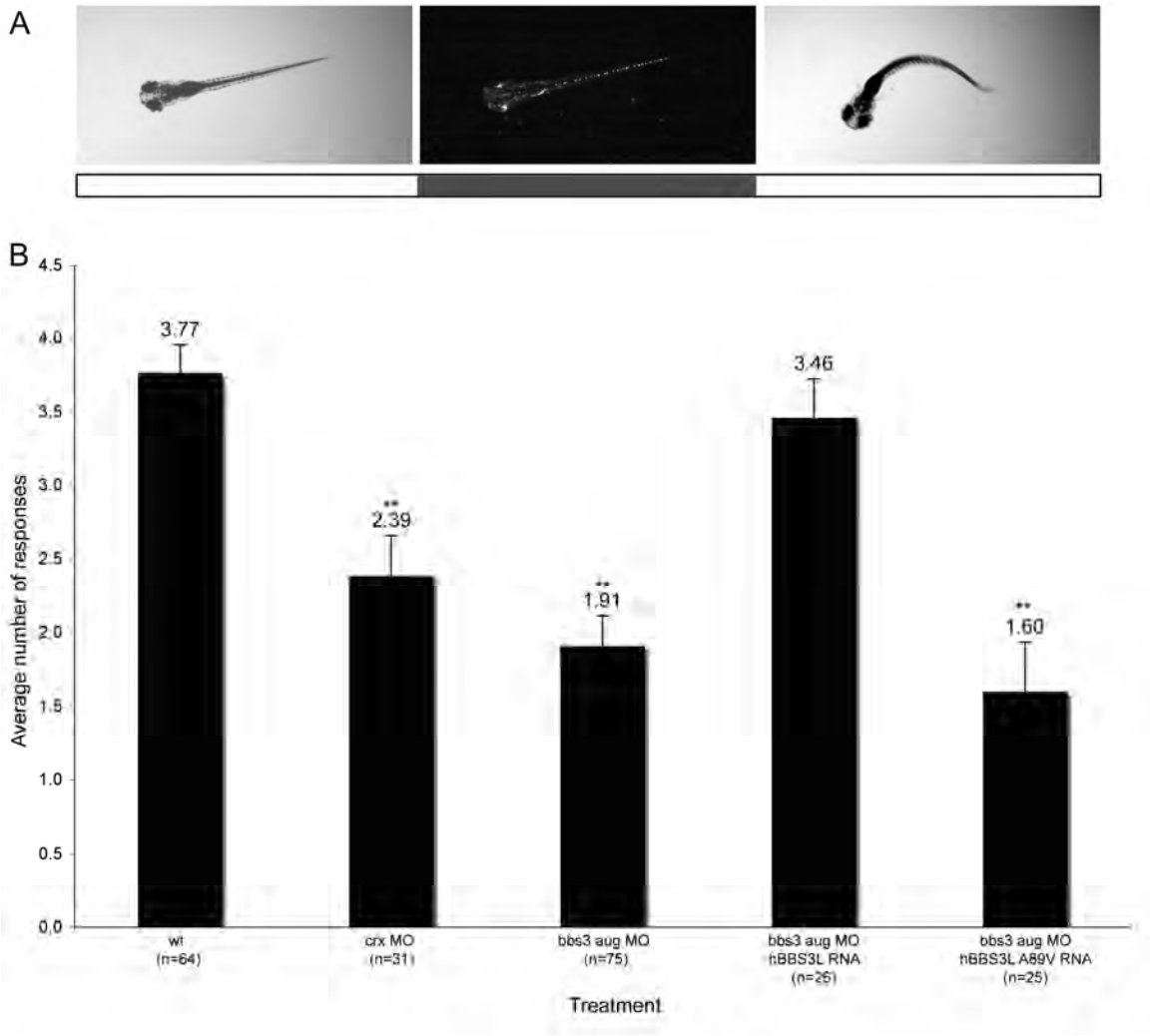

Figure 25 The BBS3L A89V mutation is not functional in vision. (A) Still images of a 5-day old zebrafish embryo illustrating the characteristic escape response elicited by a sudden change in light intensity. The white boxes below the stills indicate lights on, while the grey box indicates lights off. For visualization of the embryo in the dark, image contrast manipulation was performed in Adobe Photoshop. (B) Graphical representation of the vision startle response data. Cone-rod homeobox (*crx*) gene knockdown was used as a control for visual impairment. *hBBS3L* can rescue the vision defect whereas *hBBS3L A89V* is not able to rescue the vision defect in *bbs3* knockdown embryos. The sample size (n) is noted on the x-axis. **p<0.01, ANOVA with Tukey.

Table 5 Summary of vision assay for BBS3 A89V

	Vision (# of responses)	n
wild-type	3.8	64
bbs3 aug MO	1.9^{++}	75
bbs3 aug MO + hBBS3 RNA	1.0^{++}	15
bbs3 aug MO + hBBS3 A89V RNA	1.1^{++}	42
bbs3 aug MO + hBBS3L RNA	3.5	26
bbs3 aug MO + hBBS3L A89V RNA	1.6^{++}	25
bbs3 long MO	1.5^{++}	56
bbs3 long MO + hBBS3 A89V RNA	1.6^{++}	25
bbs3 long MO + hBBS3L A89V RNA	2.2^{++}	29
hBBS3 A89V RNA	3.8	25
hBBS3L A89V RNA	4.0	20

$^{++}$ANOVA with Tukey test, $p<0.01$ as compared to wild-type

n, sample size

Figure 26 Schematic depicting the location of the G2A, T31R and Q73L mutations in human BBS3. The G2A mutation abaltes myristoylation, while the T31R and Q73L mutations lock BBS3 in either an inactive state (GDP-bound) or an active state (GTP-bound), respectively. The red box depicts the location of the P-loop motif.

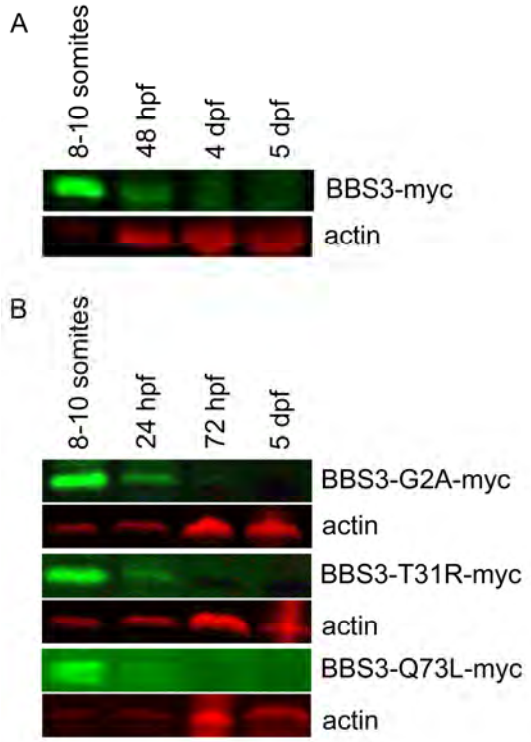

Figure 27 BBS3 G2A, T31R and Q73L protein expression. Western blot analysis of staged zebrafish embryos injected with either BBS3 or mutant BBS3 (G2A, T31R or Q73L) myc-tagged RNA. The wild-type protein is expressed through 5 dpf, while the point mutations are only robustly expressed through 24 hpf. Actin served as a control. hpf, hours post fertilization; dpf, days post fertilization.

Table 6 Summary of abnormal Kupffer's vesicle and melanosome transport times for BBS3 G2A, T31R and Q73L overexpression

	Abnormal KV (percentage)	n	Vision (# of responses)	n	Melanosome transport (min)	n
wild-type	4.9	122	3.9	29	1.7	20
BBS3 G2A RNA	6.6	91	2.5^{++}	15	1.8	21
BBS3 T31R RNA	15.3	92	3.9	16	1.4	17
BBS3 Q73L RNA	7.3	41	2.0^{++}	16	1.9	17

$^{++}$ANOVA with Tukey test, $p<0.01$ as compared to wild-type

n, sample size

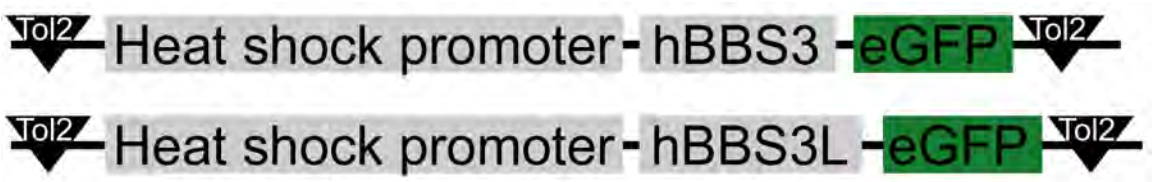

Figure 28 Schematic depicting heat shock driven BBS3 and BBS3L. The Tol2 kit was used to recombine a promoter (heat shock), the genes of interest (BBS3 and BBS3L) and a reporter (eGFP) into a single construct flanked by Tol2 sites. The heat shock promoter is cloned upstream of the gene and is turned on through the addition of heat, this leads to the expression of the gene of interest (either BBS3 or BBS3L). Protein localization can be identified through detection of the transgene (eGPF). The addition of Tol2 sites to this construct allows it to be used for the geneneration of stable transgenic zebrafish through the integration of the DNA construct into the genome.

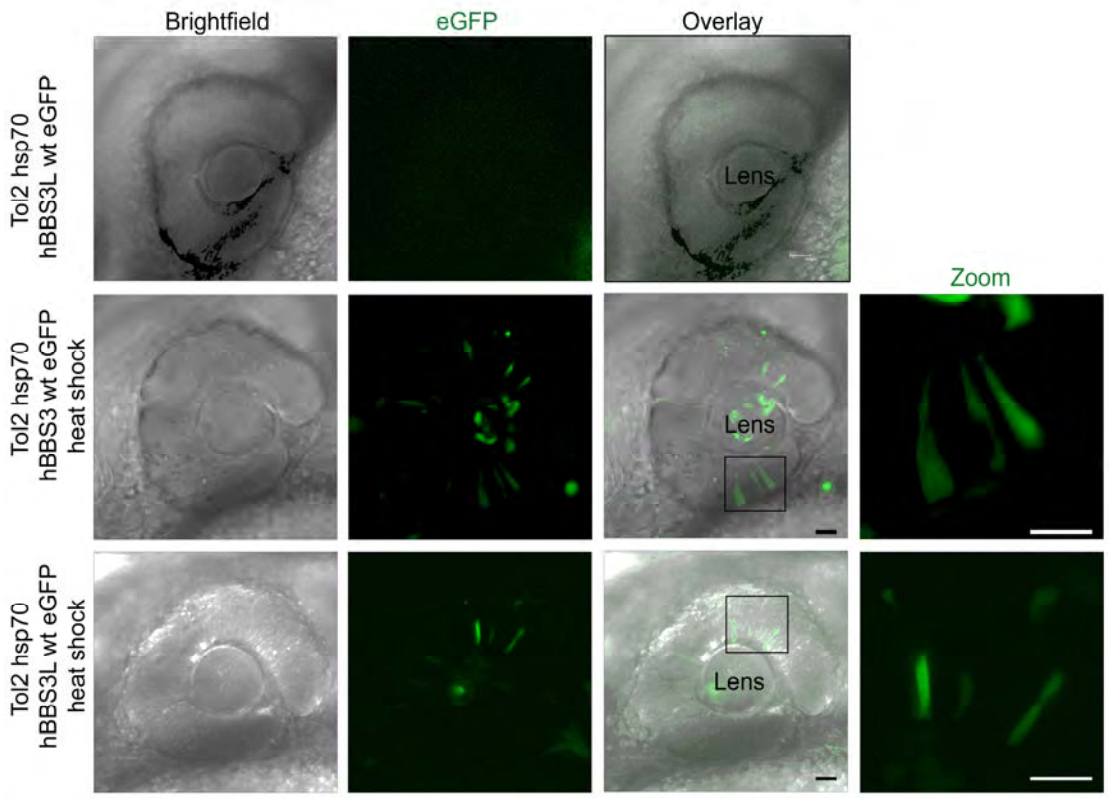

Figure 29 Localization of heat shock BBS3 and BBS3L in the undifferentiated zebrafish retina. Live imaging of 24 hour old zebrafish retinas from Tol2 hsp70 hBBS3L eGFP non-heat shocked (top), Tol2 hsp70 hBBS3 eGFP heat shocked (middle) and Tol2 hsp70 hBBS3L eGFP heat shocked (bottom) injected embryos. Heat shocked 24 hour old zebrafish retinas reveal that hBBS3 and hBBS3L have similar cytoplasmic localization patterns in the developing retina. Bright field images were overlaid with images of the fluorescently labeled protein (green). Boxed region is magnified. Scale bar 20μm.

CHAPTER IV

FUNCTIONAL VERIFICATION OF *MARK3* AS A POTENTIAL BBS GENE

Introduction

Bardet-Biedl Syndrome (BBS, OMIM 209900) is a heterogeneous genetic disorder characterized by early-onset retinal degeneration, obesity, polydactyly, learning disabilities, reproductive tract and renal abnormalities as well as an increased incidence of hypertension and diabetes. (Harnett et al. 1988; Green et al. 1989; Bardet 1995; Biedl 1995). The identification of most BBS genes has relied upon the use of large consanguineous human pedigrees for genetic mapping, with causative mutations identified in approximately 70% of BBS families (Stoetzel et al. 2006b). This indicates that additional BBS genes remain to be identified; however, the discovery of additional disease-causing mutations is hindered by the paucity of pedigrees suitable for traditional linkage studies. Additionally, due to the heterogeneous nature of BBS, it is difficult to perform molecular diagnostic studies in BBS patients as many of the mutations are implicated in only a few cases. Moreover, several of the genes have large coding regions making it both tedious and time consuming to search for mutations in each of the 14 identified disease genes.

In recent years, genome-wide analysis of copy number variation has successfully identifying rare chromosomal abnormalities that confer risk in both the development of genetically simple and complex diseases. The term copy number variation (CNV) refers to a class of chromosomal abnormalities that are defined as a chromosomal deletion or duplication that ranges in size from kilobases to megabases (Iafrate et al. 2004; Sebat et al. 2004; Redon et al. 2006; Stankiewicz and Lupski 2010). Additionally, CNVs are sometimes referred to as submicroscopic variants as their size is beyond the resolution of karyotype detection, making it difficult to detect small variations in the genome. The ability to assess for CNVs on a genome-wide level is aided by advances in microrray and

next-generation sequencing allowing for increased reliability and resolution in the detection size of copy number variation (Cheung et al. 2005; Beaudet and Belmont 2008). Moreover, CNVs are implicated in a wide range of diseases and it is estimated that 15% of all mutations involved in monogenic disorders are a result of microdeletions and duplications (Vissers et al. 2005). As a result, CNVs are now thought to play an important role in normal human variation, genetically complex traits and the development of human disease. One method to identify new BBS genes is through the use of genome-wide copy number variation assessment.

In this study, which was a collaborative effort with a graduate student in the Wassink Laboratory, 32 individuals with BBS from non-consanguineous families were evaluated for copy number variation in an effort to identify novel disease genes and to define a role for CNVs in BBS. Genome-wide analysis was performed on BBS patients with unknown mutations using Affymetrix 5.0 SNP arrays. An intragenic 4.4 kb heterozygous deletion was identified in exon 4 of *MARK3* using PennCNV software. This deletion is predicted to result in a frameshift, leading to a premature stop codon. Sequencing of the second allele in this individual revealed no additional mutations in either the coding region or the splice junctions of *MARK3*.

MARK3 (microtubule affinity-regulating kinase 3) is a member of the evolutionarily conserved Par-1 family. Par-1 stands for partitioning defective, and this family of protein kinases derives its name from cell polarity defects that were observed during early embryonic development in *Caenorhabditis elegans* (Kemphues et al. 1988). Additionally, this family of kinases is required for regulating cell polarity in worms, flies, frogs and mammals (Kemphues et al. 1988; Bullock and Ish-Horowicz 2002; Martin and St Johnston 2003; Nance 2005; Krummel and Macara 2006; Arimura and Kaibuchi 2007). The mammalian Par-1 family consists of four members, *MARK1-MARK4*. *MARK3* was initially identified in brain as playing a role in regulating microtubule dynamics through the phosphorylation of microtubule associated proteins (MAPs)

(Drewes et al. 1997). Northern blot analysis in adult mouse tissues has demonstrated that *Mark3* is widely expressed with the highest levels of expression in the kidney (Biesecker et al. 1993). Genomic analysis of the developing mouse retina also reveals expression of *Mark3* in the inner and outer segments of the retina throughout mouse development (Blackshaw et al. 2004). This expression data illustrates that *Mark3* is expressed in tissues affected by loss of BBS genes in the mouse and supports a potential role for *MARK3* in BBS.

The mechanism underlying CNV function in disease is not fully understood; however, it is thought that CNVs convey phenotypes by affecting either regulatory sequences or by altering gene dosage (Lupski et al. 1992). Thus, a functional assay is necessary to evaluate identified CNVs role in disease. For these studies, I used the zebrafish system to evaluate *MARK3* as a potential BBS gene. *mark3* is duplicated in the zebrafish and both paralogs are expressed throughout early development and indicates that utilization of antisense oligonucleotides (Morpholinos) is a viable option for manipulating *mark3* expression. Preliminary analysis in the zebrafish suggests a potential role for *mark3* in BBS.

Materials and methods

Ethics statement

All animal work in this study was approved by the by the University Animal Care and Use Committee at the University of Iowa.

Animal care

Adult zebrafish were maintained under standard conditions and embryos collected from natural spawnings (Westerfield 1993). Embryos were staged using previously described criteria (Kimmel et al. 1995).

Zebrafish *MARK3* orthologs

Using the Ensemble genome version (Zv8), zebrafish orthologs to *MARK3* were identified by performing BLAST algorithms with human *MARK3* sequences (ENSG00000075413). The BLAST search returned two loci within the zebrafish genome and synteny with the human chromosome was used to identify the duplicated gene.

RT-PCR

RNA was extracted from pools of 10-20 embryos at the following stages: maternal, 24, 48, 72, 96 hpf and 5 dpf . Additionally, RNA was extracted from the following adult tissues: fat, brain, heart, whole eye and retina. Oligo dT primers were used to synthesize cDNA and gene expression evaluated by PCR using primers specific for both *mark3* paralogs. β-actin expression served as a control.

Primers:

mark3a-F: 5'- AAACAGGAATTCTGGTTCAG-3'

mark3a-R: 5'- TTGGGTGGTTTAAATTCTTC-3'

mark3b-F: 5'- AAACAGACAAGACCCTTTACC-3'

mark3b-R: 5'- CCAGCGTGTACAGAATAACC-3'

β-actin-F: 5'-TCAGCCATGGATGATGAAAT-3'

β-actin-R: 5'-GGTCAGGATCTTCATGAGGT-3'

Morpholino injections

Antisense morpholinos (MO) were designed and purchased from Gene Tools.

Morpholino sequences:

mark3a_aug chromosome 13: ACATCGCAATCACAATTTAAGCAGC

mark3b_aug chromosome 20: GTAGTGGTGTTCTAGTTGACATTTT

MOs (2-12ng) were air-pressure-injected into one- to four-cell staged embryos.

Analysis of Kupffer's Vesicle

Embryos with a KV diameter less than the width of the notochord were scored as reduced, while embryos in which KVs could not be morphologically identified were scored as absent. Live somite staged embryos were photographed on a stereoscope equipped with a Zeiss Axiocam camera.

Melanosome transport assay

The melanosome transport assay was performed as previously described (Chiang 2006; Yen 2006; Tayeh 2008). Briefly, to evaluate retrograde transport, dark-adapted 5 dpf embryos were treated with epinephrine (500 μL/mL, Sigma E437). The continuous movement of melanosomes from the periphery to the perinuclear region was monitored and the time recorded. Live embryos were photographed on a stereoscope with a Zeiss Axiocam camera.

Statistical analysis

The Fisher's Exact test was used to evaluate statistical significance for KV formation and the two-tailed p-value was reported. Statistical significance for the melanosome transport assay was assessed using the One-Way Analysis of Variance (one-way ANOVA) paired with the Tukey Honestly Significant Difference (HSD) test.

Results

Identification of *MARK3* zebrafish orthologs

Detection of a 4.4 kb heterozygous deletion of exon 4 in *MARK3* of a patient with an unidentified BBS mutation identified a potential new BBS candidate gene. To functionally test this candidate gene the zebrafish model system was utilized. Database mining identified two *mark3* paralogs, one on chromosome 13 (designated *mark3a*) and the other on chromosome 20 (designated *mark3b*). To identify the gene duplicate the genomic intervals surrounding both zebrafish *mark3a* and *mark3b* were compared with

the chromosomal interval containing human *MARK3*. Conserved gene order, or synteny, was observed between *mark3a* and *MARK3* (Figure 30). Therefore, *mark3b* is likely the duplicated paralog of this gene.

Expression of *mark3a* and *mark3b* in zebrafish

To determine whether the two zebrafish *mark3* paralogs have similar early developmental and/or adult tissue expression an RT-PCR was performed using primer pairs specific to each paralog. A developmental expression profile of staged zebrafish embryos indicates that both *mark3* paralogs are deposited maternally and expressed throughout early development (Figure 31). Moreover, both paralogs were expressed in all adult zebrafish tissues (fat, brain, heart, whole eye and retina) evaluated (Figure 31). The expression of *mark3* early in zebrafish development indicates that utilization of antisense oligonucleotides (Morpholinos) is a viable option for manipulating *mark3* expression and allows for the evaluation of this gene as a candidate BBS gene in zebrafish.

mark3 gene targeting and gross morphology of knockdown embryos

To perform loss of function studies for *mark3* in the zebrafish a translational start site antisense morpholino (MO) was designed for each paralog. It should be noted that both *mark3* paralogs are predicted to have five alternatively spliced transcripts that vary in length as well as start codon positioning. The mark3a_aug chromosome 13 MO only targets one of the five transcripts, *mark3a.5* (Figure 32), while the mark3b_aug chromosome 20 MO targets three (*mark3b.1*, *mark3b.3* and *mark3b.4*) of the five *mark3b* transcripts (Figure 33).

mark3a knockdown did not generate any gross morphological phenotypes in the zebrafish embryo. Interestingly, loss of *mark3b* at higher concentrations (12ng) resulted in necrotic embryos with somite defects at 24 hpf. Additionally, the majority of the

mark3b MO injected embryos (morphants) were dead by 5dpf. Embryos injected with a lower concentration (6ng) of the mark3b aug MO were not necrotic; however, 25% of the embryos did have edema and curved body axes. The curly body axis is observed in zebrafish cilia mutants, such as the *ift* (intraflagellar transport) genes and *seahorse* (Sun et al. 2004; Kishimoto et al. 2008)

Loss of *mark3* results in zebrafish cardinal features of BBS

We were interested in using gene knockdown in the zebrafish system to determine if loss of *mark3* phenocopies the cardinal features of BBS. Previous work in the lab demonstrated that knockdown of *bbs* genes in zebrafish results in two overlapping phenotypes: Kuppfer's vesicle (KV) malformation and a delay in retrograde intracellular transport of melanosomes (Chiang et al. 2006; Yen et al. 2006; Tayeh et al. 2008; Pretorius et al. 2010). Thus, these two cardinal phenotypes were used to determine if *mark3* functions like other *bbs* genes in the zebrafish. The first cardinal feature evaluated was KV formation. The KV is a transient ciliated structure readily observed in the tail bud region in 8-10 somite stage (12-14 hpf) zebrafish embryos (Figure 34A) and has a role in left-right patterning (Supp et al. 1997; Essner et al. 2002; Essner et al. 2005). A normal KV is scored as being larger than the width of the notochord (approximately 50μm in diameter) (Figure 34B), while KV defects are identified as the reduction of the KV to less than the width of the notochord (Figure 34C) or the morphological absence of the KV. Knockdown of *mark3a* leads to a statistically significant difference in the percentage of embryos with abnormal KV (Table 7). Loss of *mark3b* leads to a robust dose-dependent alteration of the KV size (Table 8). This finding is consistent with KV defects observed with knockdown of other zebrafish *bbs* genes (*bbs1-12*) in zebrafish (Chiang et al. 2006; Yen et al. 2006; Tayeh et al. 2008; Pretorius et al. 2010).

A delay in the intracellular transport of melanosomes was the second cardinal feature of BBS evaluated. Zebrafish are able to adapt to their surroundings through

trafficking of melanosomes (Marks and Seabra 2001; Blott and Griffiths 2002; Skold et al. 2002; Barral and Seabra 2004). This response can be induced in the zebrafish by either light or hormonal stimulation. In the melanosome transport assay, dark-adapted 5-day-old zebrafish embryos with fully dispersed melanosomes (Figure 34D and E) are treated with epinephrine to stimulate retrograde melanosome transport (Nascimento et al. 2003; Yen et al. 2006; Tayeh et al. 2008) (Figure 34F). Knockdown of *mark3a* at a medium dose (6ng) results in a statistically significant increase in the melanosome transport time, averaging 2.57 minutes (ANOVA with Tukey, $p<0.01$) (Table 7). *mark3b* knockdown (6ng) results in a slight increase in transport time, averaging 1.82 minutes (ANOVA with Tueky, $p<0.05$) (Table 8). Taken together, this pilot study using antisense morpholino oligonucleoties to independently knockdown *mark3* paralogs supports the hypothesis that *mark3* is a potential BBS gene.

Discussion

In parallel with the zebrafish studies, CNV analysis with a non-consanguineous BBS patient with no known BBS mutation identified a 4.4 kb heterozygous deletion of exon 4 in *MARK3*. Deletion of exon 4 was predicted to result in a frameshift and a premature stop codon in *MARK3*. Sequencing of the second *MARK3* allele yielded no additional mutations. While a second mutation was not identified within the coding region of *MARK3* we cannot rule out that a second mutation may exist in either the untranslated region (UTR) or the introns, thus making *MARK3* a BBS candidate gene. Moreover, data independent of this study supports *MARK3* as a candidate BBS gene. *Mark3* is expressed throughout a range of adult mouse tissues, including heart, brain, spleen, lung, liver, muscle, kidney and testicles (Biesecker et al. 1993). Additionally, *Mark3* expression was observed in the inner and outer segments of the retina from an *in situ* performed on day 6-7 postnatal mice (Blackshaw et al. 2004). While ubiquitious tissue expression is seen with many non-BBS genes, the expression of *Mark3* is

consistent with that seen for several BBS genes in the mouse (Nishimura et al. 2004). Taken together, these data suggest that *MARK3* is a good canidate BBS gene

In this pilot study, *mark3* was evaluated as a potential BBS gene, using morpholinos to target the two *mark3* paralogs identified in zebrafish. Through the evaluation of two cardinal BBS features in the zebrafish, malformation of the KV and delays in intracellular trafficking, additional functional evidence is provided demonstrating that *MARK3* is a candidate BBS gene. While knockdown of *mark3a* does result in a statistically significant change in the percentage of embryos with abnormal KV, this response is not as robust as previous reports of *bbs* gene knockdown in the zebrafish (Chiang et al. 2006; Yen et al. 2006; Tayeh et al. 2008; Pretorius et al. 2010). Moreover, loss of *mark3b* does not lead to a robust melanosome transport phenotype.

There are two possible explanations for these weaker phenotypes. First, the morpholinos designed for these studies do not target all of the predicted splice variants for *mark3a* or *mark3b* as both paralogs are predicted to have five alternatively spliced transcripts. This would indicate that some (or all) of the non-targeted splice variants function in KV formation and intracellular transport. Secondly, *mark3* is duplicated in the zebrafish genome. Nearly 30% of the zebrafish genome is duplicated, often making analysis by gene knockdown more complex (Postlethwait and Talbot 1997; Talbot et al. 1998; Kelly et al. 2000; Postlethwait et al. 2000). There are three possible outcomes from gene duplication: sub-functionalization, neo-functionalization and non-functionalization through the loss or silencing of the duplicate gene. As *mark3* is expressed in the zebrafish, the gene copy was not lost; therefore for the purpose of the *mark3* duplication this discussion will focus on neo-functionalization and sub-functionalization.

Knockdown of *mark3b* leads to additional phenotypes, including head necrosis, edema, somite defects and curved bodies. These defects are not seen with loss of *mark3a* suggesting that neo-functionalization has occurred. In neo-functionalization one of the

duplicated genes evolves a novel function (Force et al. 1999; Lynch and Conery 2000). Conversely, sub-functionalization may have occurred with *mark3* in zebrafish, whereby the gene duplicates partition their ancestral functions between the two paralogs (Force et al. 1999; Lynch and Conery 2000). In the context of *mark3*, knockdown of *mark3b* leads to a striking increase in the percentage of embryos with KV abnormalities, while loss of *mark3a* results in melanosome transport delay. Thus, the lack of both cardinal features with individual knockdown of either *mark3a* or *mark3b* supports the idea of sub-functionalized of the *mark3* paralogs.

Several parameters of this project still warrant further investigation to decipher the role of *mark3* in BBS. First, while the temporal expression of *mark3a* and *mark3b* was assessed, whole mount in situ hybridization (WHISH) should be performed to look at spatial expression of these two paralogs. I would hypothesis that if these two paralogs have sub-functionalized we may see expression of *mark3a* and *mark3b* in different regions of the developing embryo. Secondly, the morpholino targeting strategy used in these pilot studies did not target all of the predicted splice variants for both paralogs. To confirm expression of all mark3 splice variants and to identify new splice variants, 5' rapid amplification of cDNA ends (RACE) should be performed. Once it is known which splice variants are expressed in the zebrafish new morpholinos should be designed to target the additional splice variants and phenotyping for BBS cardinal features repeated. Moreover, future experiments should be done to simultaneously knockdown both *mark3a* and *mark3b* to examine whether there is synergistic interaction of these two paralogs.

Previous work tested for interactions between *bbs1-bbs8* in the zebrafish by evaluating the cardinal features of BBS in the zebrafish. Upon pair-wise knockdown of *bbs1-bbs8* in the zebrafish eight synergistic interactions were identified (Tayeh et al. 2008). This synergy provides *in vivo* evidence for genetic interactions between a subset of *BBS* genes. The idea of synergist interactions between known *BBS* genes could be

expanded to include testing of candidate *BBS* genes. Through pair-wise knockdown of *mark3* and known *bbs* genes interactions between this potential BBS gene and known BBS genes would be identified, providing further support for *MARK3* as a BBS gene.

As mentioned previously, BBS proteins play a role in proper cilia formation. In *Bbs* knockout mice, cilia defects are observed in range of ciliated cells, including tracheal epithelia cells, ependymal cells, photoreceptor cells, spermatozoa and renal cells (Mykytyn et al. 2004; Nishimura et al. 2004; Fath et al. 2005; Davis et al. 2007; Mokrzan et al. 2007). Moreover, knockdown of *bbs* genes in the zebrafish results in the premature progressive degeneration of cilia within the Kupffer's vesicle (Yen et al. 2006). The role of *MARK3* in cilia formation and/or maintenance can be evaluated in the Kupffer's vesicle of the zebrafish. Defects in KV cilia formation would provide further support for the role of *MARK3* as a *BBS* gene.

While the zebrafish functional studies were ongoing, a study reported the characterization of a *Mark3* knockout mouse. Similar to loss of Bbs genes in the mouse, *Mark3-null* mice are not produced at the expected Mendelian ratios; however, the pups are not visibly dismorphic and survive into adult. Interestingly, *Mark3*$^{-/-}$ mice have reduced body weight as compared to their wild-type littermates and are protected against obesity induced via a high fat diet, indicating that *Mark3* has a role in maintaining metabolic homeostasis in the adult mouse (Lennerz et al. 2010). The lack of obesity in *Mark3-null* mice is in stark contrast to *Bbs* mutant mice which become obese early in life (Mykytyn et al. 2004; Nishimura et al. 2004; Fath et al. 2005; Davis et al. 2007). *Mark3* heterozygous mice were not evaluated in this study; however, it is possible that loss of a single copy of the *Mark3* allele would induce phenotypes more reminiscent of BBS.

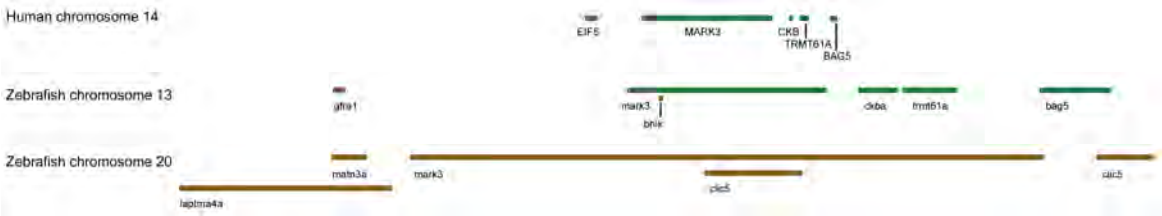

Figure 30 Syntenic relationships between human MARK3 and zebrafish *mark3* paralogs. The top image represents the region of human chromosome 14 surrounding *MARK3*, while the bottom two schematics are representative of the regions surrounding zebrafish *mark3a* (chromosome 13) and *mark3b* (chromosome 20), respectively. Conserved synteny is depicted in green. Gene order is based on Ensemble genomic sequence data (Zv8).

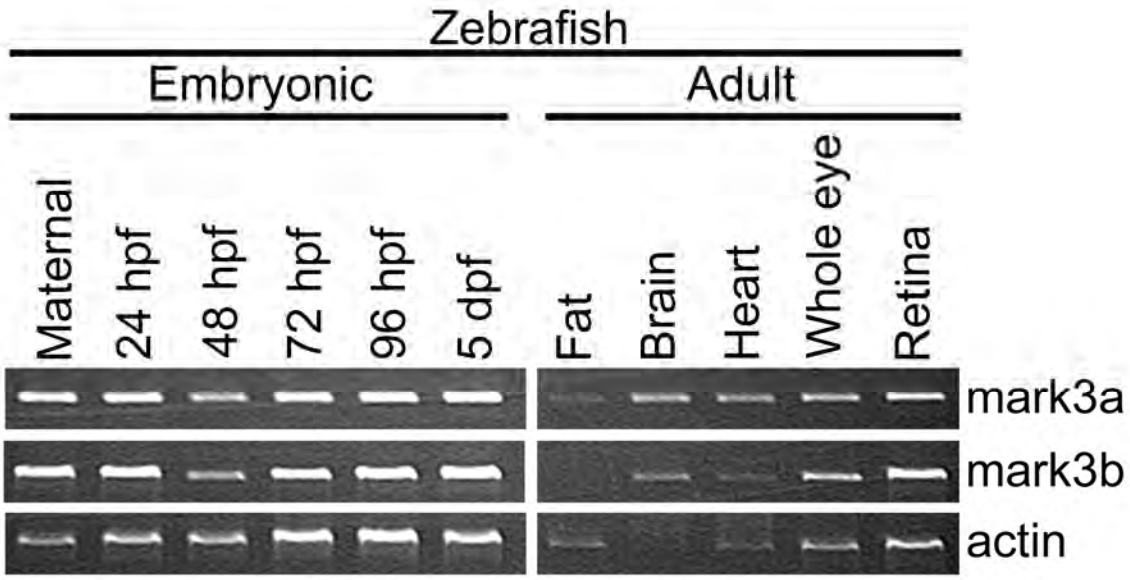

Figure 31 RT-PCR expression of *mark3a* and *mark3b* in zebrafish. The developmental profile was performed on the following stages: maternal, 24, 48, 72, 96 hpf and 5 dpf wild-type embryos. Tissue expression was evaluated in the following adult wild-type tissues: fat, brain, heart, whole and retina. β-actin was used as a positive control. Both *mark3* transcripts are expressed throughout development and in all adult tissues evaluated.

Figure 32 *mark3a* gene structure. Schematic depicting the five *mark3a* transcripts and the antisense oligonucleotide strategy used for targeting *mark3a* in zebrafish embryos. The *mark3a* aug MO (red) targets the start site of the gene and only impacts one transcript, *mark3a.5*.

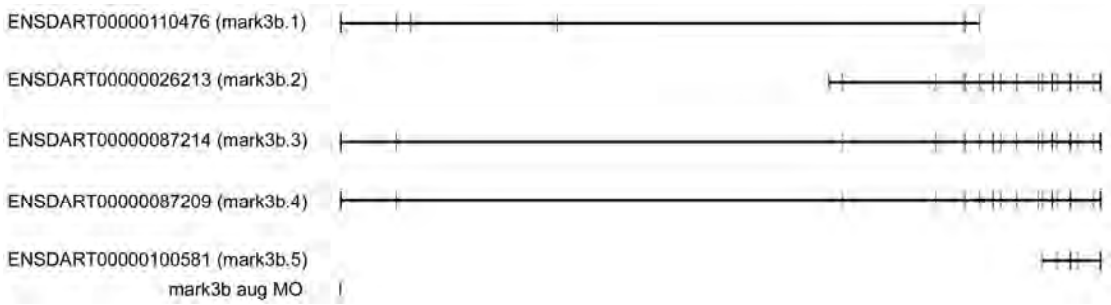

Figure 33 *mark3b* gene structure. Schematic depicting the five *mark3b* transcripts and the antisense oligonucleotide strategy used for targeting *mark3b* in zebrafish embryos. The *mark3b* aug MO (red) targets the start site of the gene and only impacts three of the transcript, *mark3b.1*, *mark3b.3* and *mark3b.4*.

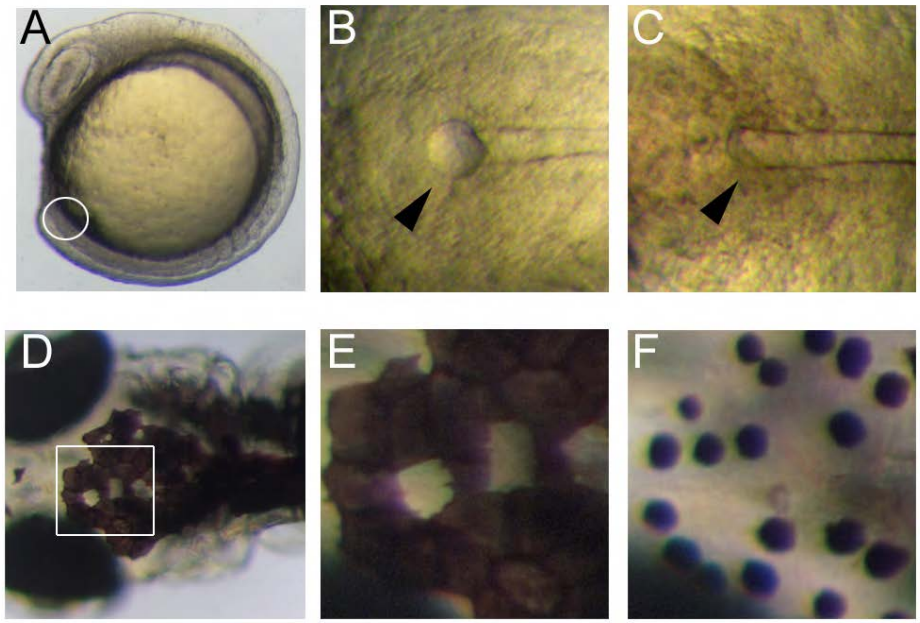

Figure 34 Cardinal features of BBS in zebrafish. (A-C) Images of live zebrafish embryos at 8-10 somite stage. (A) Tailbud view of an embryo highlighting the location of the ciliated Kupffer's vesicle (KV). (B) Dorsal view of a normal sized KV from a wild-type embryo. (C) *mark3b* morpholino-injected embryos with a reduced KV. (D-F) Epinephrine-induced melanosome transport of a wild-type 5-day old zebrafish embryo. (D) Intracellular transport of melanosomes is observed in the head of zebrafish embryos. Boxed region is magnified for E and F. (E) Wild-type embryos prior to treatment with epinephrine and (F) the endpoint of the same embryo following epinephrine treatment.

Table 7 Percentage of abnormal KV and melanosome transport for *mark3a*

	Abnormal KV (percentage)	n	Melanosome transport (min)	n
wild-type	4.2	236	1.58	29
mark3a MO (3ng)	12.5**	88	NA	NA
mark3a MO (6ng)	17.5**	120	2.57++	44
mark3a MO (12ng)	14.9**	114	2.01	40

**Fisher's exact test, $p<0.01$ as compared to wild-type

++ANOVA with Tukey test, $p<0.01$ as compared to wild-type

n, sample size

NA, not evaluated

Table 8 Percentage of abnormal KV and melanosome transport for *mark3b*

	Abnormal KV (percentage)	n	Melanosome transport (min)	n
wild-type	3.0	67	1.36	12
mark3b MO (2ng)	22.0**	97	1.47	19
mark3b MO (3ng)	23.7**	97	1.73	31
mark3b MO (6ng)	34.3**	99	1.82+	40
mark3b MO (12ng)	52.6**	38	NA	NA

**Fisher's exact test, $p<0.01$ as compared to wild-type

+ANOVA with Tukey test, $p<0.05$ as compared to wild-type

n, sample size

NA, not evaluated

CHAPTER V

SUMMARY, CONCLUSIONS AND DISCUSSION

Summary

A genetically heterogeneous disorder, Bardet-Biedl Syndrome (BBS, OMIM 209900) is characterized by retinal degeneration, early onset obesity, polydactyly, kidney malformations and learning disabilities (Harnett et al. 1988; Green et al. 1989; Bardet 1995; Biedl 1995). Additionally, patients also have an increased susceptibility to diabetes mellitus, hypertension and congenital heart disease (Harnett et al. 1988; Green et al. 1989; Elbedour et al. 1994). To date, 14 genes (*BBS1-14*) have been implicated in BBS, with more genes yet to be elucidated. The underlying pathophysiology of BBS is not well understood and has been hampered by the extensive genetic heterogeneity of this disease. The discovery of two complexes encompassing most of the BBS proteins, however, has aided in our understanding of the molecular function of these proteins. The BBSome, which functions at the ciliary membrane, was the first complex identified and consists of BBS1, 2, 4, 5, 7, 8, and 9 (Nachury et al. 2007). More recently, Jin *et al.* (Jin et al. 2010) demonstrated that BBS3 is both necessary and sufficient to recruit the BBSome to the ciliary membrane. A second complex containing BBS6, 10 and 12 as well as six other members of the chaperonin containing T-complex polypeptide 1 (CCT) family of group II chaperonins plays an essential role in BBSome assembly (Seo et al. 2010). Although progress has been made in determining the protein-protein interactions between BBS proteins, gaps remain in our understanding of the cellular functions of BBS proteins.

Using gene knockdown in zebrafish, we have previously demonstrated that loss of BBS genes results in two prototypical phenotypes: reduced size of the ciliated Kupffer's vesicle and delays in intracellular melanosome transport (Chiang et al. 2006; Yen et al. 2006; Tayeh et al. 2008; Pretorius et al. 2010). These cardinal features as well as a vision startle assay were used to determine the functional requirement of *BBS3* and *BBS3L* in

specific tissues. Knockdown of both *bbs3* transcripts results in the cardinal features of BBS as well as vision impairment in zebrafish. Unlike *bbs3*, knockdown of *bbs3L* does not result in Kupffer's Vesicle or intracellular melanosome transport defects, rather loss of *bbs3L* leads to impaired visual function and mislocalization of the photopigment green cone opsin. Moreover, BBS3L RNA, but not BBS3 RNA, is sufficient to rescue both the vision defect as well as the green cone opsin localization in the zebrafish retina. In order to demonstrate a role for *Bbs3L* function in the mammalian eye we generated a *Bbs3L-null* mouse that presents with disruption of the normal photoreceptor architecture. *Bbs3L-null* mice lack key features of previously published *Bbs-null* mice, including obesity. These data demonstrate that the *BBS3L* transcript is required for proper retinal function and organization.

With the initial characterization of BBS3 and BBS3L established, I used the zebrafish system to functionally characterize a BBS3 missense mutation (A89V) that was identified in a consanguineous family with isolated retinitis pigmentosa. The mutation falls within a conserved region of BBS3 in a wide range of vertebrate species and encodes for a single amino acid change at position 89 from an alanine to a valine. I find that BBS3 A89V is sufficient to rescue the transport delays induced by loss of *bbs3*, indicating that this mutation does not affect the function of *bbs3* as it relates to syndromic disease. Conversely, BBS3L A89V was unable to rescue vision impairment. Thus, characterization of this missense mutation highlighted a role for a specific amino acid within BBS3 that is necessary for visual function, but dispensable in other cell types. Additionally, these data aid in our understanding of why patients with the BBS3 A89V missense mutation only present with isolated retinitis pigmentosa.

Finally, I utilized the zebrafish and the cardinal features of BBS to generate functional data supporting a role for *MARK3* as a candidate BBS gene. In tandem with the zebrafish studies, a 4.4 kb heterozygous deletion of exon 4 in *MARK3* was identified. Deletion of this exon is predicted to result in a framshift that generates a premature stop

codon in *MARK3*. In zebrafish, two *MARK3* paralogs (*mark3a* and *mark3b*) were identified and both found to be expressed throughout early development as well as in an array of adult zebrafish tissues. Pilot studies demonstrate that knockdown of either *mark3a* or *mark3b* results in abnormal Kupffer's Vesicle size, while only loss of *mark3a* leads to intracellular trafficking defects. This supports the hypothesis that *MARK3* is a potential BBS candidate gene.

Conclusions

The degeneration of photoreceptors, and ultimately vision impairment and blindness, has far reaching implications for society. The term retinitis pigmentosa (RP, MIM 268000) describes a heterogeneous group of retinal dystrophies that are a result of rod and cone photoreceptor degeneration. While RP is typically non-syndromic, 20-30% of patients have additional non-ocular phenotypes (Hartong et al. 2006). Bardet-Biedl Syndrome is one form of syndromic retinitis pigmentosa in which additional tissues are affected. Patients present with early and progressive photoreceptor degeneration that results in blindness by the third decade of life (Riise 1987; Leys et al. 1988; Green et al. 1989; Jacobson et al. 1990; Fulton et al. 1993; Carmi et al. 1995a; Beales et al. 1997; Riise et al. 1997; Heon et al. 2005b). The BBS proteins are diverse and cannot all be classified within the same functional category. A common feature shared among the BBS proteins is their involvement in ciliary function and intracellular transport in a range of organs, including the eye, kidney and brain.

The vertebrate retina contains photoreceptor cells, which are highly polarized. These cells contain a primary cilium known as a connecting cilium, which connects the inner and outer segments. Proteins necessary for assembly and maintenance of the photoreceptor are transported through the connecting cilium via intraflagellar transport (IFT) (Young 1967; Horst et al. 1990; Pazour et al. 2002; Krock and Perkins 2008; Luby-Phelps et al. 2008). Disruption of IFT leads to photopigment mislocalization and

ultimately photoreceptor degeneration (Pazour et al. 2002; Tsujikawa and Malicki 2004; Sukumaran and Perkins 2009). Mouse knockout models for *Bbs2*, *4* and *6* as well as a *Bbs1 M390R* knockin model show mislocalization of the photopigment rhodopsin followed by photoreceptor cell loss, a phenotype similar to what is seen with loss of IFT proteins (Mykytyn et al. 2004; Nishimura et al. 2004; Fath et al. 2005; Abd-El-Barr et al. 2007; Davis et al. 2007; Swiderski et al. 2007). This indicates that BBS proteins are important for both proper retina structure and photopigment localization.

As BBS is a syndromic form of RP, BBS proteins role in cilia function and intracellular transport extends beyond the retina. Intracellular transport defects have been observed in airway epithelia cells as well as the brain ependymal cells of BBS mouse models (Davis et al. 2007; Shah et al. 2008). Structural ciliary defects were observed in the airway epithelium of *Bbs1*, *Bbs2*, *Bbs4* and *Bbs6* mutant mice, whereby the cilia tips displayed vesicle filled bulges (Shah et al. 2008). Similarly swollen distal tips with vesicular aggregates were seen in ependymal cell cilia of *Bbs1 M390R* knockin mice (Davis et al. 2007). The accumulation of proteins at the cilia distal tip implicates BBS proteins in the intracellular transport of proteins within the cilia. Moreover, knockdown of bbs genes (*bbs1-12*) in the zebrafish results in delays of intracellular retrograde transport of melanosomes (Chiang et al. 2006; Yen et al. 2006; Tayeh et al. 2008; Pretorius et al. 2010). Although the precise mechanisms underlying these transport defects is not known, a defect in retrograde intraflagellar transport may be responsible for these phenotypes associated with syndromic disease. While we're beginning to understand the role of BBS proteins in syndromic disease, the function of these genes in non-syndromic disease has not previously been investigated.

The overall goal of this thesis was to characterize the function of BBS3 in terms of both syndromic and non-syndromic retinal degeneration using the zebrafish and mouse model systems. This was accomplished by two independent projects. First, I characterized the newly identified BBS3L transcript, which is expressed in the mouse and

zebrafish eye. Interestingly, BBS3L is both necessary for vision and the gene product is sufficient to rescue the vision defect as well as green cone opsin localization. Thus demonstrating that BBS3L is required for proper retinal function, but dispensable for syndromic disease, providing insight into a tissue specific role for a BBS gene. Second, I functionally characterized the BBS3 A89V missense mutation associated with non-syndromic retinitis pigmentosa and identified a specific amino acid within BBS3 that is necessary for visual function, but dispensable in other cell types. These observations point to a model whereby a single gene, with multiple splice variants, can play a role in both a syndromic disease such as BBS and a non-syndromic disease such as retinitis pigmentosa. Moreover, these data highlight the importance of functionally evaluating human disease mutations for disease and/or tissue specific relevance. Taken together, my research has examined the role of BBS3 in the retina and proposes a mechanism by which a single gene can function in both syndromic and non-syndromic disease.

Discussion

Although BBS is a rare disorder, components of the phenotype, such as vision loss, are common in the general population. Understanding the pathophysiology that leads to the disease state will aid in our understanding of not only how a normal cell functions but also how a diseased cell functions. The precise molecular function of BBS genes remains elusive; however, the identification of two complexes encompassing ten of the 14 BBS genes has highlighted a role for these proteins in trafficking of cargos to the cilia (Nachury et al. 2007; Jin et al. 2010; Seo et al. 2010). While BBS3 is not part of the BBSome, it has been shown to be both necessary and sufficient for recruitment of the BBSome to the ciliary membrane (Jin et al. 2010). Additionally, recent work in the Sheffield lab has demonstrated that Bbs3 is not necessary for proper BBSome assembly in the mouse testis (Qihong Zhang personal communication). Based on this thesis, I hypothesize that BBS3 has both a BBSome dependent and independent function in the

retina and that loss of BBS3 would impact BBS1 localization within the cell. I predict that BBS3, which shows ubiquitous tissue expression in the mouse and zebrafish, functions primary through trafficking of the BBSome, while BBS3L functions independently of the BBsome, but may still play a role in proper localization of ciliary components. To investigate the BBSome-independent role for BBS3L, BBSome composition and localization should be assessed in the *Bbs3L-null* mouse retina. Furthermore, the interaction between the BBSome and BBS3 is mediated by BBS1 (Jin et al. 2010). Therefore, it will be interesting to evaluate whether loss of bbs3 in the zebrafish impacts bbs1 localization. Delineating the roles of BBS3 and BBS3L in terms of the BBSome would not only provide insight into the tissue specific roles of the BBSome but would also evaluate the individual functions of the two BBS3 transcripts in terms of BBS and syndromic disease.

The identification of a tissue specific alternatively spliced BBS3 exon highlights the importance of RNA processing as a mechanism to regulate ubiquitously expressed genes in disease. Moreover, recent work in identifying RP genes has identified genes with seemingly broad function that when mutated in tissue-specific isoforms results in a spatial restriction of the phenotype (Kirschner et al. 1999; Gupta et al. 2002; McAlinden et al. 2008). One particular gene, *NPHP6* (also known as *CEP290*, *BSB14* and *LCA10*), has been implicated in numerous diseases, including Joubert Syndrome, Meckel-Gruber Syndrome, Bardet-Biedle Syndrome and isolated blindness (Leber congenital amaurosis (Coppieters et al. 2010). While this gene has been implicated in several syndromic diseases, a mouse model for *NPHP6*, the *rd16* mouse, presents with only early onset retinal degeneration (Chang et al. 2006). Additional splice isoforms are predicted for Cep290 and Western Blot analysis supports the notion that there are retina specific isoforms (Chang et al. 2006). Taken together, it is reasonable to hypothesize that the retina isoforms are more severely impacted by the mutation identified in *Cep290*. The presence of tissue specific alternatively spliced variants in genes implicated in multiple

diseases suggests that there is a need for transcript diversity and that this diversity results in different functional properties. Identification of BBS genes with tissue-specific exons would lend further insight into gene function as well as the disease pathophysiology. The discovery of a BBS3 brain specific isoform may explain why *Bbs3-null* mice present with a more severe form of hydrocephalus than *Bbs2*, *Bbs4* or *Bbs6* knockout mice. The remaining BBS genes should also be evaluated for tissue specific exons and the expression of the splice variants confirmed through RT-PCR. Alternative splicing of additional BBS genes may point to a mechanism whereby the classic form of a given gene is ubiquitously expressed and has a more global effect when mutated while the tissue specific isoform has different functional properties with mutations resulting in a tissue specific phenotype.

This thesis has demonstrated that BBS3L function is restricted to a particular tissue, the eye. Currently, the mechanism by which two non-redundant BBS3 transcripts are produced from a single gene is unknown. Promoters, which contain transcriptional regulatory elements, are regions of DNA required for transcriptional initiation. Alternative promoters can direct the production of multiple transcripts from a single mRNA through promoter-driven exon inclusion. This results in diversified transcriptional regulation in a context specific manner, such as tissue type (Ayoubi and Van De Ven 1996). Approximately 50% of human genes have been reported to have at least one alternative promoter, indicating that alternative promoter usage is an important mechanism for gene regulation (Landry et al. 2003; Kimura et al. 2006; Baek et al. 2007; Davuluri et al. 2008). The difference in exon usage between *BBS3* and *BBS3L* in the eye could be due to alternative promoters. To further examine this, a bioinformatics approach could be applied to identify conserved regions upstream of the transcriptional start site. The presence of conserved regions would suggest that alternative promoters exist for *BBS3*. Potential promoters could be functionally tested *in vivo* using reporter constructs in the zebrafish system. Furthermore, a series of deletion mutants could be

used to identify the functional elements within the promoter regions. Regulation of *BBS3* by different promoters would explain the tissue diversity observed in the mRNA transcripts for BBS3

Work in both the zebrafish and mouse has demonstrated a role for BBS proteins in cilia function, as well as in organelle and membrane bound vesicle intracellular transport. Knockdown of *bbs* genes in zebrafish results in delayed retrograde melanosome transport, one of the cardinal features of BBS in the zebrafish (Chiang et al. 2006; Yen et al. 2006; Tayeh et al. 2008; Pretorius et al. 2010). This thesis demonstrates that loss of *bbs3*, but not *bbs3L* results in delayed intracellular trafficking. While *bbs3L* is expressed at the time melanosome transport is evaluated, we do not know whether it is expressed in melanocytes. Due to the high sequence homology between *bbs3* and *bbs3L* whole mount *in situ* hybridization could not be performed to evaluate the spatial expression of the two mRNAs in melanocytes. I would hypothesize, based on both the zebrafish and mouse data presented in this thesis, that *bbs3L* would not be expressed in the melanocytes. The expression of *bbs3* and/or *bbs3L* could be evaluated using melanocyte cDNA. The lack of *bbs3L* expression in melanocytes would explain why no delay in melanosome trafficking was observed in *bbs3L* knockdown embryos.

In the zebrafish, pigment aggregation (retrograde transport) is stimulated through treatment with epinephrine which signals through the α2-adrenoceptor (Aspengren et al. 2003; Nascimento et al. 2003). The delay in intracellular trafficking of melanosomes is thought to be a result of impaired retrograde movement and thus receptor independent; however, receptor mislocalization and thus aberrant signaling could underlie the defect. The importance of proper receptor localization in BBS was highlighted in two recent mouse studies. *Bbs2*$^{-/-}$ and *Bbs4*$^{-/-}$ mice lack somatostatin receptor 3 and melanin-concentrating hormone receptor 1ocalization to neuronal cilia, suggesting that mislocalization of ciliary signaling components is associated the disease phenotype (Berbari et al. 2008). Moreover, mistrafficking and attenuation of the leptin receptor

signal appears to underlie the energy imbalance and thus the obesity phenotype observed in *Bbs2*$^{-/-}$, *Bbs4*$^{-/-}$ and *Bbs6*$^{-/-}$ mice (Seo et al. 2009). Similar to the somatostatin receptor 3 and the melanin-concentrating hormone receptor, the α2-adrenoceptor is a G protein-coupled receptor, which functions to transfer extracellular signals across the cell membrane to intracellular effectors. Without this receptor, the epinephrine response would be diminished and a delay in melanosome transport observed. One way to test the function of the α2-adrenoceptor is by looking at the levels of cyclic adenosine monophosphate (cAMP), as intracellular levels of this second messenger decrease with binding of the ligand (epinephrine) to the receptor, resulting in melanosome aggregation (Andersson et al. 1984; Lundstrom and Svensson 1998; Aspengren et al. 2003). Moreover, epinephrine increases cytosolic Ca^{2+} leading to the aggregation of melanosomes (Kotz and McNiven 1994). The effects of epinephrine treatment on cAMP and/or Ca^{2+} in melanosomes can be evaluated through the use of live imaging of zebrafish melanocytes (Slusarski and Corces 2000; Nikolaev and Lohse 2006). It maybe necessary to perform these experiments in cell culture as the chemical used to anesthetize zebrafish embryos impacts melanosome transport, and would also potentially influence these second messengers. Finally, if changes are observed in second messenger levels upon stimulation with epinephrine, localization of α2-adrenoceptor could be investigated, as perhaps loss of bbs3 impairs the receptor localization leading to the disrupted second messenger signal. Evaluating second messenger levels after stimulation with epinephrine would provide additional insight into the mechanism underlying the intracellular trafficking defect seen in *bbs3* morphant zebrafish embryos.

This study functionally characterized a mouse and zebrafish model for BBS3 and aids in the understanding of the molecular pathophysiology of a single BBS gene. Although these models provide *in vivo* evidence for the involvement of a single gene in both syndromic and non-syndromic disease, a detailed molecular mechanism for how mutant BBS3 leads to the disease state has not yet been determined and requires

additional studies. Several human mutations (G2X, T31M, T31R, P108L, R122X, G169A and L170W) have been identified in BBS3 patients (Chiang et al. 2004; Fan et al. 2004; Pereiro et al. 2010). In nucleotide-binding assays, four of these mutations were found to abrogate nucleotide binding (Wiens et al. 2010). *In vivo* analysis of these mutations in the zebrafish may begin to decipher the nature of these mutations in the disease state.

Additionally, this thesis uncovers a specific amino acid (A89V) in BBS3 that is critical and specific for vision using *in vivo* assays in the zebrafish. Interestingly, overexpression of BBS disease causing mutations (G2A and T31R) results in a protein that is not stably expressed; however, the BBS3 A89V missense mutation that results in non-syndromic retinitis pigmentosa is stably expressed. A similar observation was made in cell culture when BBS mutations were compared to the A89V mutation (Charles Searby observation). This suggests that mutations resulting in BBS impact protein stability, while mutations in BBS genes resulting in non-syndromic disease function through a different mechanism. I would hypothesize that the BBS3 A89V missense mutation specifically disrupts protein function of BBS3L by preventing proper protein folding. It is possible the C-terminal tail of BBS3L binds to the alanine at position 89 to form a pocket necessary for interacting with binding partners in the eye. As BBS3 does not possess these additional 15 amino acids present in the long form the alanine at position 89 is dispensable for protein folding allowing BBS3 to interact with its normal binding partners.

The translation of scientific research into clinical applications is an important component of human genetics. BBS is a genetically and phenotypically heterogeneous disorder. Treatment for several of the BBS symptoms is currently available; examples include diet and exercise to treat obesity and surgery to remove extra digits resulting from polydactyly. To date, there are no effective therapies to delay or arrest retinal degeneration, thus placing a large burden on affected families and on society as a whole.

This thesis functionally characterizes the eye specific BBS3L isoform and demonstrates that it plays a critical role in both proper retinal function and organization. In particular, the data suggests that BBS3L is sufficient to restore vision. Recently, a *Bbs3-null* mouse was generated that lacks both Bbs3 transcripts and suffers from retinal degeneration. This mouse is a perfect candidate for gene therapy and could be to further examine the roles of BBS3 and BBS3L in vision. Based on this thesis, I would predict BBS3L would be sufficient to restore vision in a mouse model of Bbs3.

On a more global level, the study of Mendelian disorders can provide insight into the molecular mechanisms underlying complex diseases such as high blood pressure, obesity, cancer and psychiatric illness. Complex diseases are multifactorial and cannot be ascribed to a single gene or environmental factor, but rather arise from a combination of genetic and non-genetic factors, making it difficult to determine the precise cause of the disease (Kiberstis and Roberts 2002). In the instance of the Mendelian disorder BBS, many of the disease genes have been identified and major inroads have been made in determining the proteins precise function in the cell, especially with regards to obesity. *Bbs-null* mice become obese as a result of mistrafficking and attenuation of leptin receptor signaling (Seo et al. 2009). This knowledge can then be applied to the more complex disease state as perhaps receptor localization and/or signaling is a common mechanism between obesity in BBS and obesity in the general population. Additionally, the identification of genes contributing to complex disease is difficult, as many of the genes exert a small effect on disease susceptibility and the effect of the given gene is likely to be modified by unrelated genes (Kiberstis and Roberts 2002). The study of Mendelian disorders provides an understanding of the basic biological function both in the normal and diseased state. This basic biological understanding can then be applied to complex disease. Moreover, it is possible that some of these monogenic entities may act as modifier or susceptibility locus to complex disease which often have variable expressivity (Antonarakis and Beckmann 2006). Most cases of retinitis pigmentosa are

thought to be monogenic; however, in some instances the variable expressivity is best explained through complex inheritance. Kajiwara *et al*. (Kajiwara et al. 1994) identified three families with seemingly dominant retinitis pigmentosa; however, several asymptomatic individuals also carried the disease causing mutation. The authors hypothesized that a mutation at a second locus must be necessary for disease. This was in fact the case, as all three families had heterozygous mutations in the peripherin/retinal degeneration slow (*RDS*) gene and retinal outer segment membrane protein 1 (*ROM1*) gene (Kajiwara et al. 1994). Based on the tissue specific role of BBS3L in the eye, it is reasonable to hypothesize that BBS3L act as a susceptibility locus for retinal degeneration, and should be screened in instances where the phenotype cannot be explained by a single mutation.

REFERENCES

Abd-El-Barr MM, Sykoudis K, Andrabi S, Eichers ER, Pennesi ME et al. (2007) Impaired photoreceptor protein transport and synaptic transmission in a mouse model of Bardet-Biedl syndrome. Vision Res 47(27): 3394-3407.

Abu Safieh L, Aldahmesh M, Shamseldin H, Hashem M, Shaheen R et al. (2009) Clinical and Molecular Characterization of Bardet-Biedl Syndrome in Consanguineous Populations: The Power of Homozygosity Mapping. J Med Genet.

Adams AE, Rosenblatt M, Suva LJ (1999) Identification of a novel parathyroid hormone-responsive gene in human osteoblastic cells. Bone 24(4): 305-313.

Aldahmesh MA, Safieh LA, Alkuraya H, Al-Rajhi A, Shamseldin H et al. (2009) Molecular characterization of retinitis pigmentosa in Saudi Arabia. Mol Vis 15: 2464-2469.

Andersson RG, Karlsson JO, Grundstrom N (1984) Adrenergic nerves and the alpha 2-adrenoceptor system regulating melanosome aggregation within fish melanophores. Acta Physiol Scand 121(2): 173-179.

Ansley SJ, Badano JL, Blacque OE, Hill J, Hoskins BE et al. (2003) Basal body dysfunction is a likely cause of pleiotropic Bardet-Biedl syndrome. Nature 425(6958): 628-633.

Antonarakis SE, Beckmann JS (2006) Mendelian disorders deserve more attention. Nat Rev Genet 7(4): 277-282.

Antoshechkin I, Han M (2002) The C. elegans evl-20 gene is a homolog of the small GTPase ARL2 and regulates cytoskeleton dynamics during cytokinesis and morphogenesis. Dev Cell 2(5): 579-591.

Arimura N, Kaibuchi K (2007) Neuronal polarity: from extracellular signals to intracellular mechanisms. Nat Rev Neurosci 8(3): 194-205.

Aspengren S, Skold HN, Quiroga G, Martensson L, Wallin M (2003) Noradrenaline- and melatonin-mediated regulation of pigment aggregation in fish melanophores. Pigment Cell Res 16(1): 59-64.

Avidor-Reiss T, Maer AM, Koundakjian E, Polyanovsky A, Keil T et al. (2004) Decoding cilia function: defining specialized genes required for compartmentalized cilia biogenesis. Cell 117(4): 527-539.

Ayoubi TA, Van De Ven WJ (1996) Regulation of gene expression by alternative promoters. Faseb J 10(4): 453-460.

Baala L, Audollent S, Martinovic J, Ozilou C, Babron MC et al. (2007) Pleiotropic effects of CEP290 (NPHP6) mutations extend to Meckel syndrome. Am J Hum Genet 81(1): 170-179.

Badano JL, Ansley SJ, Leitch CC, Lewis RA, Lupski JR et al. (2003a) Identification of a novel Bardet-Biedl syndrome protein, BBS7, that shares structural features with BBS1 and BBS2. Am J Hum Genet 72(3): 650-658.

Badano JL, Kim JC, Hoskins BE, Lewis RA, Ansley SJ et al. (2003b) Heterozygous mutations in BBS1, BBS2 and BBS6 have a potential epistatic effect on Bardet-Biedl patients with two mutations at a second BBS locus. Hum Mol Genet 12(14): 1651-1659.

Badano JL, Leitch CC, Ansley SJ, May-Simera H, Lawson S et al. (2006) Dissection of epistasis in oligogenic Bardet-Biedl syndrome. Nature 439(7074): 326-330.

Baek D, Davis C, Ewing B, Gordon D, Green P (2007) Characterization and predictive discovery of evolutionarily conserved mammalian alternative promoters. Genome Res 17(2): 145-155.

Bardet G (1995) On congenital obesity syndrome with polydactyly and retinitis pigmentosa (a contribution to the study of clinical forms of hypophyseal obesity). 1920. Obes Res 3(4): 387-399.

Barral DC, Seabra MC (2004) The melanosome as a model to study organelle motility in mammals. Pigment Cell Res 17(2): 111-118.

Beales PL, Warner AM, Hitman GA, Thakker R, Flinter FA (1997) Bardet-Biedl syndrome: a molecular and phenotypic study of 18 families. J Med Genet 34(2): 92-98.

Beales PL, Elcioglu N, Woolf AS, Parker D, Flinter FA (1999) New criteria for improved diagnosis of Bardet-Biedl syndrome: results of a population survey. J Med Genet 36(6): 437-446.

Beales PL, Badano JL, Ross AJ, Ansley SJ, Hoskins BE et al. (2003) Genetic interaction of BBS1 mutations with alleles at other BBS loci can result in non-Mendelian Bardet-Biedl syndrome. Am J Hum Genet 72(5): 1187-1199.

Beaudet AL, Belmont JW (2008) Array-based DNA diagnostics: let the revolution begin. Annu Rev Med 59: 113-129.

Berbari NF, Lewis JS, Bishop GA, Askwith CC, Mykytyn K (2008) Bardet-Biedl syndrome proteins are required for the localization of G protein-coupled receptors to primary cilia. Proc Natl Acad Sci U S A 105(11): 4242-4246.

Besharse JC, Horst CJ (1990) The photoreceptor connecting cilium. A model for for the transition zone. In: Bloodgood RA, editor. Ciliary and Flagellar Membranes. New York: Plenum Publishing Corp. pp. 389-417.

Bhamidipati A, Lewis SA, Cowan NJ (2000) ADP ribosylation factor-like protein 2 (Arl2) regulates the interaction of tubulin-folding cofactor D with native tubulin. J Cell Biol 149(5): 1087-1096.

Biedl A (1995) A pair of siblings with adiposo-genital dystrophy. 1922. Obes Res 3(4): 404.

Biesecker LG, Gottschalk LR, Emerson SG (1993) Identification of four murine cDNAs encoding putative protein kinases from primitive embryonic stem cells differentiated in vitro. Proc Natl Acad Sci U S A 90(15): 7044-7048.

Billingsley G, Bin J, Fieggen KJ, Duncan JL, Gerth C et al. (2010) Mutations in chaperonin-like BBS genes are a major contributor to disease development in a multiethnic Bardet-Biedl syndrome patient population. J Med Genet 47(7): 453-463.

Bilotta J, Saszik S, Sutherland SE (2001) Rod contributions to the electroretinogram of the dark-adapted developing zebrafish. Dev Dyn 222(4): 564-570.

Bin J, Madhavan J, Ferrini W, Mok CA, Billingsley G et al. (2009) BBS7 and TTC8 (BBS8) mutations play a minor role in the mutational load of Bardet-Biedl syndrome in a multiethnic population. Hum Mutat 30(7): E737-746.

Bisgrove BW, Yost HJ (2006) The roles of cilia in developmental disorders and disease. Development 133(21): 4131-4143.

Blackshaw S, Harpavat S, Trimarchi J, Cai L, Huang H et al. (2004) Genomic analysis of mouse retinal development. PLoS Biol 2(9): E247.

Blacque OE, Reardon MJ, Li C, McCarthy J, Mahjoub MR et al. (2004) Loss of C. elegans BBS-7 and BBS-8 protein function results in cilia defects and compromised intraflagellar transport. Genes Dev 18(13): 1630-1642.

Blatch GL, Lassle M (1999) The tetratricopeptide repeat: a structural motif mediating protein-protein interactions. Bioessays 21(11): 932-939.

Blott EJ, Griffiths GM (2002) Secretory lysosomes. Nat Rev Mol Cell Biol 3(2): 122-131.

Borovina A, Superina S, Voskas D, Ciruna B (2010) Vangl2 directs the posterior tilting and asymmetric localization of motile primary cilia. Nat Cell Biol 12(4): 407-412.

Brady ST, Lasek RJ, Allen RD (1982) Fast axonal transport in extruded axoplasm from squid giant axon. Science 218(4577): 1129-1131.

Brancati F, Dallapiccola B, Valente EM (2010) Joubert Syndrome and related disorders. Orphanet J Rare Dis 5: 20.

Branchek T (1984) The development of photoreceptors in the zebrafish, brachydanio rerio. II. Function. J Comp Neurol 224(1): 116-122.

Bullock SL, Ish-Horowicz D (2002) Cell polarity: Oskar seeks PARtner for a stable relationship. Nat Cell Biol 4(5): E117-118.

Carmi R, Elbedour K, Stone EM, Sheffield VC (1995a) Phenotypic differences among patients with Bardet-Biedl syndrome linked to three different chromosome loci. Am J Med Genet 59(2): 199-203.

Carmi R, Rokhlina T, Kwitek-Black AE, Elbedour K, Nishimura D et al. (1995b) Use of a DNA pooling strategy to identify a human obesity syndrome locus on chromosome 15. Hum Mol Genet 4(1): 9-13.

Chang B, Khanna H, Hawes N, Jimeno D, He S et al. (2006) In-frame deletion in a novel centrosomal/ciliary protein CEP290/NPHP6 perturbs its interaction with RPGR and results in early-onset retinal degeneration in the rd16 mouse. Hum Mol Genet 15(11): 1847-1857.

Cheung SW, Shaw CA, Yu W, Li J, Ou Z et al. (2005) Development and validation of a CGH microarray for clinical cytogenetic diagnosis. Genet Med 7(6): 422-432.

Chiang AP, Nishimura D, Searby C, Elbedour K, Carmi R et al. (2004) Comparative genomic analysis identifies an ADP-ribosylation factor-like gene as the cause of Bardet-Biedl syndrome (BBS3). Am J Hum Genet 75(3): 475-484.

Chiang AP, Beck JS, Yen HJ, Tayeh MK, Scheetz TE et al. (2006) Homozygosity mapping with SNP arrays identifies TRIM32, an E3 ubiquitin ligase, as a Bardet-Biedl syndrome gene (BBS11). Proc Natl Acad Sci U S A 103(16): 6287-6292.

Cole DG, Chinn SW, Wedaman KP, Hall K, Vuong T et al. (1993) Novel heterotrimeric kinesin-related protein purified from sea urchin eggs. Nature 366(6452): 268-270.

Cole DG, Diener DR, Himelblau AL, Beech PL, Fuster JC et al. (1998) Chlamydomonas kinesin-II-dependent intraflagellar transport (IFT): IFT particles contain proteins required for ciliary assembly in Caenorhabditis elegans sensory neurons. J Cell Biol 141(4): 993-1008.

Coppieters F, Lefever S, Leroy BP, De Baere E (2010) CEP290, a gene with many faces: mutation overview and presentation of CEP290base. Hum Mutat 31(10): 1097-1108.

Davis RE, Swiderski RE, Rahmouni K, Nishimura DY, Mullins RF et al. (2007) A knockin mouse model of the Bardet-Biedl syndrome 1 M390R mutation has cilia defects, ventriculomegaly, retinopathy, and obesity. Proc Natl Acad Sci U S A 104(49): 19422-19427.

Davuluri RV, Suzuki Y, Sugano S, Plass C, Huang TH (2008) The functional consequences of alternative promoter use in mammalian genomes. Trends Genet 24(4): 167-177.

Deffert C, Niel F, Mochel F, Barrey C, Romana C et al. (2007) Recurrent insertional polydactyly and situs inversus in a Bardet-Biedl syndrome family. Am J Med Genet A 143(2): 208-213.

den Hollander AI, Koenekoop RK, Yzer S, Lopez I, Arends ML et al. (2006) Mutations in the CEP290 (NPHP6) gene are a frequent cause of Leber congenital amaurosis. Am J Hum Genet 79(3): 556-561.

Drewes G, Ebneth A, Preuss U, Mandelkow EM, Mandelkow E (1997) MARK, a novel family of protein kinases that phosphorylate microtubule-associated proteins and trigger microtubule disruption. Cell 89(2): 297-308.

Easter SS, Jr., Nicola GN (1996) The development of vision in the zebrafish (Danio rerio). Dev Biol 180(2): 646-663.

Elbedour K, Zucker N, Zalzstein E, Barki Y, Carmi R (1994) Cardiac abnormalities in the Bardet-Biedl syndrome: echocardiographic studies of 22 patients. Am J Med Genet 52(2): 164-169.

Essner JJ, Amack JD, Nyholm MK, Harris EB, Yost HJ (2005) Kupffer's vesicle is a ciliated organ of asymmetry in the zebrafish embryo that initiates left-right development of the brain, heart and gut. Development 132(6): 1247-1260.

Essner JJ, Vogan KJ, Wagner MK, Tabin CJ, Yost HJ et al. (2002) Conserved function for embryonic nodal cilia. Nature 418(6893): 37-38.

Evans JE, Snow JJ, Gunnarson AL, Ou G, Stahlberg H et al. (2006) Functional modulation of IFT kinesins extends the sensory repertoire of ciliated neurons in Caenorhabditis elegans. J Cell Biol 172(5): 663-669.

Fan Y, Esmail MA, Ansley SJ, Blacque OE, Boroevich K et al. (2004) Mutations in a member of the Ras superfamily of small GTP-binding proteins causes Bardet-Biedl syndrome. Nat Genet 36(9): 989-993.

Fath MA, Mullins RF, Searby C, Nishimura DY, Wei J et al. (2005) Mkks-null mice have a phenotype resembling Bardet-Biedl syndrome. Hum Mol Genet 14(9): 1109-1118.

Force A, Lynch M, Pickett FB, Amores A, Yan YL et al. (1999) Preservation of duplicate genes by complementary, degenerative mutations. Genetics 151(4): 1531-1545.

Frank V, den Hollander AI, Bruchle NO, Zonneveld MN, Nurnberg G et al. (2008) Mutations of the CEP290 gene encoding a centrosomal protein cause Meckel-Gruber syndrome. Hum Mutat 29(1): 45-52.

Frosk P, Weiler T, Nylen E, Sudha T, Greenberg CR et al. (2002) Limb-girdle muscular dystrophy type 2H associated with mutation in TRIM32, a putative E3-ubiquitin-ligase gene. Am J Hum Genet 70(3): 663-672.

Frydman J, Nimmesgern E, Erdjument-Bromage H, Wall JS, Tempst P et al. (1992) Function in protein folding of TRiC, a cytosolic ring complex containing TCP-1 and structurally related subunits. Embo J 11(13): 4767-4778.

Fulton AB, Hansen RM, Glynn RJ (1993) Natural course of visual functions in the Bardet-Biedl syndrome. Arch Ophthalmol 111(11): 1500-1506.

Goldstein LS (2001) Molecular motors: from one motor many tails to one motor many tales. Trends Cell Biol 11(12): 477-482.

Green JS, Parfrey PS, Harnett JD, Farid NR, Cramer BC et al. (1989) The cardinal manifestations of Bardet-Biedl syndrome, a form of Laurence-Moon-Biedl syndrome. N Engl J Med 321(15): 1002-1009.

Gupta SK, Leonard BC, Damji KF, Bulman DE (2002) A frame shift mutation in a tissue-specific alternatively spliced exon of collagen 2A1 in Wagner's vitreoretinal degeneration. Am J Ophthalmol 133(2): 203-210.

Haimo LT, Rosenbaum JL (1981) Cilia, flagella, and microtubules. J Cell Biol 91(3 Pt 2): 125s-130s.

Harnett JD, Green JS, Cramer BC, Johnson G, Chafe L et al. (1988) The spectrum of renal disease in Laurence-Moon-Biedl syndrome. N Engl J Med 319(10): 615-618.

Hartong DT, Berson EL, Dryja TP (2006) Retinitis pigmentosa. Lancet 368(9549): 1795-1809.

Helou J, Otto EA, Attanasio M, Allen SJ, Parisi MA et al. (2007) Mutation analysis of NPHP6/CEP290 in patients with Joubert syndrome and Senior-Loken syndrome. J Med Genet 44(10): 657-663.

Heon E, Westall C, Carmi R, Elbedour K, Panton C et al. (2005a) Ocular phenotypes of three genetic variants of Bardet-Biedl syndrome. Am J Med Genet A 132A(3): 283-287.

Heon E, Westall C, Carmi R, Elbedour K, Panton C et al. (2005b) Ocular phenotypes of three genetic variants of Bardet-Biedl syndrome. Am J Med Genet A 132(3): 283-287.

Hichri H, Stoetzel C, Laurier V, Caron S, Sigaudy S et al. (2005) Testing for triallelism: analysis of six BBS genes in a Bardet-Biedl syndrome family cohort. Eur J Hum Genet 13(5): 607-616.

Hjortshoj TD, Gronskov K, Philp AR, Nishimura DY, Riise R et al. (2010) Bardet-Biedl syndrome in Denmark--report of 13 novel sequence variations in six genes. Hum Mutat 31(4): 429-436.

Hori Y, Kobayashi T, Kikko Y, Kontani K, Katada T (2008) Domain architecture of the atypical Arf-family GTPase Arl13b involved in cilia formation. Biochem Biophys Res Commun 373(1): 119-124.

Horst CJ, Johnson LV, Besharse JC (1990) Transmembrane assemblage of the photoreceptor connecting cilium and motile cilium transition zone contain a common immunologic epitope. Cell Motil Cytoskeleton 17(4): 329-344.

Hu M, Easter SS (1999) Retinal neurogenesis: the formation of the initial central patch of postmitotic cells. Dev Biol 207(2): 309-321.

Iafrate AJ, Feuk L, Rivera MN, Listewnik ML, Donahoe PK et al. (2004) Detection of large-scale variation in the human genome. Nat Genet 36(9): 949-951.

Iannaccone A, Mykytyn K, Persico AM, Searby CC, Baldi A et al. (2005) Clinical evidence of decreased olfaction in Bardet-Biedl syndrome caused by a deletion in the BBS4 gene. Am J Med Genet A 132(4): 343-346.

Ingley E, Williams JH, Walker CE, Tsai S, Colley S et al. (1999) A novel ADP-ribosylation like factor (ARL-6), interacts with the protein-conducting channel SEC61beta subunit. FEBS Lett 459(1): 69-74.

Jacobson SG, Borruat FX, Apathy PP (1990) Patterns of rod and cone dysfunction in Bardet-Biedl syndrome. Am J Ophthalmol 109(6): 676-688.

Jin H, White SR, Shida T, Schulz S, Aguiar M et al. (2010) The conserved Bardet-Biedl syndrome proteins assemble a coat that traffics membrane proteins to cilia. Cell 141(7): 1208-1219.

Kahn RA, Cherfils J, Elias M, Lovering RC, Munro S et al. (2006) Nomenclature for the human Arf family of GTP-binding proteins: ARF, ARL, and SAR proteins. J Cell Biol 172(5): 645-650.

Kajiwara K, Berson EL, Dryja TP (1994) Digenic retinitis pigmentosa due to mutations at the unlinked peripherin/RDS and ROM1 loci. Science 264(5165): 1604-1608.

Katsanis N (2004) The oligogenic properties of Bardet-Biedl syndrome. Hum Mol Genet 13 Spec No 1: R65-71.

Katsanis N, Beales PL, Woods MO, Lewis RA, Green JS et al. (2000) Mutations in MKKS cause obesity, retinal dystrophy and renal malformations associated with Bardet-Biedl syndrome. Nat Genet 26(1): 67-70.

Katsanis N, Eichers ER, Ansley SJ, Lewis RA, Kayserili H et al. (2002) BBS4 is a minor contributor to Bardet-Biedl syndrome and may also participate in triallelic inheritance. Am J Hum Genet 71(1): 22-29.

Katsanis N, Ansley SJ, Badano JL, Eichers ER, Lewis RA et al. (2001) Triallelic inheritance in Bardet-Biedl syndrome, a Mendelian recessive disorder. Science 293(5538): 2256-2259.

Kelly PD, Chu F, Woods IG, Ngo-Hazelett P, Cardozo T et al. (2000) Genetic linkage mapping of zebrafish genes and ESTs. Genome Res 10(4): 558-567.

Kemphues KJ, Priess JR, Morton DG, Cheng NS (1988) Identification of genes required for cytoplasmic localization in early C. elegans embryos. Cell 52(3): 311-320.

Kiberstis P, Roberts L (2002) It's Not Just the Genes. Science 296(5568): 685.

Kim JC, Badano JL, Sibold S, Esmail MA, Hill J et al. (2004) The Bardet-Biedl protein BBS4 targets cargo to the pericentriolar region and is required for microtubule anchoring and cell cycle progression. Nat Genet 36(5): 462-470.

Kimmel CB, Ballard WW, Kimmel SR, Ullmann B, Schilling TF (1995) Stages of embryonic development of the zebrafish. Dev Dyn 203(3): 253-310.

Kimura K, Wakamatsu A, Suzuki Y, Ota T, Nishikawa T et al. (2006) Diversification of transcriptional modulation: large-scale identification and characterization of putative alternative promoters of human genes. Genome Res 16(1): 55-65.

Kirschner R, Rosenberg T, Schultz-Heienbrok R, Lenzner S, Feil S et al. (1999) RPGR transcription studies in mouse and human tissues reveal a retina-specific isoform that is disrupted in a patient with X-linked retinitis pigmentosa. Hum Mol Genet 8(8): 1571-1578.

Kishimoto N, Cao Y, Park A, Sun Z (2008) Cystic kidney gene seahorse regulates cilia-mediated processes and Wnt pathways. Dev Cell 14(6): 954-961.

Kotz KJ, McNiven MA (1994) Intracellular calcium and cAMP regulate directional pigment movements in teleost erythrophores. J Cell Biol 124(4): 463-474.

Kozminski KG, Johnson KA, Forscher P, Rosenbaum JL (1993) A motility in the eukaryotic flagellum unrelated to flagellar beating. Proc Natl Acad Sci U S A 90(12): 5519-5523.

Krock BL, Perkins BD (2008) The intraflagellar transport protein IFT57 is required for cilia maintenance and regulates IFT-particle-kinesin-II dissociation in vertebrate photoreceptors. J Cell Sci 121(Pt 11): 1907-1915.

Krummel MF, Macara I (2006) Maintenance and modulation of T cell polarity. Nat Immunol 7(11): 1143-1149.

Kudryashova E, Kudryashov D, Kramerova I, Spencer MJ (2005) Trim32 is a ubiquitin ligase mutated in limb girdle muscular dystrophy type 2H that binds to skeletal muscle myosin and ubiquitinates actin. J Mol Biol 354(2): 413-424.

Kulaga HM, Leitch CC, Eichers ER, Badano JL, Lesemann A et al. (2004) Loss of BBS proteins causes anosmia in humans and defects in olfactory cilia structure and function in the mouse. Nat Genet 36(9): 994-998.

Kwan KM, Fujimoto E, Grabher C, Mangum BD, Hardy ME et al. (2007) The Tol2kit: a multisite gateway-based construction kit for Tol2 transposon transgenesis constructs. Dev Dyn 236(11): 3088-3099.

Kwitek-Black AE, Carmi R, Duyk GM, Buetow KH, Elbedour K et al. (1993) Linkage of Bardet-Biedl syndrome to chromosome 16q and evidence for non-allelic genetic heterogeneity. Nat Genet 5(4): 392-396.

Kyttala M, Tallila J, Salonen R, Kopra O, Kohlschmidt N et al. (2006) MKS1, encoding a component of the flagellar apparatus basal body proteome, is mutated in Meckel syndrome. Nat Genet 38(2): 155-157.

Landry JR, Mager DL, Wilhelm BT (2003) Complex controls: the role of alternative promoters in mammalian genomes. Trends Genet 19(11): 640-648.

Larkin MA, Blackshields G, Brown NP, Chenna R, McGettigan PA et al. (2007) Clustal W and Clustal X version 2.0. Bioinformatics 23(21): 2947-2948.

Laurier V, Stoetzel C, Muller J, Thibault C, Corbani S et al. (2006) Pitfalls of homozygosity mapping: an extended consanguineous Bardet-Biedl syndrome family with two mutant genes (BBS2, BBS10), three mutations, but no triallelism. Eur J Hum Genet 14(11): 1195-1203.

Leitch CC, Zaghloul NA, Davis EE, Stoetzel C, Diaz-Font A et al. (2008) Hypomorphic mutations in syndromic encephalocele genes are associated with Bardet-Biedl syndrome. Nat Genet 40(4): 443-448.

Lennerz JK, Hurov JB, White LS, Lewandowski KT, Prior JL et al. (2010) Loss of Par-1a/MARK3/C-TAK1 kinase leads to reduced adiposity, resistance to hepatic steatosis, and defective gluconeogenesis. Mol Cell Biol 30(21): 5043-5056.

Leys MJ, Schreiner LA, Hansen RM, Mayer DL, Fulton AB (1988) Visual acuities and dark-adapted thresholds of children with Bardet-Biedl syndrome. Am J Ophthalmol 106(5): 561-569.

Li JB, Gerdes JM, Haycraft CJ, Fan Y, Teslovich TM et al. (2004) Comparative genomics identifies a flagellar and basal body proteome that includes the BBS5 human disease gene. Cell 117(4): 541-552.

Li Y, Wei Q, Zhang Y, Ling K, Hu J (2010) The small GTPases ARL-13 and ARL-3 coordinate intraflagellar transport and ciliogenesis. J Cell Biol 189(6): 1039-1051.

Liu Y, Shen Y, Rest JS, Raymond PA, Zack DJ (2001) Isolation and characterization of a zebrafish homologue of the cone rod homeobox gene. Invest Ophthalmol Vis Sci 42(2): 481-487.

Loken AC, Hanssen O, Halvorsen S, Jolster NJ (1961) Hereditary renal dysplasia and blindness. Acta Paediatr 50: 177-184.

Luby-Phelps K, Fogerty J, Baker SA, Pazour GJ, Besharse JC (2008) Spatial distribution of intraflagellar transport proteins in vertebrate photoreceptors. Vision Res 48(3): 413-423.

Lundstrom I, Svensson S (1998) Biosensing with G-protein coupled receptor systems. Biosens Bioelectron 13(6): 689-695.

Lupski JR, Wise CA, Kuwano A, Pentao L, Parke JT et al. (1992) Gene dosage is a mechanism for Charcot-Marie-Tooth disease type 1A. Nat Genet 1(1): 29-33.

Lynch M, Conery JS (2000) The evolutionary fate and consequences of duplicate genes. Science 290(5494): 1151-1155.

Marks MS, Seabra MC (2001) The melanosome: membrane dynamics in black and white. Nat Rev Mol Cell Biol 2(10): 738-748.

Martin SG, St Johnston D (2003) A role for Drosophila LKB1 in anterior-posterior axis formation and epithelial polarity. Nature 421(6921): 379-384.

Masai I, Lele Z, Yamaguchi M, Komori A, Nakata A et al. (2003) N-cadherin mediates retinal lamination, maintenance of forebrain compartments and patterning of retinal neurites. Development 130(11): 2479-2494.

McAlinden A, Majava M, Bishop PN, Perveen R, Black GC et al. (2008) Missense and nonsense mutations in the alternatively-spliced exon 2 of COL2A1 cause the ocular variant of Stickler syndrome. Hum Mutat 29(1): 83-90.

Mecke S, Passarge E (1971) Encephalocele, polycystic kidneys, and polydactyly as an autosomal recessive trait simulating certain other disorders: the Meckel syndrome. Ann Genet 14(2): 97-103.

Memon AR (2004) The role of ADP-ribosylation factor and SAR1 in vesicular trafficking in plants. Biochim Biophys Acta 1664(1): 9-30.

Mokrzan EM, Lewis JS, Mykytyn K (2007) Differences in renal tubule primary cilia length in a mouse model of Bardet-Biedl syndrome. Nephron Exp Nephrol 106(3): e88-96.

Moore SJ, Green JS, Fan Y, Bhogal AK, Dicks E et al. (2005) Clinical and genetic epidemiology of Bardet-Biedl syndrome in Newfoundland: a 22-year prospective, population-based, cohort study. Am J Med Genet A 132(4): 352-360.

Mykytyn K, Mullins RF, Andrews M, Chiang AP, Swiderski RE et al. (2004) Bardet-Biedl syndrome type 4 (BBS4)-null mice implicate Bbs4 in flagella formation but not global cilia assembly. Proc Natl Acad Sci U S A 101(23): 8664-8669.

Mykytyn K, Braun T, Carmi R, Haider NB, Searby CC et al. (2001) Identification of the gene that, when mutated, causes the human obesity syndrome BBS4. Nat Genet 28(2): 188-191.

Mykytyn K, Nishimura DY, Searby CC, Shastri M, Yen HJ et al. (2002) Identification of the gene (BBS1) most commonly involved in Bardet-Biedl syndrome, a complex human obesity syndrome. Nat Genet 31(4): 435-438.

Mykytyn K, Nishimura DY, Searby CC, Beck G, Bugge K et al. (2003) Evaluation of complex inheritance involving the most common Bardet-Biedl syndrome locus (BBS1). Am J Hum Genet 72(2): 429-437.

Nachury MV, Loktev AV, Zhang Q, Westlake CJ, Peranen J et al. (2007) A core complex of BBS proteins cooperates with the GTPase Rab8 to promote ciliary membrane biogenesis. Cell 129(6): 1201-1213.

Nakane T, Biesecker LG (2005) No evidence for triallelic inheritance of MKKS/BBS loci in Amish Mckusick-Kaufman syndrome. Am J Med Genet A 138(1): 32-34.

Nance J (2005) PAR proteins and the establishment of cell polarity during C. elegans development. Bioessays 27(2): 126-135.

Nascimento AA, Roland JT, Gelfand VI (2003) Pigment cells: a model for the study of organelle transport. Annu Rev Cell Dev Biol 19: 469-491.

Nikolaev VO, Lohse MJ (2006) Monitoring of cAMP synthesis and degradation in living cells. Physiology (Bethesda) 21: 86-92.

Nishimura DY, Swiderski RE, Searby CC, Berg EM, Ferguson AL et al. (2005) Comparative genomics and gene expression analysis identifies BBS9, a new Bardet-Biedl syndrome gene. Am J Hum Genet 77(6): 1021-1033.

Nishimura DY, Fath M, Mullins RF, Searby C, Andrews M et al. (2004) Bbs2-null mice have neurosensory deficits, a defect in social dominance, and retinopathy associated with mislocalization of rhodopsin. Proc Natl Acad Sci U S A 101(47): 16588-16593.

Nishimura DY, Baye LM, Perveen R, Searby CC, Avila-Fernandez A et al. (2010) Discovery and Functional Analysis of a Retinitis Pigmentosa Gene, C2ORF71. Am J Hum Genet.

Nishimura DY, Searby CC, Carmi R, Elbedour K, Van Maldergem L et al. (2001) Positional cloning of a novel gene on chromosome 16q causing Bardet-Biedl syndrome (BBS2). Hum Mol Genet 10(8): 865-874.

Pan Q, Shai O, Lee LJ, Frey BJ, Blencowe BJ (2008) Deep surveying of alternative splicing complexity in the human transcriptome by high-throughput sequencing. Nat Genet 40(12): 1413-1415.

Pasqualato S, Renault L, Cherfils J (2002) Arf, Arl, Arp and Sar proteins: a family of GTP-binding proteins with a structural device for 'front-back' communication. EMBO Rep 3(11): 1035-1041.

Pazour GJ, Wilkerson CG, Witman GB (1998) A dynein light chain is essential for the retrograde particle movement of intraflagellar transport (IFT). J Cell Biol 141(4): 979-992.

Pazour GJ, Baker SA, Deane JA, Cole DG, Dickert BL et al. (2002) The intraflagellar transport protein, IFT88, is essential for vertebrate photoreceptor assembly and maintenance. J Cell Biol 157(1): 103-113.

Pereiro I, Valverde D, Pineiro-Gallego T, Baiget M, Borrego S et al. (2010) New mutations in BBS genes in small consanguineous families with Bardet-Biedl syndrome: detection of candidate regions by homozygosity mapping. Mol Vis 16: 137-143.

Piperno G, Siuda E, Henderson S, Segil M, Vaananen H et al. (1998) Distinct mutants of retrograde intraflagellar transport (IFT) share similar morphological and molecular defects. J Cell Biol 143(6): 1591-1601.

Postlethwait JH, Talbot WS (1997) Zebrafish genomics: from mutants to genes. Trends Genet 13(5): 183-190.

Postlethwait JH, Woods IG, Ngo-Hazelett P, Yan YL, Kelly PD et al. (2000) Zebrafish comparative genomics and the origins of vertebrate chromosomes. Genome Res 10(12): 1890-1902.

Pretorius PR, Baye LM, Nishimura DY, Searby CC, Bugge K et al. (2010) Identification and functional analysis of the vision-specific BBS3 (ARL6) long isoform. PLoS Genet 6(3): e1000884.

Radcliffe PA, Vardy L, Toda T (2000) A conserved small GTP-binding protein Alp41 is essential for the cofactor-dependent biogenesis of microtubules in fission yeast. FEBS Lett 468(1): 84-88.

Redon R, Ishikawa S, Fitch KR, Feuk L, Perry GH et al. (2006) Global variation in copy number in the human genome. Nature 444(7118): 444-454.

Riazuddin SA, Iqbal M, Wang Y, Masuda T, Chen Y et al. (2010) A splice-site mutation in a retina-specific exon of BBS8 causes nonsyndromic retinitis pigmentosa. Am J Hum Genet 86(5): 805-812.

Riise R (1987) Visual function in Laurence-Moon-Bardet-Biedl syndrome. A survey of 26 cases. Acta Ophthalmol Suppl 182: 128-131.

Riise R, Andreasson S, Borgastrom MK, Wright AF, Tommerup N et al. (1997) Intrafamilial variation of the phenotype in Bardet-Biedl syndrome. Br J Ophthalmol 81(5): 378-385.

Robinow M, Shaw A (1979) The McKusick-Kaufman syndrome: recessively inherited vaginal atresia, hydrometrocolpos, uterovaginal duplications, anorectal anomalies, postaxial polydactyly, and congenital heart disease. J Pediatr 94(5): 776-778.

Rogers SL, Gelfand VI (1998) Myosin cooperates with microtubule motors during organelle transport in melanophores. Curr Biol 8(3): 161-164.

Rohlich P (1975) The sensory cilium of retinal rods is analogous to the transitional zone of motile cilia. Cell Tissue Res 161(3): 421-430.

Sapp JC, Nishimura D, Johnston JJ, Stone EM, Heon E et al. (2010) Recurrence risks for Bardet-Biedl syndrome: Implications of locus heterogeneity. Genet Med 12(10): 623-627.

Sayer JA, Otto EA, O'Toole JF, Nurnberg G, Kennedy MA et al. (2006) The centrosomal protein nephrocystin-6 is mutated in Joubert syndrome and activates transcription factor ATF4. Nat Genet 38(6): 674-681.

Schmitt EA, Dowling JE (1999) Early retinal development in the zebrafish, Danio rerio: light and electron microscopic analyses. J Comp Neurol 404(4): 515-536.

Sebat J, Lakshmi B, Troge J, Alexander J, Young J et al. (2004) Large-scale copy number polymorphism in the human genome. Science 305(5683): 525-528.

Senior B, Friedmann AI, Braudo JL (1961) Juvenile familial nephropathy with tapetoretinal degeneration. A new oculorenal dystrophy. Am J Ophthalmol 52: 625-633.

Seo S, Guo DF, Bugge K, Morgan DA, Rahmouni K et al. (2009) Requirement of Bardet-Biedl syndrome proteins for leptin receptor signaling. Hum Mol Genet 18(7): 1323-1331.

Seo S, Baye LM, Schulz NP, Beck JS, Zhang Q et al. (2010) BBS6, BBS10, and BBS12 form a complex with CCT/TRiC family chaperonins and mediate BBSome assembly. Proc Natl Acad Sci U S A.

Shah AS, Farmen SL, Moninger TO, Businga TR, Andrews MP et al. (2008) Loss of Bardet-Biedl syndrome proteins alters the morphology and function of motile cilia in airway epithelia. Proc Natl Acad Sci U S A 105(9): 3380-3385.

Sheffield VC (2004) BBS genes and the Bardet-Biedl syndrome. In: Epstein CJ, Erickson RP, Wynshaw-Boris A, editors. Inborn Errors of Development. New York: Oxford University Press. pp. 1044-1050.

Sheffield VC, Carmi R, Kwitek-Black A, Rokhlina T, Nishimura D et al. (1994) Identification of a Bardet-Biedl syndrome locus on chromosome 3 and evaluation of an efficient approach to homozygosity mapping. Hum Mol Genet 3(8): 1331-1335.

Shen YC, Raymond PA (2004) Zebrafish cone-rod (crx) homeobox gene promotes retinogenesis. Dev Biol 269(1): 237-251.

Signor D, Wedaman KP, Orozco JT, Dwyer ND, Bargmann CI et al. (1999) Role of a class DHC1b dynein in retrograde transport of IFT motors and IFT raft particles along cilia, but not dendrites, in chemosensory neurons of living Caenorhabditis elegans. J Cell Biol 147(3): 519-530.

Skold HN, Aspengren S, Wallin M (2002) The cytoskeleton in fish melanophore melanosome positioning. Microsc Res Tech 58(6): 464-469.

Slavotinek AM, Stone EM, Mykytyn K, Heckenlively JR, Green JS et al. (2000) Mutations in MKKS cause Bardet-Biedl syndrome. Nat Genet 26(1): 15-16.

Sloboda RD (2005) Intraflagellar transport and the flagellar tip complex. J Cell Biochem 94(2): 266-272.

Slusarski DC, Corces VG (2000) Calcium imaging in cell-cell signaling. Methods Mol Biol 135: 253-261.

Smaoui N, Chaabouni M, Sergeev YV, Kallel H, Li S et al. (2006) Screening of the eight BBS genes in Tunisian families: no evidence of triallelism. Invest Ophthalmol Vis Sci 47(8): 3487-3495.

Stankiewicz P, Lupski JR (2010) Structural variation in the human genome and its role in disease. Annu Rev Med 61: 437-455.

Stoetzel C, Laurier V, Faivre L, Megarbane A, Perrin-Schmitt F et al. (2006a) BBS8 is rarely mutated in a cohort of 128 Bardet-Biedl syndrome families. J Hum Genet 51(1): 81-84.

Stoetzel C, Muller J, Laurier V, Davis EE, Zaghloul NA et al. (2007) Identification of a novel BBS gene (BBS12) highlights the major role of a vertebrate-specific branch of chaperonin-related proteins in Bardet-Biedl syndrome. Am J Hum Genet 80(1): 1-11.

Stoetzel C, Laurier V, Davis EE, Muller J, Rix S et al. (2006b) BBS10 encodes a vertebrate-specific chaperonin-like protein and is a major BBS locus. Nat Genet 38(5): 521-524.

Stone DL, Slavotinek A, Bouffard GG, Banerjee-Basu S, Baxevanis AD et al. (2000) Mutation of a gene encoding a putative chaperonin causes McKusick-Kaufman syndrome. Nat Genet 25(1): 79-82.

Sukumaran S, Perkins BD (2009) Early defects in photoreceptor outer segment morphogenesis in zebrafish ift57, ift88 and ift172 Intraflagellar Transport mutants. Vision Res 49(4): 479-489.

Sun Z, Amsterdam A, Pazour GJ, Cole DG, Miller MS et al. (2004) A genetic screen in zebrafish identifies cilia genes as a principal cause of cystic kidney. Development 131(16): 4085-4093.

Supp DM, Witte DP, Potter SS, Brueckner M (1997) Mutation of an axonemal dynein affects left-right asymmetry in inversus viscerum mice. Nature 389(6654): 963-966.

Swiderski RE, Nishimura DY, Mullins RF, Olvera MA, Ross JL et al. (2007) Gene expression analysis of photoreceptor cell loss in bbs4-knockout mice reveals an early stress gene response and photoreceptor cell damage. Invest Ophthalmol Vis Sci 48(7): 3329-3340.

Tabb JS, Molyneaux BJ, Cohen DL, Kuznetsov SA, Langford GM (1998) Transport of ER vesicles on actin filaments in neurons by myosin V. J Cell Sci 111 (Pt 21): 3221-3234.

Takada T, Iida K, Sasaki H, Taira M, Kimura H (2005) Expression of ADP-ribosylation factor (ARF)-like protein 6 during mouse embryonic development. Int J Dev Biol 49(7): 891-894.

Takai Y, Sasaki T, Matozaki T (2001) Small GTP-binding proteins. Physiol Rev 81(1): 153-208.

Talbot WS, Egan ES, Gates MA, Walker C, Ullmann B et al. (1998) Genetic analysis of chromosomal rearrangements in the cyclops region of the zebrafish genome. Genetics 148(1): 373-380.

Tayeh MK, Yen HJ, Beck JS, Searby CC, Westfall TA et al. (2008) Genetic interaction between Bardet-Biedl syndrome genes and implications for limb patterning. Hum Mol Genet.

Tsujikawa M, Malicki J (2004) Intraflagellar transport genes are essential for differentiation and survival of vertebrate sensory neurons. Neuron 42(5): 703-716.

Vale RD (2003) The molecular motor toolbox for intracellular transport. Cell 112(4): 467-480.

Valente EM, Brancati F, Dallapiccola B (2008) Genotypes and phenotypes of Joubert syndrome and related disorders. Eur J Med Genet 51(1): 1-23.

Valente EM, Silhavy JL, Brancati F, Barrano G, Krishnaswami SR et al. (2006) Mutations in CEP290, which encodes a centrosomal protein, cause pleiotropic forms of Joubert syndrome. Nat Genet 38(6): 623-625.

Vihtelic TS, Doro CJ, Hyde DR (1999) Cloning and characterization of six zebrafish photoreceptor opsin cDNAs and immunolocalization of their corresponding proteins. Vis Neurosci 16(3): 571-585.

Vissers LE, Veltman JA, van Kessel AG, Brunner HG (2005) Identification of disease genes by whole genome CGH arrays. Hum Mol Genet 14 Spec No. 2: R215-223.

Wang ET, Sandberg R, Luo S, Khrebtukova I, Zhang L et al. (2008) Alternative isoform regulation in human tissue transcriptomes. Nature 456(7221): 470-476.

Westerfield M (1993) The Zebrafish book. A guide for the laboratory use of zebrafish (*Brachydanio rerio*). Eugene, OR: University of Oregon Press.

Wheatley DN, Wang AM, Strugnell GE (1996) Expression of primary cilia in mammalian cells. Cell Biol Int 20(1): 73-81.

Wiens CJ, Tong Y, Esmail MA, Oh E, Gerdes JM et al. (2010) The Bardet-Biedl syndrome-associated small GTPase ARL6 (BBS3) functions at or near the ciliary gate and modulates Wnt signalling. J Biol Chem.

Wu X, Hammer JA, 3rd (2000) Making sense of melanosome dynamics in mouse melanocytes. Pigment Cell Res 13(4): 241-247.

Yen HJ, Tayeh MK, Mullins RF, Stone EM, Sheffield VC et al. (2006) Bardet-Biedl syndrome genes are important in retrograde intracellular trafficking and Kupffer's vesicle cilia function. Hum Mol Genet 15(5): 667-677.

Young RW (1967) The renewal of photoreceptor cell outer segments. J Cell Biol 33(1): 61-72.

Young RW (1985) Cell differentiation in the retina of the mouse. Anat Rec 212(2): 199-205.